Applied Geochemistry xxx (2016) 1–16

Contents lists available at ScienceDirect

Applied Geochemistry

journal homepage: www.elsevier.com/locate/apgeochem

Reversible adsorption and flushing of arsenic in a shallow, Holocene aquifer of Bangladesh

Kathleen A. Radloff [a, b, *, 1], Yan Zheng [a, c], Martin Stute [a, d], Beth Weinman [e, 2], Benjamin Bostick [a], Ivan Mihajlov [b], Margaret Bounds [d], M.Moshiur Rahman [c, f], M.Rezaul Huq [f], Kazi M. Ahmed [f], Peter Schlosser [a, b], Alexander van Geen [a]

[a] Lamont-Doherty Earth Observatory of Columbia University, Palisades, NY 10964, USA
[b] Columbia University, New York, NY 10027, USA
[c] Queens College, City University of New York, Flushing, NY 11367, USA
[d] Barnard College, Columbia University, New York, NY 10027, USA
[e] Vanderbilt University, Nashville, TN 37240, USA
[f] Department of Geology, University of Dhaka, Dhaka, Bangladesh

ARTICLE INFO

Article history:
Received 1 June 2015
Received in revised form
9 November 2015
Accepted 16 November 2015
Available online 23 November 2015

Keywords:
Arsenic
Bangladesh
Adsorption
Hydrology
Groundwater age dating
Push–pull tests

ABSTRACT

The spatial heterogeneity of dissolved arsenic (As) concentrations in shallow groundwater of the Bengal Basin has been attributed to transport of As (and reactive carbon) from external sources or to the release of As from within grey sand formations. We explore the latter scenario in this detailed hydrological and geochemical study along a 300 m transect of a shallow aquifer extending from a groundwater recharge area within a sandy channel bar to its discharge into a nearby stream. Within the 10–20 m depth range, groundwater ages along the transect determined by the ^{3}H–^{3}He method increase from <10 yr in the recharge area to a maximum of 40 yr towards the stream. Concentrations of groundwater As within the same grey sands increase from 10 to 100 to ~500 μg/L along this transect. Evidence of reversible adsorption of As between the groundwater and sediment was obtained from a series of push–pull experiments, traditional batch adsorption experiments, and the accidental flooding of a shallow monitoring well. Assuming reversible adsorption and a distribution coefficient, K_d, of 0.15–1.5 L/kg inferred from these observations, a simple flushing model shows that the increase in As concentrations with depth and groundwater age at this site, and at other sites in the Bengal and Red River Basins, can be attributed to the evolution of the aquifer over 100–1000 years as aquifer sands are gradually flushed of their initial As content. A wide range of As concentrations can thus be maintained in groundwater with increases with depth governed by the history of flushing and local recharge rates, without external inputs of reactive carbon or As from other sources.

1. Introduction

The spatial variability of arsenic (As) in groundwater pumped from shallow Holocene aquifers of South and Southeast Asia has been well documented by various research teams at dozens of sites over the past decade and half (e.g. BGS/DPHE, 2001; Harvey et al., 2002; McArthur et al., 2004, 2008; Polizzotto et al., 2008; Kocar et al., 2008; Postma et al., 2007, 2012; van Geen et al., 2003a). A commonly observed feature is an order-of-magnitude increase of As concentrations in groundwater within the upper 30 m of an aquifer. The underlying reasons for this feature, and why the increase in groundwater As with depth can change considerably from one location to the other, are still poorly understood. The question needs attention, because tens of millions of villagers throughout the affected region continue to rely on shallow wells as their main source of drinking water. Without a quantitative understanding of the mechanisms as to how and why As increases with depth, doubts will remain concerning how long a shallow well that once tested low for As can continue to be used for drinking and cooking (McArthur et al., 2010; Fendorf et al., 2010).

* Corresponding author. Lamont-Doherty Earth Observatory of Columbia University, Palisades, NY 10964, USA.
E-mail address: kradloff@gradientcorp.com (K.A. Radloff).
[1] Present address: Gradient, Cambridge, MA 02138, USA.
[2] Present address: California State University, Fresno, CA 93740, USA.

http://dx.doi.org/10.1016/j.apgeochem.2015.11.003
0883-2927/

In the much smaller number of detailed As studies that include profiles of bomb-produced ^{3}H and its radiogenic daughter ^{3}He, groundwater ages relative to the time of recharge inferred from these measurements also increase with depth (Klump et al., 2006; Postma et al., 2007, 2012; Stute et al., 2007). One of these studies, which included paired profiles of both As and ^{3}H–^{3}He ages for 6 sites separated by a few kilometers in Bangladesh, showed that As concentrations rose more rapidly with depth at sites where groundwater ages also increased faster with depth (Stute et al., 2007). This relationship was subsequently interpreted as an indication that the rate of flushing of a Holocene aquifer determined the amount of exchangeable As remaining in the sediment and, therefore, also As concentrations in groundwater (Aziz et al., 2008; van Geen et al., 2008). Another study, conducted at 4 sites across a 10-km transect in Vietnam, has since shown that the depth gradient of As concentrations in shallow aquifers can also be a function of sediment age (Postma et al., 2012).

The common theme underlying these and many other studies is the extent to which the release of As to groundwater in Holocene aquifers is regulated by the availability of reactive carbon and/or exchangeable As (Harvey et al. 2002; Zheng et al., 2005; Mladenov et al. 2015). For both reactive carbon and exchangeable As, either transport from a shallow source that affects a shallow aquifer or *in situ* reaction from sediment within the aquifer has been invoked for different sites (Polizzotto et al., 2008; Neumann et al., 2010; Desbarats et al., 2014; Harvey et al., 2006; Mladenov et al., 2009; Mailloux et al., 2013). The goal of our study was to test the limits of internal As release by thoroughly characterizing a site that seemed hydrologically tractable and had groundwater As depth profiles that varied markedly over a very short distance. The observations from the site were integrated with a simple model which assumes that reversible adsorption and the extent of flushing are the key parameters. We demonstrate the relevance of this new understanding by applying the same model to other well-studied aquifers in the Bengal and Red River Basins.

2. Methods

2.1. Study site

The study site (90.63° E, 23.79° N) in a small village located 25 km northeast of Dhaka Araihazar, Bangladesh, is a sandy point bar where a cluster of low-As concentrations (at <50 m depth) was documented in a blanket survey of private wells (van Geen et al., 2003b; Weinman et al., 2008). Sediment incubation experiments were previously conducted using material from the site (Radloff et al., 2008). The land surface of the site is characterized by a sandy, raised area in the village with a gradually thickening silty-clay layer extending beneath the adjacent agricultural fields, which are bordered by a small stream (Fig. 1). Weinman et al. (2008) described several of the fine scale patterns (10^{1}–10^{2} m) of local fluvial subsurface stratigraphy that are found within Araihazar. Using their classification scheme, the study site described here can be characterized as having near-surface sandy outcrops underlain by clean sands (Facies A or B), which are characteristic of channel bars and levees formed under high flow regimes (Weinman et al., 2008).

The stratigraphy of the area was confirmed with a surface electromagnetic conductivity survey and extensive coring (Aziz et al., 2008). The surface sediments at the site have a lower EM conductivity (and therefore are coarser) than the average sediments in the region. Recharge is therefore likely to be concentrated in particularly coarse areas found in and along the border of the raised sandy village. The surface elevation decreases about 2 m from the village to the stream; depths across the transect are referenced throughout the paper relative to one location, the base of a concrete utility pole in the village, and were determined using a clear water-filled tube. From the surface to 10 m depth, the sediment is a silty sand. A thin (<5 cm) clay layer located at approximately 10 m depth was identified while drilling at several locations. Below 10 m the sandy aquifer is physically homogeneous and no other extensive clay lenses were identified. A thick grey clay layer (>5 m) provides a lower confinement of this aquifer and is found between 30 and 35 m depth. On the basis of these observations, groundwater was expected to flow from the elevated sand bar, presumed to be the main recharge area, to the zone of discharge in a local stream at a distance of 300 m (Fig. 1).

2.2. Monitoring wells

2.2.1. Installation and sample collection

The village to stream transect includes 6 locations that are labeled by referring to their distance (in meters) from the nearby stream. The main transect includes four monitoring locations which are in a line from the village to the stream (K240, K150, K60 and K5). Up to 5 wells were installed at each location with 1-m screens centered at approximately 7, 10, 15, 20 and 30 m depth. At two additional locations located off of the main transect, 3 wells were installed in the shallow aquifer at 7, 10 and 15 m depth (K80W and K40E). Additional wells were installed within a 0.25 km^{2} area surrounding the transect, totaling 41 monitoring wells distributed across 24 locations. Profiles of groundwater and sediment were also obtained by needle-sampling (van Geen et al., 2004).

Groundwater samples for metal and anion analysis were collected at 18 monitoring wells biweekly from December 2006 through 2009. For the remaining wells, samples were collected every 3 months from February 2008 through 2009. The most extensive sampling campaigns took place in March 2007, 2008 and 2009. Groundwater was collected using a submersible pump (Typhoon, Proactive) after purging the well for at least 3 well volumes. During collection, groundwater was continuously monitored for temperature, pH and conductivity using a multiparameter water monitoring probe in a flow cell (MP 556 from YSI, Inc.), while dissolved oxygen was measured using 0–40 ppb kits (Chemetrics). Samples for metal and anion analyses were filtered inline through 0.45 μm syringe filters (Whatman 6753–2504) and collected in 20 mL plastic scintillation vials; the samples for metal analysis were also acidified to 1% HCl (Optima) in the field.

2.2.2. Field protocols

Dissolved Fe(II) was measured in the field using ferrozine (Stookey, 1970). The alkalinity of groundwater was determined within a day after sampling (Gran, 1952). As speciation was determined by difference by filtering groundwater in the field through columns that retain As(V) but not As(III) (Meng et al., 2001). Ammonia concentrations were measured on the day of sampling by colorimetry (Sorzano, 1969).

2.2.3. Water level measurements and loggers

Groundwater levels were monitored in 41 wells and at two locations within the stream, from the bridge and in an L-shaped pipe near K5, over a 2 year period from March 2007 to 2009. Manual water level measurements were taken biweekly for 18 wells and the stream locations from December 2006 to November 2009, and approximately every 3 months from February 2008 to November 2009 for all locations. In order to prevent floodwater intrusion, 1.5 m-long galvanized iron (GI) extensions were added to the wells located in low-lying areas during the monsoon season. Pressure transducers (Leveloggers, Solinst) were deployed in 8 wells and recorded pressures every 20 min from March or May 2007 through

Please cite this article in press as: Radloff, K.A., et al., Reversible adsorption and flushing of arsenic in a shallow, Holocene aquifer of Bangladesh, Applied Geochemistry (2016), http://dx.doi.org/10.1016/j.apgeochem.2015.11.003

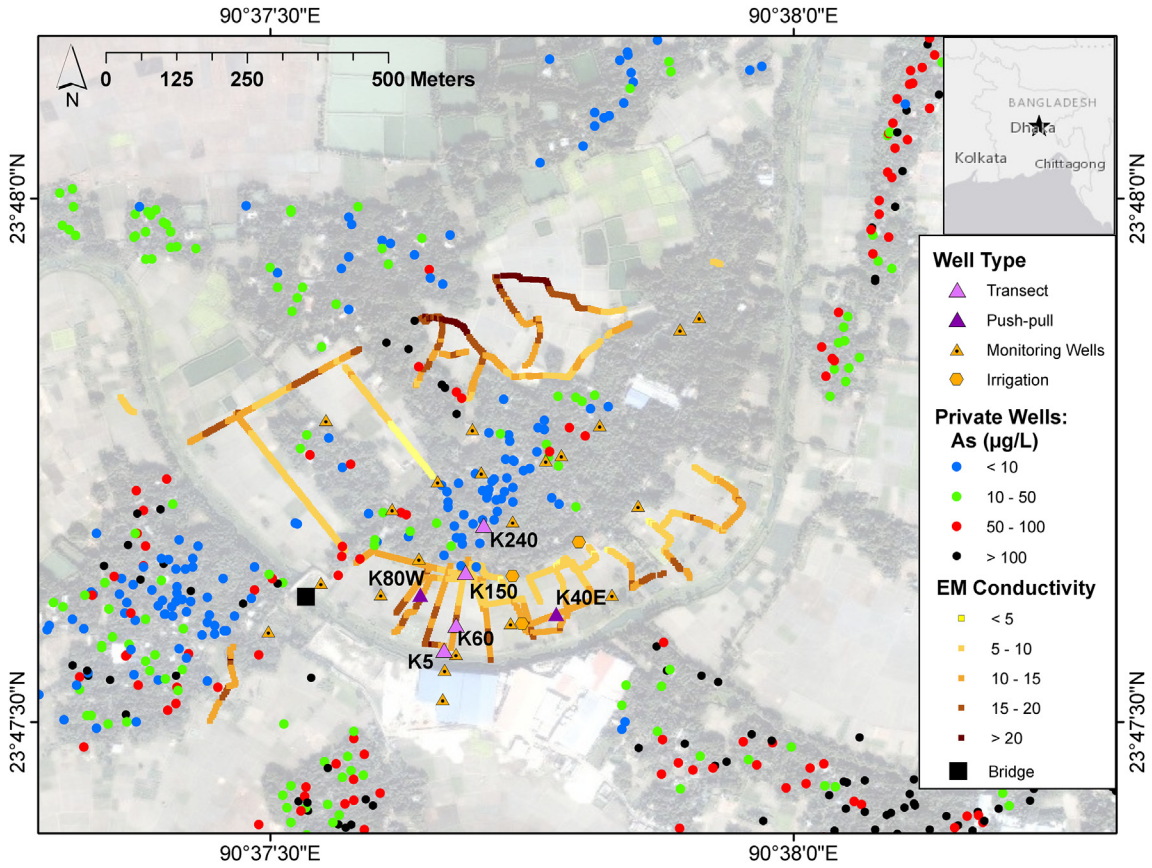

Fig. 1. Site map with private well data and EM survey. A satellite image of the study area is shown; the village is located under the tree cover and the stream crosses the southern portion of the image. 24 well locations are shown and differentiated by their use. Light purple triangles show multi-well nests with up to 5 wells, screened at 7, 10, 15, 20 and 30 m. Dark purple triangles show wells locations were the push–pull experiments were conducted. Orange triangles show single well location where groundwater samples were collected and water levels were measured. Results of the EM survey are shown (EM conductivity reported in mS/m). Arsenic concentrations measured in private wells are shown in colored circles, ranging from blue for low As (<10 µg/L) to black for high As (>100 µg/L) wells. (For interpretation of the references to color in this figure legend, the reader is referred to the web version of this article.)

2009. All water levels are reported relative to the base of the concrete utility pole in the village. Pressure transducer data were corrected for barometric pressure changes, as recorded by a pressure transducer in the village, to determine the water height above the transducers.

2.2.4. Water analyses

Groundwater As, Fe, Mn, P, and S and major ion concentrations were measured by high-resolution inductively coupled plasma mass spectrometry (HR ICP-MS) and has a precision of ±3% (1σ, Cheng et al., 2004). Anion concentrations were measured by ion chromatography (IC) using a DIONEX-500 IC system, following the standard protocol of EPA method 300. Methane concentrations were measured on samples collected in 50 mL glass crimp vials using blue butyl rubber septa (Bellco) with no headspace and poisoned with 0.1 mL of saturated $HgCl_2$ solution (Fisher Scientific) to prevent degradation. The samples were analyzed approximately one month after collection by introducing an N_2 gas headspace and letting the water reequilibrate with the headspace. The re-equilibrated headspace was then analyzed by gas chromatography with a flame ionization detector (FID). As(III) concentrations were measured in select samples using differential pulse cathodic stripping voltammetry (DPCSV) using an Eco Chemie Autolab voltammeter and a Metrohm 663 VA electrode stand (Brinkmann Instruments) (He et al., 2004; Jung and Zheng, 2006).

Stable water isotope samples were collected in 60 mL glass bottles with polyseal caps from all shallow (<15 m) wells in March 2008 and the deeper wells (20 and 30 m depth) in March 2009. These samples were analyzed at the Environmental Isotope Laboratory of the University of Waterloo with a precision of 0.1‰ ($\delta^{18}O$) and 1‰ ($\delta^{2}H$). Groundwater for radiocarbon analysis was collected in 250 mL glass bottles with polyseal caps and was poisoned with 0.2 mL of saturated $HgCl_2$.

2.2.5. Groundwater dating

Samples for ^{3}H were collected in 125 mL glass bottles with polyseal caps, while samples for ^{3}He were collected in 16 cm long, 1-cm- OD copper tubes (volume approximately 16 mL) crimped sealed on the ends with stainless steel clamps (Weiss, 1968). Analysis of ^{3}H in groundwater was performed using the ^{3}He in-growth technique (Bayer et al., 1989; Clarke et al., 1976; Ludin et al., 1998). For samples collected in 2007, the full suite of noble gases were measured by mass spectrometry (Stute et al., 1995), while only He and Ne measurements were performed on the samples collected in 2008 and 2009, also by mass spectrometry (Ludin et al., 1998). The precision of the ^{3}H measurements is ±0.05 at 1.0 TU and the detection limit is 0.05 TU. The precision of noble gas measurements is typically <± 2% (standard error) and the precision of He and Ne only measurements 0.5–1%. Analyses of $^{13}C/^{12}C$ and $^{14}C/^{12}C$ in dissolved inorganic carbon (DIC) were performed at the NOSAMS facility at Woods Hole Oceanographic Institution following standard protocols with a precision of 0.1%

Please cite this article in press as: Radloff, K.A., et al., Reversible adsorption and flushing of arsenic in a shallow, Holocene aquifer of Bangladesh, Applied Geochemistry (2016), http://dx.doi.org/10.1016/j.apgeochem.2015.11.003

(Elder et al., 1998).

2.3. Sediment collection and analysis

2.3.1. Sediment collection

Intact sediment cores were recovered at regular intervals from the surface until approximately 15 m depth within a few meters of monitoring nests K240, K150 and K60. The traditional sludger method (Horneman et al., 2004) created a borehole to a specified depth and a manual push soil corer (AMS 424.45) was then used to recover a core from the bottom of the borehole. The top few centimeters of each core were discarded to ensure that only undisturbed material was analyzed. At greater depths, core recovery was poor and drill cuttings were therefore collected instead. The drill cuttings are biased towards the larger grain sizes, as some of the clay and silt particles are removed in the drilling process (Horneman et al., 2004). Needle sampling was also used to collect groundwater and sediment slurries from several depths to compare with the core and cuttings (van Geen et al., 2004). Sediment collected from all methods were used to characterize the sediment, but only cores and cuttings were used in the adsorption experiments.

2.3.2. Field measurements

Drilling logs recorded during the installation of the 24 well nests provided a physical description of the sediment lithology of the shallow aquifer. Sediment color was quantified on the basis of diffuse reflectance spectra at about half of the well locations and at nine locations along the northern stream bank. The slope of the diffuse spectral reflectance of the sediment between 530 and 520 nm, reported in units of percent reflectance per 10 nm (%/10 nm) and referred to here as ΔR without units, was used as an indication of Fe speciation in the solid phase (Horneman et al., 2004; van Geen et al., 2006). The reflectance of the drill cuttings was measured every 1.5 m from the surface to the lower (35 m depth) clay layer.

2.3.3. Sediment extractions

Three separate extractions in (a) water, (b) 1M phosphate and (c) 1.2N hot HCl were performed on the cores, needle samples, and drill cuttings within one day of collection in the field to target readily desorbed As, adsorbed As and As associated with less crystalline Fe oxyhydroxides, respectively. Prior to extraction, samples were stored in the sampling container (plastic core liner or needle sampling tube) in air tight mylar bags with oxygen adsorbents (Sorbent Systems) to minimize oxidation. Sediment samples were well mixed before aliquots were taken for each extraction. For (a) water extraction, ~1 g of wet sediment was mixed with 10 mL of distilled water that had been bubbled with N_2 for 1 h and was then crimped sealed in glass bottles. The water extracts were collected 31 days later by drawing the water from the serum bottles using a syringe and filtered immediately. Some solutions were also passed through Meng et al. (2001) columns for As speciation. For (b) phosphate extractions, ~1 g of wet sediment was mixed with 10 mL of a 1 M sodium phosphate solution with 0.1 M of L-ascorbic acid and shaken for 24 h, after which the solution was passed through a 0.45 μm syringe filter (Jung and Zheng, 2006; Keon et al., 2001). For (c) HCl extractions, ~1 g of wet sediment was mixed with 10 mL of 1.2 N HCl (Optima) and warmed to 100° C for 1 h, after which the solution was allowed to settle and a portion of the supernatant was collected. Arsenic concentrations in all three extraction types were analyzed by HR ICP-MS following a protocol similar to the one used for groundwater. Iron speciation of the sediment was determined by analyzing the HCl extraction using the ferrozine method (Horneman et al., 2004).

2.3.4. Bulk sediment analyses

Sediment cores were collected in 5 locations for detailed grain size analysis and XRF analysis. Using approximately 30 g of sediment, the coarse fraction (sand) analysis was completed following a modified version of the USGS East Coast Sediment Analysis Procedures to separate the sediment into three size fractions: >150 μm, 63–150 μm, and <63 μm (Poppe et al., 2000). Two handheld X-ray fluorescence devices (Innov-X Systems Alpha model with a Hewlett–Packard iPAQ PocketPC and an Innov-X Delta Premium for a subset of samples) were used for analyzing the bulk sediment composition. With the Alpha instrument, measurements were collected using the 60-s standard test and a 30–60-s light elements test in soil mode. Bulk concentration of As were measured using the more sensitive Delta Premium instrument for 300 s. Standardization of the instruments was checked with two USGS or NIST soil reference samples approximately once every twelve measurements.

2.3.5. As speciation by X-ray absorption spectroscopy (XAS)

Synchrotron X-ray absorption spectroscopy (XAS) for As was performed on beamline 11–2 at the Stanford Synchrotron Radiation Laboratory in California using sediment samples preserved in glycerol. Arsenic XANES spectra were collected using the protocol described in Jung et al. 2012. All data averaging, normalization, and linear combination fitting was done with SIXPack software (Webb, 2005). Arsenic XANES fits were performed on normalized spectra. Arsenate and arsenite adsorbed on ferrihydrite (100 g As/kg ferrihydrite, pH 7) were used to represent adsorbed As(V) and As(III), and orpiment (As_2S_3) was used to model arsenic sulfides. Arsenopyrite (FeAsS), which contains As(-I), was also used in fitting but was not required to fit any spectra. The estimated errors in least-squares fitting are determined using SixPack software, and were determined to be ~3% for the As XANES fits.

2.4. Batch adsorption experiments

2.4.1. Preparation

Batch As adsorption experiments were conducted within a day of collecting groundwater and sediment. Groundwater was collected into 150-mL glass serum bottles with no headspace and was allowed to over flow into a bucket, before capping with gas impermeable blue butyl rubber septa (Bellco) and crimp sealed. Sediment was stored in air-tight mylar bags with oxygen adsorbents (Sorbent Systems). The batch samples were mixed in a glove bag (Sigma Aldrich Z555525), which was flushed with ultra-high purity nitrogen gas and monitored with an oxygen indicator strip (Becton Dickinson) to maintain close to anaerobic conditions (less than 1% O_2). Sediment was removed from the cores in the glove bag and thoroughly mixed in a re-sealable bag before dispensing 4–6 g of sediment into individual glass vials. Then 11 mL of groundwater was added to the vials and were capped with butyl rubber septa and crimp sealed while still in the glove bag. A range of volumes of an As(III) spike (1000 mg/L) were added to samples from all depths to increase the As concentration up to 15,500 μg/L, while an As(V) spike (1000 mg/L) was added to samples taken from 7 to 12 m only. One sample from 7 to 12 m, at each location, also received an addition of phosphate (approximately 4000 μg/L P) and no As addition. The spike solutions of 1000 mg/L As(III), As(V) and P were freshly prepared using reagent grade $NaAsO_2$, $NaHAsO_4 \cdot 7H_2O$ and $NaH_2PO_4 \cdot 2H_2O$, respectively.

2.4.2. Water and sediment analyses

After 31 days, groundwater from the adsorption experiments was sampled through the septum with a syringe to prevent exposure to oxygen and filtered immediately through a 0.45 μm syringe

Please cite this article in press as: Radloff, K.A., et al., Reversible adsorption and flushing of arsenic in a shallow, Holocene aquifer of Bangladesh, Applied Geochemistry (2016), http://dx.doi.org/10.1016/j.apgeochem.2015.11.003

filter for analysis by ICP-MS. As(III) concentrations in the adsorption experiments were determined using Meng et al. (2001) columns as well as differential pulse cathodic stripping voltammetry (DPCSV) using an Eco Chemie Autolab voltammeter and a Metrohm 663 VA electrode stand (Brinkmann Instruments) (He et al., 2004; Jung and Zheng, 2006). The sediment from the batch adsorption experiments underwent a sequential extraction to remove the sorbed As. First, 10 mL of the phosphate solution was added to the sediment in the batch vials, crimp sealed and shaken for 24 h. Next, the sediment was moved to larger vials with 50 mL of 1.2 N HCl (Optima) and warmed to 60° C for 24 h, but not shaken. The supernatants from these two extractions were analyzed for As content only.

2.5. Push-pull experiments

2.5.1. Preparation and sampling

The push–pull tests were conducted at two well nests, K40E and K80W (Fig. 1). Four experiments lowered the groundwater As concentration surrounding the well and an additional experiment injected higher As groundwater into a well with less As (Table 1). Each experiment required two wells; one functioned as the source and the other well received groundwater. Bromide was added as a conservative tracer to assess dilution and was dynamically mixed with the source water as it was pumped from the source well directly into the receiving well. The source well was pumped with a locally-available irrigation pump and a high-pressure gradient piston pump (Cole–Parmer) was used to introduce the concentrated Br solution into the flow from the irrigation pump. Approximately 14 L/min of source water was mixed in-line with 2 mL/min of the concentrated solution for an injected Br concentration between 50 and 60 mg/L. Approximately 1000 L of the modified groundwater was then immediately injected into the receiving well. Groundwater samples were collected over the following 15 days and monitored for bromide and alkalinity in the field. Each experiment is referred to by the name of the receiving well.

Three desorption tests were performed at K40E where low As groundwater (7 μg/L) from a well screened in a deeper aquifer (at 45 m depth) was injected into shallow wells screened at 7, 10 and 15 m, with groundwater As concentrations between 200 and 400 μg/L. In the K40E − 7 m test, 1005 L of groundwater with 7 μg/L of As and 56.0 mg/L Br was added to a well with an initial groundwater As concentration of 233 μg/L. The K40E − 10 m test added 1034 L of the same groundwater with 50.9 mg/L of Br into a well with 343 μg/L of As, while K40E − 15 m test added 812 L of water with 62.6 mg/L of Br into a well with 412 μg/L of As. The injection rate was slower for the K40E − 15 m test compared to the other experiment, with the source water entering at 6 L/min and the tracer added at 1 mL/min.

Two tests were performed at K80W using three wells screened in the shallow aquifer (screened at 7, 10 and 15 m, respectively). The only adsorption test that was conducted as part of this study injected 1012 L of water from K80W − 15 m with 204 μg/L of As and 58.4 mg/L of Br into K80W − 7 m with an initial groundwater As concentration of 71 μg/L and is referred to hereon as the K80W − 7 m test. Subsequently, a desorption test injected 1010 L of water from 10 m depth with 97 μg/L of As and 53.8 mg/L of Br into the well at 15 m with an initial groundwater As concentration of 204 μg/L, and is referred to as the K80W − 15 m test.

2.5.2. Modeling

Analysis of the push–pull experiments requires a simple box model to address both the spatial distribution and kinetic limitations of adsorption in the aquifer; the same approach is described in Radloff et al. (2011). This model assumes homogenous plug flow during injection (push) and the step-wise withdrawal (pull). Only samples moderately affected by mixing, as indicated by $Br/Br_0 > 0.7$, were used for model fitting. Adsorption was modeled as reversible, kinetically-limited Langmuir sorption.

The box model was used to evaluate two potential adsorption scenarios. The first and simplest adsorption scenario, also known as the single porosity model, assumes that all adsorption sites are equally accessible. The second scenario sets the Langmuir adsorption constant, K, to the distribution coefficient (K_d) derived from the batch adsorption experiments and assumes two types of adsorption sites with different accessibility, but the same distribution partitioning (Wood et al., 1990; Harvey and Gorelick, 2000; Hellerich et al., 2003). Rapid adsorption occurs on one type of site and diffusion limits the rate of adsorption onto the second type of site. The fraction of rapidly adsorbing sites (x_f), the adsorption constant (K), the adsorption rate constant (k_f), and the diffusion rate (k_{diff}) are all determined by fitting the undiluted samples from all five experiments to a single set of parameters. The best model fit was determined by minimizing the sum of the squared residuals between modeled and measured groundwater As concentrations.

2.6. Models of groundwater age and sediment flushing

2.6.1. Groundwater age profile in a simple aquifer

The idealized Vogel model for a homogeneous aquifer presented by Schlosser et al. (1989) is used to estimate vertical flow velocities from the vertical profiles of groundwater ages derived from ^3H–^3He data. The model predicts a logarithmic increase in groundwater ages with depth that is inversely proportional to the rate of recharge and the groundwater age at depth z is described using:

$$t(z) = \frac{z_{max}}{v_0} * \ln\left(\frac{z_{max}}{z_{max} - z}\right) \quad (1)$$

where v_0 is the vertical flow velocity and z_{max} is the thickness of the aquifer, which is assumed to be constant. The vertical flow velocity

Table 1
Groundwater properties of push–pull wells. Dissolved As, Fe, P, SO_4, Mn and pH are reported for the wells used in the push–pull experiment. As concentrations at 400 h and 2 months after the push-phase are also included.

Well	Purpose	Depth m	As ug/L	Fe mg/L	P mg/L	SO_4 mg/L	Mn mg/L	pH	As after experiment	
									~400 h	~2months
K40E − 7 m	Recv. Well	8	233	12.0	0.9	0.3	3.1	6.6	159	207
K40E − 10 m	Recv. Well	11	343	8.7	1.1	0.1	0.7	6.7	218	310
K40E − 15 m	Recv. Well	16	412	8.7	0.9	0.2	0.6	6.8	348	415
K40E − 45 m	Source for K40E tests	45	7	8.9	1.4	0.3	0.1	6.7		
K80W − 7 m	Recv. Well	8	71	1.2	0.2	2.2	3.4	6.7	102	89
K80W − 10 m	Source to K80W − 15 m	11	97	6.7	1.1	0.2	1.3	6.7		94
K80W − 15 m	Recv. Well, Source to K80W − 7 m	17	204	8.8	0.7	0.2	3.1	6.9	183	217

Please cite this article in press as: Radloff, K.A., et al., Reversible adsorption and flushing of arsenic in a shallow, Holocene aquifer of Bangladesh, Applied Geochemistry (2016), http://dx.doi.org/10.1016/j.apgeochem.2015.11.003

is simply the recharge rate divided by the porosity and is also assumed to be constant.

Assuming a uniform rate of recharge of a two-dimensional aquifer, the model predicts that the profile of groundwater age is independent of its location within a two-dimensional aquifer; thus the vertical age profile is constant. Using this simplified approach, knowledge of specific flowpaths, and the specific horizontal and vertical velocities associated with them, is not needed. Thus, the groundwater age can be used to approximate the extent of flushing without specific knowledge of the flowpath.

2.6.2. Advection dispersion model

van Geen et al. (2008) used a simple model to predict the impact of gradually flushing a shallow aquifer of its original content of exchangeable As by recharge by water without As. We use the same model here to estimate how the relationship between groundwater As concentrations and groundwater age could evolve over geologic time due to flushing. Using the same one-dimensional advection dispersion model, the relationship between groundwater age and As concentration can be evaluated for any K_d, which are converted to retardation factors, R, using the aquifer bulk density (2.65 g/cm^3) and porosity (0.3). The model solution (from van Genuchten and Alves, 1982) calculates the groundwater As concentration at a given distance along the flowpath (x) at a specified time (t) since flushing began assuming that the recharging water contains no As and is:

$$C(x,t) = C_i\left[1 - \frac{1}{2}erfc\frac{(Rx-vt)}{2(DRt)^{\frac{1}{2}}} + \frac{1}{2}\exp\left(\frac{vx}{D}\right)erfc\frac{(Rx+vt)}{2(DRt)^{\frac{1}{2}}}\right] \quad (2)$$

where C_i is the initial groundwater As concentration, v is the advection velocity, and D is the hydraulic dispersion coefficient. The C_i was set to 1000 μg/L as an upper limit to what has been observed in Bangladesh. A new aspect of the modeling is that the velocity and flowpath distance (x) were estimated at specific depths in the aquifer using the estimated vertical flow velocity derived for this site using the model of Vogel described by Schlosser et al. (1989). The scaling of v and x is proportional using the Vogel model, therefore the model solution is the same for a long, fast flowpath or a short, slow flowpath if the groundwater ages are the same. Hydraulic dispersivity was estimated to be 10 m, which is representative of sandy aquifers across spatial scales of ~100 m (Gelhar et al., 1992). Hydraulic dispersion is estimated to be the vertical flow velocity multiplied by the dispersivity. Groundwater As concentration were predicted over a range of years after flushing began and for a range of distribution coefficients.

3. Results

3.1. Water levels

The hydrology of the site is dominated by the monsoon that induces a nearly 5 m rise in hydraulic head and submerges almost half of the study area for several months each year (Fig. 2). Changes in groundwater levels typically lag behind the stream, in both the rising and falling phases. Groundwater levels are lower than the stream level at the beginning of the dry season (December) and are drawn even lower due to irrigation pumping. Stream levels rise faster than groundwater levels in April and May and reach their maximum difference of 1 m. Flood water arrives in July and equalize stream and groundwater levels. Most of the agricultural fields at Site K are submerged while the village remains above the flood water. As the flood water begins to recede in October, groundwater levels remain higher than stream levels until the start of the dry season. In the dry season, the stream is frequently dammed to form ponds for aquaculture and is largely stagnant. Net flow direction at the site was estimated using manual measurements made biweekly in ten wells located along the transect from K240 to the stream. The lowest annual average water level was recorded in the village and water levels increased towards the stream (Table 2, Supplementary Material Figure A1.1). The implication is that net flow under current conditions is directed from the stream towards the village instead of the anticipated opposite direction. Biweekly water levels measured in the wells located on the other side of the stream mirror the main transect; they are a similar amount above or below the stream water levels at the same times of year (Supplementary Material Figure A1.3). This indicates that the stream hydraulically separates the groundwater on either side at all times of the year.

3.2. Groundwater ages

The age of groundwater relative to recharge in the study area was determined on the basis of ^{3}H and ^{3}He concentrations for a total of 33 wells (Fig. 1). All wells screened at less than 20 m depth contained detectable ^{3}H, an unambiguous indication of recharge since the input reached a maximum in the 1950s and 1960s due to atmospheric testing of nuclear weapons. Tritium was also detected in some wells in the 20–30 m depth range, primarily those within and closest to the village (Supplementary Material, Table A2.1). With the exception of two samples, groundwater ages calculated from paired ^{3}H and ^{3}He measurements are consistent with the original content of ^{3}H (measured in TU) of water derived from these measurements and a simple model of ^{3}H input based on the historical record of tritium content in precipitation in Asia, indicating that little mixing is occurring (Stute et al., 2007 and Supplementary Material Figure A2.2).

The ^{3}H–^{3}He data show that groundwater from wells within the village is particularly young (<5 yr). At the other end of the spectrum, the oldest (~35 yr) groundwater containing ^{3}H is located primarily near the stream both on and off the main transect. The groundwater in two shallow wells on the other side of the stream (KW15 and KW32) is younger and consistent with the observation from the water levels that the stream is a hydrologic boundary (Supplementary Material Figure A2.1). Vertical profiles in the northern portion of the transect show an increase in age with depth and towards the stream (Fig. 3B). At K240, K150, and K60, the age of groundwater is between 1 and 12 yr in the 7–10 m depth range and converges to 30–35 yr at ~20 m depth. Groundwater ages are more homogeneous and average 30–40 yr at K5 and K40E in the southern portion of the aquifer. The ^{14}C content of DIC, reported in FMC (fraction modern carbon), is lowest in the deeper wells located closed to the stream (Supplementary Material, A2.2). In five wells, ^{3}H–^{3}He data alone cannot provide an estimated age.

The presence of younger groundwater in the village and fields and older groundwater closer to the stream indicate long-term flow from the village towards the stream, as anticipated based on the topography of the site but opposite to the direction indicated by recent water-level measurements. The presence of younger groundwater at K150 than K240 at 10 and 15 m suggests that the original assumption that water flows in the north-south direction from K240 to K150 was also incorrect.

3.3. Groundwater chemistry

The composition of groundwater was measured in March 2007, 2008 and 2009 in the 25 monitoring wells at 6 locations along the transect. By and large, the composition of groundwater did not vary substantially from one sampling occasion to the next (Supplementary Material, Figure A3.2). Results from the most

Please cite this article in press as: Radloff, K.A., et al., Reversible adsorption and flushing of arsenic in a shallow, Holocene aquifer of Bangladesh, Applied Geochemistry (2016), http://dx.doi.org/10.1016/j.apgeochem.2015.11.003

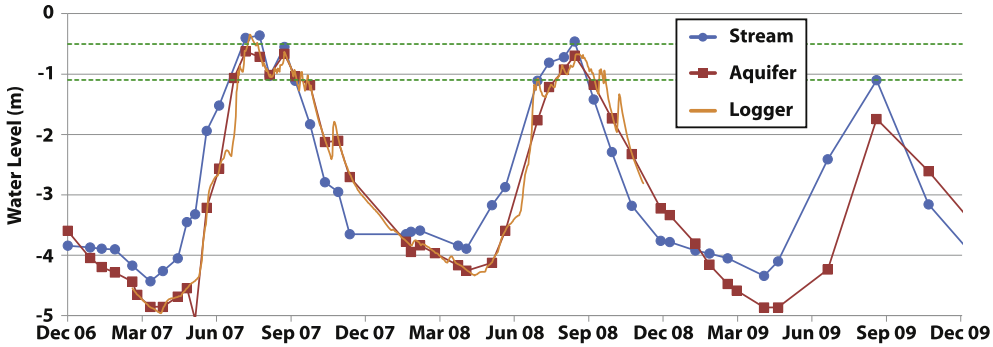

Fig. 2. Seasonal hydrograph. Biweekly water levels were measured from December 2006 until June 2009 and then reduced in frequency to every 2 months. Data shown is from the bridge monitoring location (in blue) and K240 (in red). Water levels in the aquifer (at K240) were also recorded every 20 min with a pressure transducer (shown in orange). Dashed green lines indicate relative elevation of the fields. (For interpretation of the references to color in this figure legend, the reader is referred to the web version of this article.)

Table 2
Annual average of manually-measured water levels. Average water level determined from biweekly manual measurements collected from February 2007 to 2009. Depth of water table is reported relative to one location in the village.

Well nest	Water level (m)				
	K240	K150	K60	K5	Stream
Well depth					
7 m	−2.87	−2.83	−2.80	−2.81	−2.76
10 m	−2.87	−2.85	−2.81		
15 m	−2.87	−2.84	−2.85		

recent sampling are presented for all wells, which was March 2009 for most parameters. In wells located within the village, As levels typically remain below 50 μg/L As. At nest K240 located within southern portion of the village, groundwater As concentrations rise to nearly 100 μg/L at 15 m. Groundwater As concentrations increase further towards the stream and reach a maximum of 600 μg/L between 15 and 30 m (Fig. 3A). At shallower depths (<15 m), As concentrations as high as 400 μg/L are reached at a distance of 50 m from the stream (at K40E and K80W) but decrease to 200 μg/L at closer to it (K5). With the exception of the shallowest well at K240

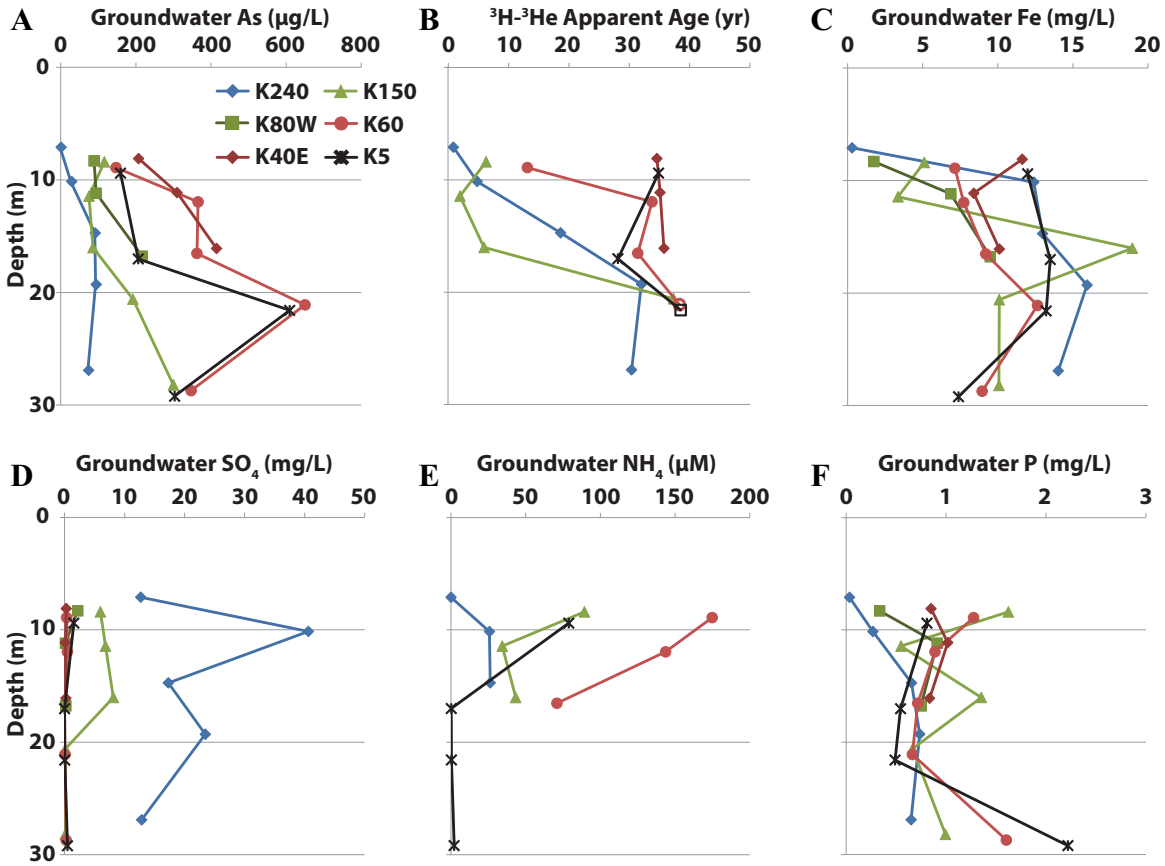

Fig. 3. Selected Groundwater Properties at Site K. Vertical profiles extending from the surface to about 30 m depth are shown for 6 locations. Color indicates distance from stream, changing from blue in the village to green to red to black near the stream bank. Six parameters are shown here: As in μg/L (A), $^{3}H-^{3}He$ Apparent Age in years (B), Fe in mg/L (C), SO_4 in mg/L (D), NH_4 in μM (E) and P in mg/L (F). Unfilled symbols in the apparent groundwater age indicate samples with evidence of groundwater mixing and are not included in later analyses. (For interpretation of the references to color in this figure legend, the reader is referred to the web version of this article.)

Please cite this article in press as: Radloff, K.A., et al., Reversible adsorption and flushing of arsenic in a shallow, Holocene aquifer of Bangladesh, Applied Geochemistry (2016), http://dx.doi.org/10.1016/j.apgeochem.2015.11.003

within the village, which contains only 2 μg/L As, over 90% of the As in groundwater is present as As(III) (Supplementary Material, Table A3.1).

Concentrations of other groundwater constituents confirm the reducing nature of the aquifer indicated by field measurement of dissolved O_2 (<0.025 mg/L) and ORP (−12 to −182 mV), even in the most rapidly recharged northern portion of the transect. Groundwater Fe concentrations generally increase with depth and range from 0.3 to 19 mg/L (Fig. 3C). Groundwater Mn concentrations range from 0.2 to 3.7 mg/L and peak between 10 and 15 m (Supplementary Material, Figure A3.1). Groundwater SO_4 concentrations were highest at K240 within the village location (40 mg/L at 10 m) and undetectable (<0.1 mg/L) near the stream (Fig. 3D). Concentrations of ammonium increase from the village to the stream, with a peak concentration of ~150 μM at 7 m depth at K60, before decreasing to 80 μM at well K5 closest to the stream (Fig. 3E). In contrast, groundwater P ranges from 0.3 to 2.2 mg/L without a systematic trend with depth or distance from the stream (Fig. 3F). Methane was detected in shallow (<15 m) wells at several locations along the transect and increase to 3.1 mg/L toward the stream (Supplementary Material, Figure A3.1). The deeper wells were not sampled for methane, however numerous bubbles were observed in groundwater from deeper samples near the stream, suggesting particularly high concentrations (20 and 30 m at K60 and K5).

Measurements of ^{2}H and ^{18}O in groundwater can distinguish different sources of recharge of the aquifer. The isotopic composition of shallow (<15 m) groundwater at Site K was comparable to that of precipitation in the area; the deuterium excess ($\delta^{2}H$-8*$\delta^{18}O$) of precipitation is approximately 10 and shallow wells had values ranging from 7.8 to 12. This indicates that much of the shallow groundwater is derived from rain or flood waters during the monsoon rather than from ponds or irrigated fields during the dry season (Supplementary Material, A3.3).

3.4. Flooded-well observations

Unusually high flood waters evidently flowed into the 10 m well at K150 on July 31, 2007 (Fig. 4A). A rapid increase in water level was recorded by the levelogger installed in this well as the stream water entered the wells through the small holes in the well cap used to ensure the well remained at barometric pressure. On August 3, 2007, the stream water intrusion was stopped after a 1.5 m GI pipe extension was installed and a sample was collected. This well was routinely sampled every 2 weeks, however, and groundwater composition changes induced by this unintended push–pull experiment were therefore documented. The time series shows that groundwater As concentrations were relatively steady and averaged 350 μg/L before the intrusion and then decreased to 18 μg/L (Fig. 4B). Groundwater Fe concentrations also decreased from 9 mg/L to 1.3 mg/L, Mn concentrations from 2.0 to 0.2 mg/L, P concentrations from 1.0 to 0.1 mg/L and major cation concentrations decreased from 3.5 to 0.9 meq/L. Conversely, sulfate concentrations increased from 0.2 mg/L to 3.7 mg/L and then to 4.9 mg/L, before decreasing again. Over the next 10 weeks, concentrations of all groundwater constituents gradually returned to levels recorded before the perturbation. A similar observation was also made at the 7 m well at KW16, which also had a levelogger installed. However only samples collected every two months are available for this well (Supplementary Material, Figure A3.2).

3.5. Sediment chemistry

The shallowest depth of the sandy portion of the aquifer, defined here by a proportion of sand in sediment cores >50%, ranges from 5 to 9 m along the transect (Fig. 5A). The silty-clay layer that caps the aquifer thickens and becomes more dominated by clay away from the village and eventually extends to 10 m depth near the stream (Supplementary Material, Figure A4.3). Bulk concentrations of Fe in aquifer sands measured by XRF vary from 10 to 35 g/kg without showing any systematic spatial pattern (Fig. 5B). The ratio of Fe(II) to total Fe in the HCl-extractable fraction of the aquifer sands averages 0.7 ± 0.1, with values < 0.5 recorded in only a few sandy intervals. In the surficial clay and silt layer, several values < 0.25 were measured at K240 and K150 (Fig. 5C). These patterns are broadly consistent with reflectance data obtained on fresh cuttings showing that Fe oxides are reduced throughout the sandy aquifer, with the exception of a few sandy intervals <10 m deep at K240 (Supplementary Material, Figure A4.1).

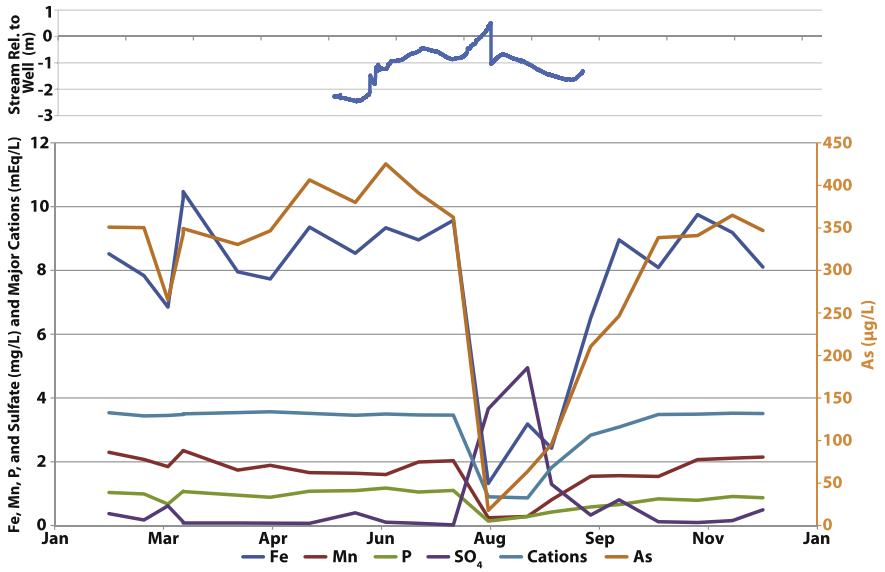

Fig. 4. Flood Water Perturbation. Unusually high flood waters (shown as stream height relative to the well) breached the well casing at K60–10 m resulting in floodwater entering the wells on July 31, 2007 the next sample was collected on August 3rd and a 1.5 m extension pipe was added to the well to prevent further intrusion. Groundwater concentrations of As, Fe, Mn, P and the major cations all decreased, while sulfate concentrations increased over this time. Concentrations returned to normal 10 weeks later.

Please cite this article in press as: Radloff, K.A., et al., Reversible adsorption and flushing of arsenic in a shallow, Holocene aquifer of Bangladesh, Applied Geochemistry (2016), http://dx.doi.org/10.1016/j.apgeochem.2015.11.003

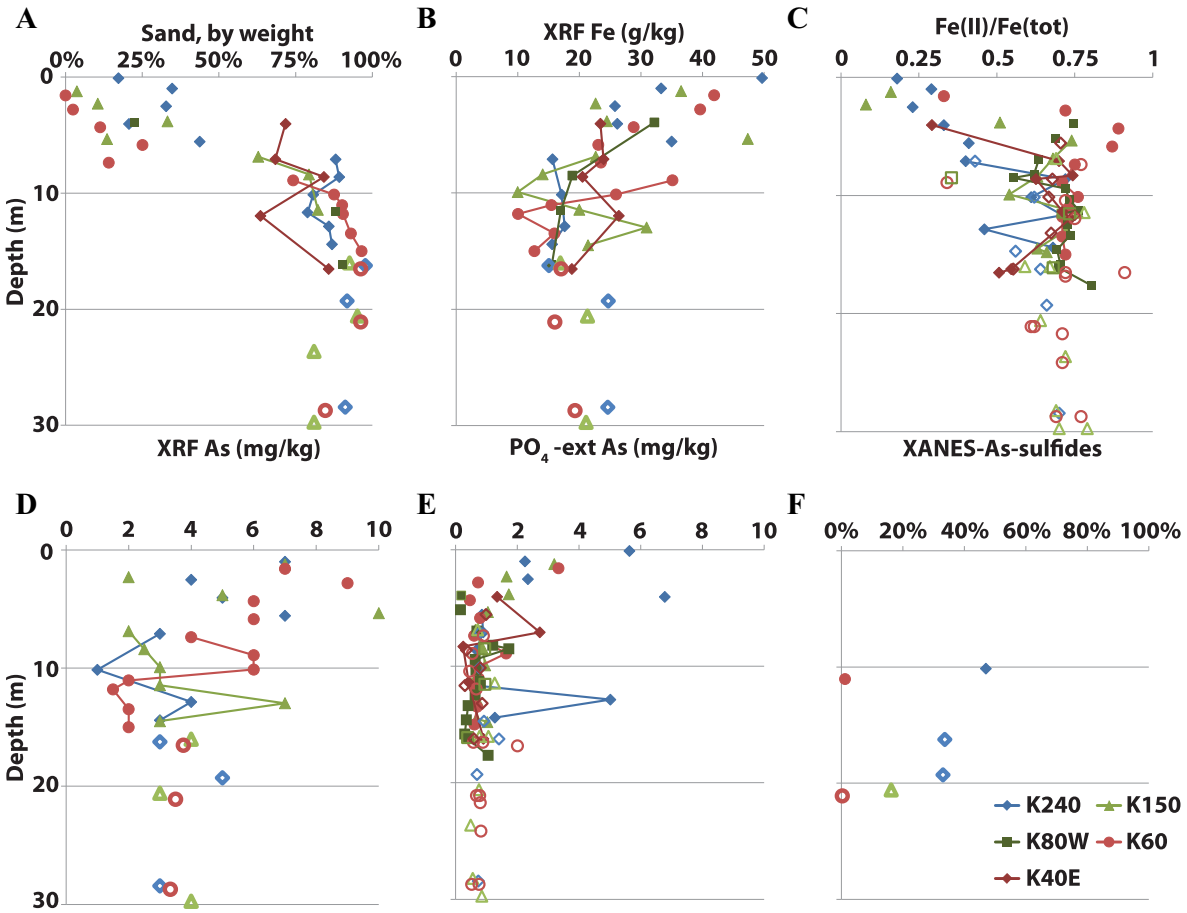

Fig. 5. Selected Sediment Properties at Site K. Vertical profiles extending from the surface to about 30 m depth are shown for 5 locations. Color indicates distance from stream, changing from blue in the village to green to red to black near the stream bank. Sediment collected by coring are shown with solid markers and are connected by a line in the sandy portion of the aquifer. Sediment collected from needle sampling or as drill cuttings are shown as open markers. Six parameters are shown here: percent sand (>150 μm, by weight) (A), Fe in g/kg by XRF (B), Fe(II)/Fe from HCl-extractions (C), As in mg/kg by XRF (D), PO_4-extractable As in mg/kg (F) and percent As-sulfides by XANES (G). (For interpretation of the references to color in this figure legend, the reader is referred to the web version of this article.)

Bulk As measurements in aquifer sands measured by XRF indicate concentrations ranging from 1 to 10 mg/kg and averaging 4.3 ± 2.3 mg/kg (Fig. 5D). With the exception of two intervals, concentrations of P-extractable As in aquifer sands are about a factor of three lower (Fig. 5E). Arsenic speciation was determined using X-ray absorption near edge spectroscopy (XANES) in six sediment samples and indicate a large fraction of As bound to sulfide at K240 (47, 34 and 33% at 10, 15 and 20 m, respectively), less at K150 (16% at 10 m), and none at K60 (10 and 20 m, Fig. 5F). With the exception of the 10 m interval at K240, about 60% of the remaining arsenic in aquifer is As(III), with As(V) not exceeding 40% anywhere (Supplementary Material, Figure A4.1).

3.6. Batch adsorption experiments

The degree to which As adsorbs to aquifer sands was quantified with batch experiments at 3 locations (K240, K150 and K60) and at 5 depths (7, 10, 15, 20, 30 m) at each location. Of the 15 sediments selected for the batch experiments, only the sands from 7 m at K240 were less reduced (Fe(II)/Fe ~ 0.4) than the other locations where Fe(II)/Fe ranged from 0.6 to 0.9. In all 15 experiments, additions of either As(III) or As(V) up to 15,500 μg/L were readily adsorbed within a month. Most samples show little to no dampening of adsorption due to site saturation. Dissolved Fe concentrations in the incubation bottles remained near ambient concentrations of 0.4–16 mg/L for the duration of the experiment (Supplementary Material, Table A5.5). This indicates the batch adsorption experiments were not compromised by the precipitation of Fe oxides, which could have occurred with a large influx of oxygen.

We use the additions up to 8000 μg/L As to infer the most representative K_ds because of the non-linear response in some of the samples for the highest addition of 15,500 μg/L. We focus on the experiments conducted with aquifer sands collected by coring at 7 and 10 m depth rather than cuttings because the grain size distribution is unbiased in the cores and the material is less likely to have been exposed to atmospheric oxygen during sample collection. In the less reduced sediment of K240-7 m, the K_d was estimated to be 2.8 L/kg, while in the 5 more reduced samples the K_d averaged 1.1 ± 0.2 L/kg. There was no discernible difference in the amount of added As(III) or As(V) adsorbed on aquifer sands from these samples (Supplementary Material, Figure A5.2). The distribution coefficients obtained for cuttings at 15, 20 and 30 m depth are comparable, ranging from 1.0 to 2.7 L/kg, and show no clear spatial trends (Table 3). Overall, the range of measured K_ds was small, with an average of 1.7 ± 0.6 L/kg for the 14 reduced intervals with Fe(II)/Fe > 0.5.

At the end of the adsorption experiments, the speciation of As was determined in groundwater, and in the P-extractable fraction. The speciation of As in groundwater was dominated (>85%) by As(III), even in the incubation bottles that were spiked with As (V).

Please cite this article in press as: Radloff, K.A., et al., Reversible adsorption and flushing of arsenic in a shallow, Holocene aquifer of Bangladesh, Applied Geochemistry (2016), http://dx.doi.org/10.1016/j.apgeochem.2015.11.003

Table 3
Measured K_ds from experiments and sediment extractions. Distribution coefficients, K_d, determined in the push–pull experiments, batch adsorption isotherms and in the phosphate and water extractions are reported in L/kg.

Push–pull tests					Model results
Single porosity					0.17
Dual porosity					1.50
Batch methods	Core material		Drill cuttings		
Adsorption isotherm	7 m	10 m	15 m	20 m	30 m
K240	2.8	1.2	2.2	2.7	1.2
K150	1.1	0.8	2.4	1.7	1.0
K60	1.4	1.0	2.0	2.1	2.4
Phosphate-extraction					
K240	539.4	33.1	15.3	8.4	10.8
K150	8.5	7.9	12.4	4.6	3.2
K60	12.4	2.3	1.4	1.3	2.6
K80W	13.6	8.2	4.9	–	–
K40E	1.2	1.4	2.2	–	–
Water-extraction					
K240	8.3	2.8	0.8	1.1	0.9
K150	0.8	1.4	1.6	1.0	0.7
K60	3.0	2.1	0.7	0.3	0.8

P-extractions at the completion of the experiment recovered 50–70% of the newly adsorbed As and was dominated by As(III) in all cases, including batches spiked with As(V) (Supplementary Material, Figure A5.3).

3.7. Push-pull experiments

The push–pull experiments were designed to observe changes in groundwater As concentrations after a perturbation of the presumed adsorptive equilibrium in the field rather with an incubation bottle containing a diluted sediment slurry. The Br tracer added during the push phase was used to calculate expected As concentrations in the absence of exchange between groundwater and aquifer sediments. In the push–pull experiments where lower As groundwater was injected, As concentrations after injection (<100 h) were higher than predicted from conservative mixing, indicating a release from the sediment (Fig. 6). For tests at K40E, groundwater with 7 μg/L of As was added to wells containing between 233 and 412 μg/L. After 24 h, groundwater concentrations ranged from 101 to 127 μg/L (31–43% of the original concentration) and after 100 h from 134 to 216 μg/L (44–58%, Fig. 6A–C). For the test at K80W- 7 m, water with 97 μg/L of As was added to a well with 204 μg/L. After 24 h, the groundwater As concentration was 136 μg/L, or 67% of the original concentration, and remained at this concentration after 100hr (Fig. 6E). The one experiment where groundwater with higher than ambient As concentrations was injected, groundwater with 204 μg/L As was pumped into a well containing 71 μg/L. By 24 h, the As concentration was 135 μg/L and after 140 h had dropped to 114 μg/L, indicating that about 70% of added As was retained in the aquifer (Fig. 6D). Groundwater Fe, SO_4 and P concentrations were also measured during the push–pull tests, even though the experiments were designed to minimize differences between source and receiving wells (Table 1). When ambient concentrations differed from the injected groundwater, the expected adsorption or desorption of F and P was observed (Supplementary Material, A6).

Using the box model of Radloff et al. (2011) and assuming all sites are equally accessible (fraction of rapid sites, x_f, = 100%), a reasonable fit to all the undiluted samples from all five experiments is obtained for K of 0.17 L/kg and an adsorption rate constant (k_f) of 0.02 hr^{-1} (Fig. 6). Predicted As concentration reach a plateau after about 100 h even though the measured concentrations continue to increase. The fit improves when more rapid adsorption is modeled to occur on a small subset of readily accessible sites and slower adsorption occurs on the remaining less accessible sites. The main reason is that the dual porosity model predicts a gradual rebound of As concentrations over the entire duration of the experiment. Under this scenario, K has to be assumed and a value of 1.5 kg/L, based on adsorption experiments for the more reduced sediments, was selected. Fitting yields a proportion of interior sites of 94% ($x_f = 6\%$) and a k_f of 1.24 hr^{-1} and a k_{diff} of 0.0006 hr^{-1}, respectively. The proportion of less accessible sites is at the high end the 70–80% range reported for less accessible sites in similar sandy aquifers (Wood et al., 1990; Harvey and Gorelick, 2000; Hellerich et al., 2003). Both the single- and dual-porosity models underestimate the decline in As concentrations attributable to adsorption following the single experiment where groundwater with a higher than ambient As concentration was injected (Fig. 6). Measured As concentrations decreased to 125 μg/L in 50 h, while the modeled concentrations were higher (~150 μg/L).

4. Discussion

4.1. Recent reversal in flow direction

Seasonal reversal of groundwater flow due to monsoon flooding has been observed in other areas of Bangladesh, Cambodia, and Vietnam where elevated As levels in shallow groundwater pose a serious health threat (Harvey et al., 2006; Benner et al., 2008; Larsen et al., 2008; van Geen et al., 2013). Benner et al. (2008) confirmed in Cambodia, where groundwater is not used for irrigation, that the net flow of water through river banks is determined by elevation and leads from groundwater aquifers into rivers in non-arid regions. This is the flow direction indicated at our study site by groundwater ages increasing from <10 to 30–40 years along the transect (Fig. 4). Water level measurements averaged over 2007–09, however, indicate net flow in the opposite direction, i.e. from the river into the aquifer (Table 2). Such reversals have been attributed elsewhere in Bangladesh and in Vietnam to large-volume pumping for irrigation and municipal water supply, respectively (Harvey et al., 2006; van Geen et al., 2013).

Transient decreases of 5–15 cm in water levels at one well located near an irrigation pump (KW16, Supplementary Material, Figure A1.5) indicate that irrigation pumping for growing rice during winter probably contributed to flow reversal at the study site. At the height of the irrigation season, the lowest water levels were recorded in the fields south of our study village where three irrigation wells are located (Supplementary Material, Figure A1.3). On average, however, the lowest water levels were observed within the village and therefore to the north of the rice fields, where there are only domestic hand-pumps. The observations therefore suggest an additional perturbation, likely to be the large cotton-spinning mill built between 2003 and 2006 on the other side of the stream, which started operating around the time when water level surveys were initiated (Supplementary Material A1.5). The factory discharges water pumped from a deeper aquifer into the stream. The discharge volume is not known, but interviews of local staff indicate that the factory pumps an estimated 400,000 L/day from the deeper aquifer (R. Mozumder, personal communication). This amount of water could have significantly raised the level of the stream during the dry season, when it does not flow and local farmers build temporary dams across it to retain water for aquaculture. The net flow reversal is therefore probably very recent and should not have affected the composition of water near the stream. This is confirmed by both the groundwater age of 35 yr and the precipitation-like stable isotope signature in the shallow wells at

Please cite this article in press as: Radloff, K.A., et al., Reversible adsorption and flushing of arsenic in a shallow, Holocene aquifer of Bangladesh, Applied Geochemistry (2016), http://dx.doi.org/10.1016/j.apgeochem.2015.11.003

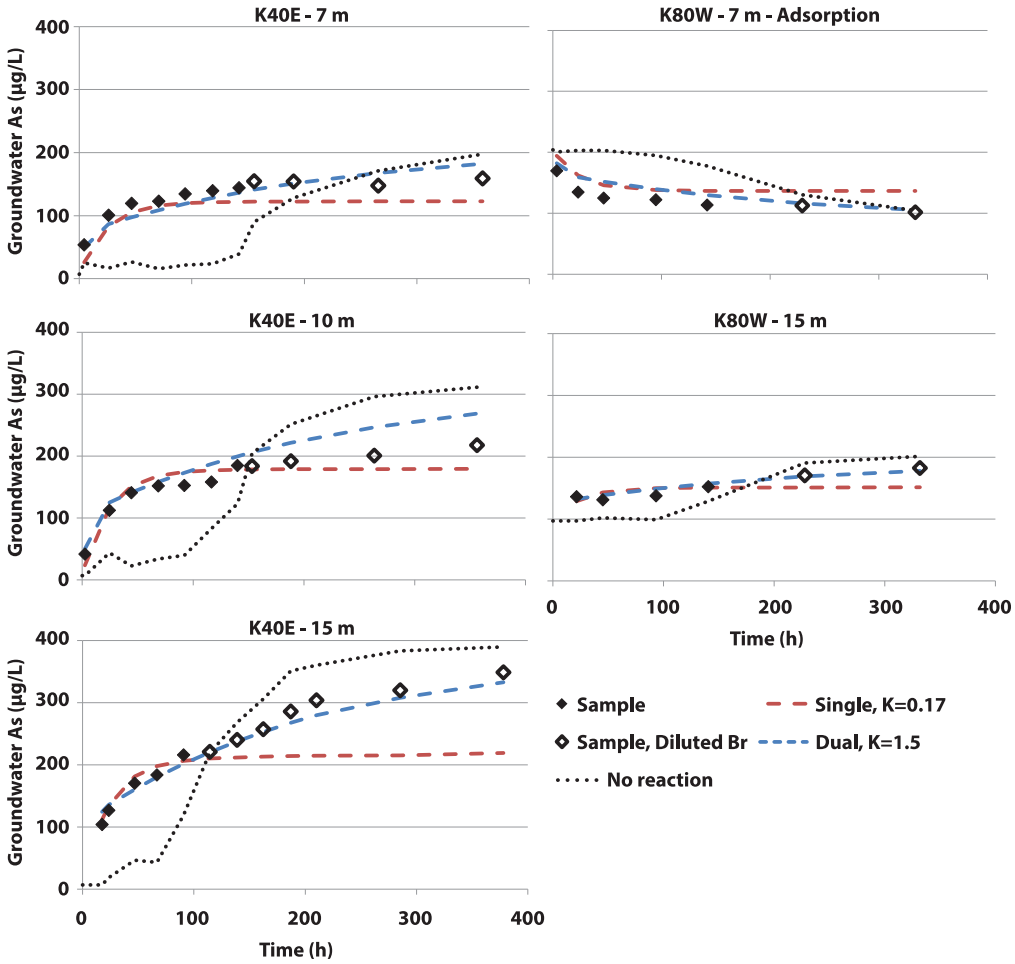

Fig. 6. Push-pull time series for As. Groundwater As concentrations are shown for the five push–pull tests. Dashed lines indicate expected concentration if there was no reaction (estimated from change in [Br]); samples with significant dilution (e.g. $[Br]/[Br]_0<0.7$) are shown as unfilled diamonds. Best fits are shown for two scenarios – a single porosity model (red dash, K = 0.17), and a dual porosity model, where K was set to 1.5 L/kg (blue dash). (For interpretation of the references to color in this figure legend, the reader is referred to the web version of this article.)

K5, which is similar to that of groundwater to the north rather than river water subject to evaporation during the dry season.

4.2. Exchange of As between groundwater and aquifer sands

A previous push–pull experiment conducted in a shallow aquifer of Bangladesh composed of grey sands, combined with selective extractions of As and Fe from sediment at the same site, has been interpreted as an indication that sediments are saturated with As once groundwater concentrations are greater than 100 µg/L (Harvey et al., 2002; Swartz et al., 2004). In contrast, As adsorption occurred readily in our adsorption push–pull experiment, in which groundwater with an As content of over 200 µg/L was injected into a well with an initial concentration of 97 µg/L of As, indicating that the sediment was not saturated. In addition, our batch experiments show that the adsorption capacity of grey sands is high and not sensitive to the redox state of As. Similar observations were reported by Jung et al. (2012) using grey riverbank sands. Itai et al. (2010) also conducted a series of batch adsorption experiments and saw no evidence of saturation for groundwater As concentrations less than 1000 µg/L. These results suggest that a linear distribution coefficient, K_d, adequately represents both adsorption and desorption of As in reducing aquifers at ambient groundwater As concentrations.

The push–pull and batch adsorption experiments, combined, constrain the distribution coefficient, K_d, for As in reducing aquifers to the 0.15–1.5 L/kg range. The high end might over-estimate the extent of As adsorption, because the sediment-water ratio used in the batch adsorption experiments was lower than in the actual aquifer (Limousin et al., 2007). Even a K_d of 1.5 L/kg is a factor of 2–3 lower than the value of predicted from 1 M P-extractions of As from grey Bangladesh sediment for the southern portion of the transect (3–15 L/kg) and results from previous studies across the Bengal Basin (van Geen et al., 2008 and Itai et al. 2010), suggesting that P-extractions over-estimate the proportion of exchangeable As in aquifer sands. The push–pull derived K_d using the single-porosity model of 0.15 L/kg provides a plausible lower bound for As adsorption. The limited range of adsorption affinity observed in both the batch and push–pull experiments suggests that the characteristics that most influence As adsorption do not vary substantially within this aquifer, even though groundwater redox conditions vary from suboxic (sulfate-reducing) to methane-generating. Adsorption of As is known be sensitive to Fe mineralogy (Jung et al. 2012, and references therein) and sediment Fe(II)-total Fe ratios were indeed comparable throughout the aquifer, with the exception of some of the shallowest intervals (Fig. 5). The observations also suggest that the degree of As adsorption remains stable soon after reducing conditions are established.

Please cite this article in press as: Radloff, K.A., et al., Reversible adsorption and flushing of arsenic in a shallow, Holocene aquifer of Bangladesh, Applied Geochemistry (2016), http://dx.doi.org/10.1016/j.apgeochem.2015.11.003

The extent of partitioning of As between aquifer sands and groundwater has significant practical implications. The kinetics of adsorption and desorption estimated from the push–pull experiments are sufficiently fast that equilibrium is expected under normal flow conditions. Assuming a K_d of 1.5 L/kg, the redistribution of As from a hot spot into a low-As area by irrigation pumping would be delayed by a factor of ~14 relative to the movement of groundwater. This delay would provide considerable protection for the large number of villagers who have relied on shallow low-As wells to lower their exposure. If instead the partitioning of As between groundwater and aquifer sands is determined by a distribution coefficient closer to 0.15 L/kg, aquifers would be flushed of their initial content of exchangeable As over time scales of decades instead of centuries, but the migration of plumes of high As concentrations would be more rapid, slowed by a retardation factor of only ~2. In addition, under intensive irrigation pumping scenarios, adsorptive equilibrium may not be reached, and therefore the effective K_d may be more similar to the lower estimate. This lower estimate is consistent with early indications of flushing and movement of As in reducing aquifers reported from West Bengal (McArthur et al., 2010).

4.3. Low As concentrations due to precipitation as arsenic-sulfide

The several-fold lower dissolved As concentration from the northern portion of the transect is not likely due to adsorptive equilibrium alone. With the exception of the shallowest, less-reduced sample from K240, the K_ds derived from the batch adsorption experiments with grey sands from within the village are not different from the values obtained in the southern portion of the transect. This uniformity contrasts with the 10-fold higher K_ds calculated from the P-extractions and the low ambient groundwater As levels in the northern portion of the transect. The simplest explanation is precipitation of As-sulfides, which was previously proposed as a mechanism for suppressing the release of As to groundwater under reducing conditions (Polizzotto et al., 2006; Lowers et al., 2007; Buschmann and Berg, 2009). The data indicate that sulfide precipitation at our study site retains considerable quantities of As, on the order of 0.4–1.7 mg/kg (based on total As estimates from XRF), and presumably limits the As available for desorption and flushing from the sediment. Within the northern portion of the transect, this mechanism is supported by the detection of As-sulfide in aquifer sands at two points along the transect where sulfate concentrations are elevated (5–50 mg/L) and the lack of As-sulfides at one location where sulfate levels are also undetectable (Fig. 5). The association also suggests that the supply of sulfur is a limiting factor for the formation of As-sulfides. High groundwater sulfate levels have been observed in both sandy, rapidly recharged areas and clay-capped, slowly recharged areas of Araihazar (Stute et al., 2007; Dhar et al., 2008; Aziz et al., 2008). Recharge may therefore not be the primary source of sulfur to groundwater. An alternative source is decaying organic matter contained in the fine-grained sediment layer (Schroth et al., 2007; Planer-Friedrich et al., 2012).

4.4. Evolution of the arsenic-depth relation with time

The estimates of adsorption equilibrium and flushing rate of the aquifer allow us to create a simple yet plausible model to predict the evolution of the vertical distribution of As in groundwater over time. In addition to the distribution coefficient, K_d, the model requires an initial concentration of exchangeable As after an aquifer becomes reducing and sands have turned grey. The value selected is somewhat arbitrary and could vary with the depositional history of the sediment. An upper limit for groundwater As concentration of 1000 μg/L As in groundwater is set by the few reports of higher concentrations in South and Southeast Asia. This amount corresponds to concentrations of 0.15–1.5 mg/kg for exchangeable As for K_d of 0.15–1.5 kg/L, respectively. The assumed initial concentration of exchangeable As, 1.5 mg/kg for the K_d of 1.5 kg/L scenario, is below the current bulk concentration of ~3 mg/kg and similar to the P-extractable concentration of 1 mg/kg at the study site (Fig. 5). Both of these concentrations are likely to overestimate the exchangeable As concentrations today but, on the other hand, could already have been substantially reduced from initial conditions by flushing.

To apply the flushing model, groundwater velocity is first estimated from the profiles of groundwater ages (Fig. 7A). Current groundwater As concentrations are then matched with modeled flushing times, starting from the time when conditions became sufficiently reducing. Assuming first a K_d of 1.5 L/kg, the profile of groundwater age and As concentrations in the southern portion of the study transect resembles predictions for a vertical flow velocity of 0.25 m/yr and a flushing time of about 500 yr (Fig. 7B). When the recharge velocity is doubled to 0.5 m/yr to match the profile of groundwater ages in the northern portion of the transect, the otherwise identical model predicts groundwater As concentrations that are considerably higher than most of those observed. Assuming instead a K_d of 0.15 L/kg, observed As profiles across the entire transect are more closely matched by the model if a much shorter flushing time of 50 yr is assumed (Fig. 7C). Sediment dating of the site by Optically Stimulated Luminescence (B. Weinman, unpublished) indicates that the shallow aquifer was deposited 4000 years ago in the village (at K240) and was deposited only 400 yrs ago closer to the stream (at K60). However, the available dates cannot rule out the possibility that the upper 7 m of the aquifer was deposited only 50 instead of 500 years ago and therefore do not help constrain the estimated range of K_ds.

4.5. Impact of flushing on Groundwater As elsewhere

The vertical age and As profiles from a dozen other sites across South and Southeast Asia can be used to evaluate whether the parameters estimated for the present site are more broadly relevant. Vertical flow velocities estimated for other 4 other sites in Araihazar using the Vogel model, which range from 0.7 to 5 m/yr, agree with previously estimated recharge rates of Stute et al. (2007) that do not consider aquifer thickness (Table 4, Fig. 7D). At 4 sites in the Red River basin of Vietnam, reported vertical flow velocities derived from ^3H–^3He dating, ranging from 0.25 to 0.5 m/yr, are consistent with the profiles generated using the Vogel model (Postma et al., 2012, Table 4, Fig. 7F). The model is also applied to a few other sites in Bangladesh and West Bengal, India, where vertical flow velocities ranging from 0.5 to 2 m/yr (i.e. 0.15–0.6 m/yr recharge) have been estimated (Klump et al., 2006; McArthur et al., 2010). Finally, the flushing model is applied to a site in Cambodia where particularly slow recharge of 0.04 m/yr was derived from a groundwater flow model and could not be verified with ^3H–^3He dating (Polizzotto et al., 2008; Kocar et al., 2008; Benner et al., 2008). Model results for the additional sites in Bangladesh, West Bengal and Cambodia are reported in the Supplementary Material (Section A7).

The flushing model is used primarily to predict where groundwater As concentrations rapidly increase with depth. Even for a distribution coefficient, K_d, of 1.5 L/kg, the high recharge rates at Sites C and F in Araihazar suggest that very little time (50–75 yrs) was required to reduce concentrations to their present level (Fig. 7B); no higher As concentrations are observed within the shallow aquifer at these sites. At Sites A and B within Araihazar, the model correctly predicts a rapid increase in As with depth with

Please cite this article in press as: Radloff, K.A., et al., Reversible adsorption and flushing of arsenic in a shallow, Holocene aquifer of Bangladesh, Applied Geochemistry (2016), http://dx.doi.org/10.1016/j.apgeochem.2015.11.003

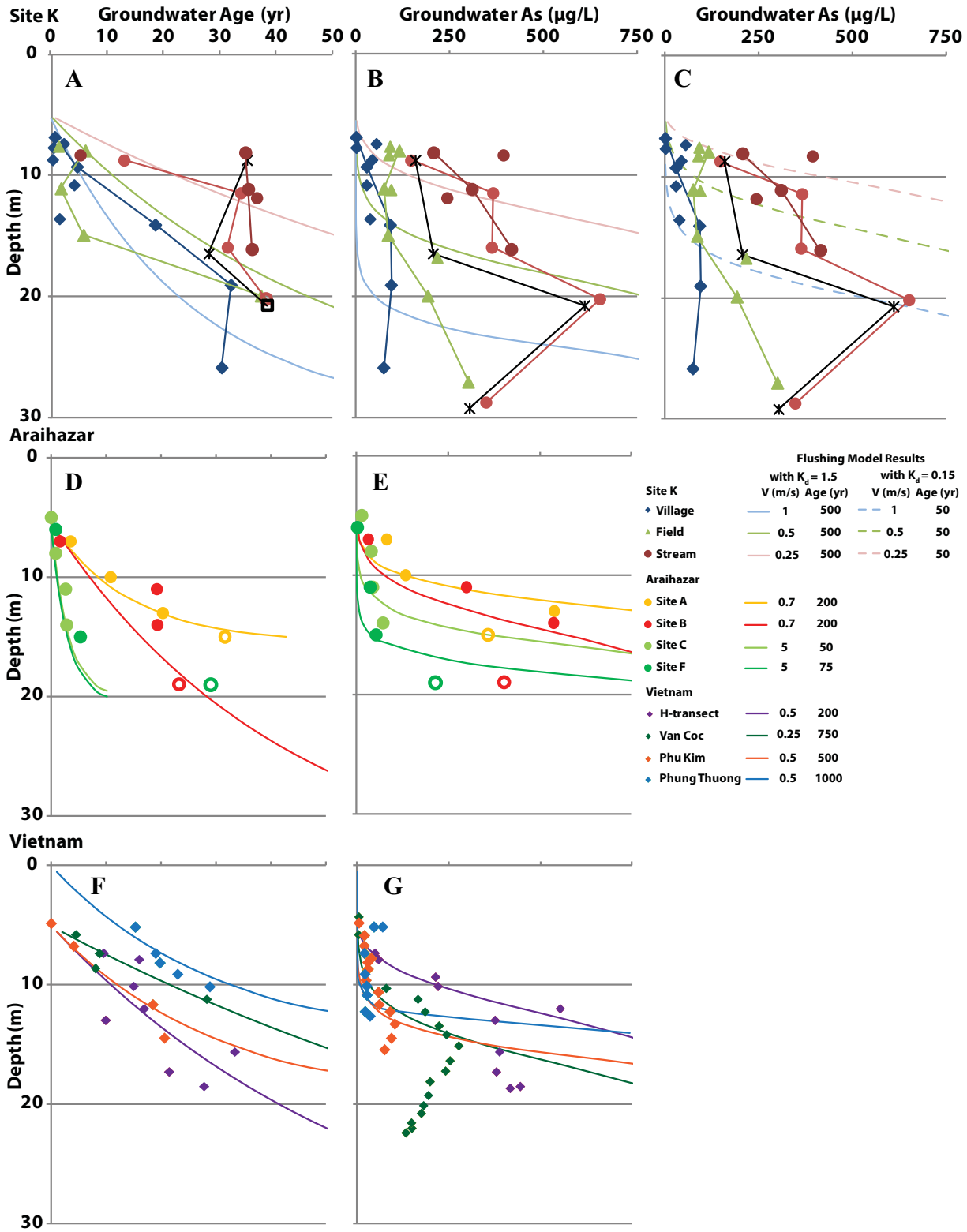

Fig. 7. Groundwater As and Age profiles with depth. Measurements and model results for Site K are shown in Panels A, B and C; for other sites in Araihazar in D and E (Stute et al. 2007); and for Vietnam in F and G (Postma et al. 2012). Measured groundwater ages and modeled age profiles based on the Vogel model are shown in A, D and F. Groundwater As concentrations and estimated concentration based on the idealized flushing model for a K_d of 1.5 L/kg are shown in B, E and G, with model results for a K_d of 0.15 L/kg shown only in panel C.

slower recharge and a flushing time of about 200 yr for K_d of 1.5 L/kg (Fig. 7E). For a K_d of 0.15 L/kg, the required flushing time would be about an order of magnitude lower, which seems unlikely given the depositional history of the area (Weinman et al., 2008).

Using again a K_d of 1.5 L/kg in the Red River basin, the model confirms that sediment deposited 500–1000 yr ago would be

Please cite this article in press as: Radloff, K.A., et al., Reversible adsorption and flushing of arsenic in a shallow, Holocene aquifer of Bangladesh, Applied Geochemistry (2016), http://dx.doi.org/10.1016/j.apgeochem.2015.11.003

Table 4
Velocity and flushing extent estimated for other sites using the idealized flushing model. The Vogel model was used to estimate vertical velocities in Araihazar. Velocities reported in Postma et al. 2012 were used, and indicated with an asterisk (*). The As depth profiles for other sites were then compared to the results of the idealized flushing model to approximate the extent of flushing.

Site	Aquifer thickness (m)	Est. Vertical velocity (m/s)	Flushing time (yr)	Reference
Araihazar, Site K	**25**	**0.25 to 1**	**500**	**This study**
Araihazar, Site A	10	0.7	200	Stute et al., 2007
Araihazar, Site B	30	0.7	200	Stute et al., 2007
Araihazar, Site C	15	5	50	Stute et al., 2007
Araihazar, Site F	15	5	75	Stute et al., 2007
Vietnam, H-transect	55	0.5*	200	Postma et al., 2012
Vietnam, Van Coc	30	0.25*	750	Postma et al., 2012
Vietnam, Phu Kim	15	0.5*	500	Postma et al., 2012
Vietnam, Phung Thuong	15	0.5*	1000	Postma et al., 2012

nearly flushed of their As content (Fig. 7G). The duration of flushing for the more recently deposited sediments at H −transect was estimated to be 200 yr (Fig. 7G) based on the observation that peak groundwater As concentrations occur between 10 and 15 m depth. These flushing times are in line with estimates of sediment ages of from 500 to 6000 yrs at these sites (Postma et al., 2012). The match with independently dated sediments suggest that the lower K_d of 0.15 L/kg is less likely for this site. Flushing times for a few other sites in the Bengal Basin range between 250 and 1000 yrs for different recharge rates. Finally, the model indicates that the groundwater As distribution and very slow rate of recharge in Cambodia require >5000 yr of flushing, which is consistent with age dating of the sediment at the site (Supplementary Material, A7). Taken together, the idealized flushing model predicts flushing times that are in line with known estimates of sediment ages across a wide range of settings for a distribution coefficient, K_d, of about 1.5 L/kg rather than the lower value inferred from the single porosity model applied to the push–pull data.

4.6. Evolution of the As-age relation over time

The idealized flushing model provides a context for revisiting the observation of Stute et al. (2007) that groundwater As concentration generally increased with groundwater age across several sites within Araihazar. According to the flushing model, differences in hydrology across sites are in principle normalized by this representation. The new data from Site K clearly indicate a more gradual increase in As concentrations with age than at the other sites in Araihazar (Fig. 8A). The scatter in the As-age relationship does not increase markedly, however, when data are added from the limited number of sites elsewhere in the Bengal Basin and the Red River delta where groundwater has been dated (Fig. 8B).

Using what appears to be the more widely applicable K_d of 1.5 L/kg, the flushing model is used to illustrate the effects of groundwater velocity and aquifer age. The results show the effect of different flow velocities on the groundwater As-age relationship is detectable but modest (Fig. 8A). Much more significant is the effect of flushing time (and therefore sediment age) (Fig. 8B). The slope of groundwater As-age relationship shifts over flushing time, such that less flushed aquifers may have high As concentrations in relatively young groundwater, while high As concentrations are only found in older groundwater in more flushed aquifers. Flushing gradually reduces the range of As concentrations across the range of groundwater ages (Fig. 8B) and deepens the location of the peak As concentration. The model cannot claim to explain all the available observations, but it indicates that a wide range of As concentration should be expected for a given groundwater age and that this variability may reflect an aquifer's age and extent of flushing.

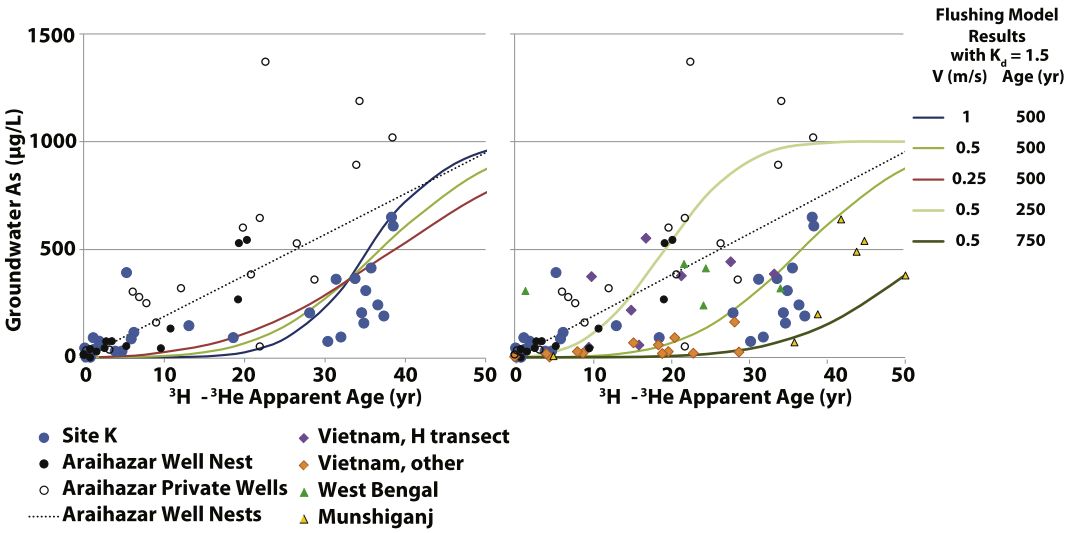

Fig. 8. Groundwater As and Age Relationship. Results from Site K and other sites in Araihazar (Stute et al., 2007) are shown in Panel A. The original observed As- age relationship (dotted line) is shown along with idealized flushing model results for various groundwater velocities using a K_d of 1.5 L/kg and a flushing extent of 500 years (colored lines). Results from other sites (Postma et al., 2012; Klump et al., 2006 and McArthur et al. 2010) are included in Panel B along with idealized flushing model results for flushing extents of 250, 500 and 750 years using a groundwater velocity of 0.5 m/yr and a K_d of 1.5 L/kg. (For interpretation of the references to color in this figure legend, the reader is referred to the web version of this article).

Please cite this article in press as: Radloff, K.A., et al., Reversible adsorption and flushing of arsenic in a shallow, Holocene aquifer of Bangladesh, Applied Geochemistry (2016), http://dx.doi.org/10.1016/j.apgeochem.2015.11.003

5. Conclusion

A number of studies from both Bangladesh and Cambodia have suggested that the release of As during Fe reduction in near surface sediments is the primary contributor to groundwater As concentrations deeper within the aquifer, with little exchange of As occurring further downstream. The push–pull tests conducted at our study site clearly demonstrate that the aquifer instead responds rapidly to perturbations in groundwater concentrations by either desorbing or adsorbing As. The tests also indicate the presence of a dispersed source of As throughout the aquifer. Adsorption modeling constrains the distribution coefficients for As to between 0.15 and 1.5 L/kg. The high end of this range is consistent with a series of batch adsorption experiments and with the estimated age of the aquifer formation based on an idealized model of As flushing. Despite its limitations, the idealized flushing model appears to be consistent with shallow groundwater As profiles elsewhere in the Bengal and Red River basins where groundwater has been dated and locations are subject to different recharge rates and extent of irrigation pumping. While external sources such as ponds, wetlands, and fine grained deposits may be important sources of As or reactive carbon at these sites, they are not necessary to explain the broad distribution of As in a way that is consistent with the range of recharge rates encountered in low-lying fluvial-deltaic aquifers.

Acknowledgments

Columbia University and the University of Dhaka's research in Araihazar has been supported since 2000 by NIEHS Superfund Basic Research Program grant NIEHS 5 P42 ES010349. Additional support for these experiments was received from Barnard College and the Earth Institute at Columbia University. The authors thank H. C. Siu for the grain size analysis (Bronx Science High School). This is Lamont-Doherty Earth Observatory contribution number 7953.

Appendix A. Supplementary data

Supplementary data related to this article can be found at http://dx.doi.org/10.1016/j.apgeochem.2015.11.003.

References

Aziz, Z., et al., 2008. Impact of local recharge on arsenic concentrations in shallow aquifers inferred from the electromagnetic conductivity of soils in Araihazar, Bangladesh. Water Resour. Res. 44 (7).

Bayer, R., et al., 1989. Performance and blank components of a mass spectrometric system for routine measurement of helium isotopes and tritium by 3He ingrowth method. Sitzungsberichte der Heidelberger Akademie der Wissenschaften, Mathematisch-naturwissenschaftliche Klasse. Jahrgang 5, 241–279.

Benner, S.G., et al., 2008. Groundwater flow in an arsenic-contaminated aquifer, Mekong Delta, Cambodia. Appl. Geochem. 23 (11), 3072–3087.

BGS/DPHE (British Geological Survey, Dept of Public Health Engineering), 2001. Arsenic Contamination of Groundwater in Bangladesh. Final Report. British Geological Survey, Dept. of Public Health Engineering, Keyworth, UK.

Buschmann, J., Berg, M., 2009. Impact of sulfate reduction on the scale of arsenic contamination in groundwater of the Mekong, bengal and Red river deltas. Appl. Geochem. 24 (7), 1278–1286.

Cheng, Z., Zheng, Y., Mortlock, R., van Geen, A., 2004. Rapid multi-element analysis of groundwater by high-resolution inductively coupled plasma mass spectrometry. Anal. Bioanal. Chem. 379 (3), 512–518.

Clarke, W.B., Jenkins, W.J., Top, Z., 1976. Determination of tritium by mass-spectrometric measurement of 3He. Int. J. Appl. Radiat. Isotopes 27 (9), 515–522.

Desbarats, A.J., Koenig, C.E.M., Pal, T., Mukherjee, P.K., Beckie, R.D., 2014. Groundwater flow dynamics and arsenic source characterization in an aquifer system of West Bengal, India. Water Resour. Res. 50, 4974–5002. http://dx.doi.org/10.1002/2013WR014034.

Dhar, R.K., Zheng, Y., Stute, M., van Geen, A., Cheng, Z., Shanewaz, M., Ahmed, K.M., 2008. Temporal variability of groundwater chemistry in shallow and deep aquifers of araihazar, Bangladesh. J. Contam. Hydrol. 99 (1–4), 97–111. http://dx.doi.org/10.1016/j.jconhyd.2008.03.007.

Elder, K.L., McNichol, A., Gagnon, A.R., 1998. Reproducibility of seawater, inorganic and organic carbon C-14 results at NOSAMS. Radiocarbon 40 (1), 223–230.

Fendorf, S., Michael, H.A., van Geen, A., 2010. Spatial and temporal variations of groundwater arsenic in South and Southeast Asia. Science 328 (5982), 1123–1127.

Gelhar, L.W., Welty, C., Rehfeldt, K.R., 1992. A critical review of data on field-scale dispersion in aquifers. Water Resour. Res. 28, 1955–1974.

Gran, G., 1952. A new method to linearize titration curves. Analyst 77 (661–671).

Harvey, C., Gorelick, S.M., 2000. Rate-limited mass transfer or macrodispersion: which dominates plume evolution at the macrodispersion experiment (MADE) site? Water Resour. Res. 36 (3), 637–650.

Harvey, C.F., et al., 2002. Arsenic mobility and groundwater extraction in Bangladesh. Science 298 (5598), 1602–1606.

Harvey, C.F., et al., 2006. Groundwater dynamics and arsenic contamination in Bangladesh. Chem. Geol. 228 (1–3), 112–136.

He, Y., Zheng, Y., Ramnaraine, M., Locke, D.C., 2004. Differential pulse cathodic stripping voltammetric speciation of trace level inorganic arsenic compounds in natural water samples. Anal. Chim. Acta 511 (1), 55–61.

Hellerich, L.A., Oates, P.M., Johnson, C.R., Nikolaidis, N.P., Harvey, C.F., Gschwend, P.M., 2003. Bromide transport before, during, and after colloid mobilization in push-pull tests and the implications for changes in aquifer properties. Water Resour. Res. 39 (10).

Horneman, A., et al., 2004. Decoupling of as and Fe release to Bangladesh groundwater under reducing conditions. Part I: evidence from sediment profiles. Geochimica Cosmochimica Acta 68 (17), 3459–3473.

Itai, T., Takahashi, Y., Seddique, A.A., Maruoka, T., Mitamura, M., 2010. Variations in the redox state of as and Fe measured by X-ray absorption spectroscopy in aquifers of Bangladesh and their effect on as adsorption. Appl. Geochem. 25 (1), 34–47.

Jung, H.B., Bostick, B.C., Zheng, Y., 2012. Field, experimental, and modeling study of arsenic partitioning across a redox transition in a Bangladesh aquifer. Environ. Sci. Technol. 46 (3), 1388–1395.

Jung, H.B., Zheng, Y., 2006. Enhanced recovery of arsenite sorbed onto synthetic oxides by L-ascorbic acid addition to phosphate solution: calibrating a sequential leaching method for the speciation analysis of arsenic in natural samples. Water Res. 40 (11), 2168–2180.

Keon, N.E., Swartz, C.H., Brabander, D.J., Harvey, C., Hemond, H.F., 2001. Validation of an arsenic sequential extraction method for evaluating mobility in sediments. Environ. Sci. Technol. 35 (13), 2778–2784.

Klump, S., et al., 2006. Groundwater dynamics and arsenic mobilization in Bangladesh assessed using noble gases and tritium. Environ. Sci. Technol. 40 (1), 243–250.

Kocar, B.D., Polizzotto, M.L., et al., 2008. Integrated biogeochemical and hydrologic processes driving arsenic release from shallow sediments to groundwaters of the Mekong delta. Appl. Geochem. 23 (11), 3059–3071. http://dx.doi.org/10.1016/j.apgeochem.2008.06.026.

Larsen, F., et al., 2008. Controlling geological and hydrogeological processes in an arsenic contaminated aquifer on the Red river flood plain. Vietnam. Appl. Geochem. 23 (11), 3099–3115.

Limousin, G., Gaudet, J.P., et al., 2007. Sorption isotherms: a review on physical bases, modeling and measurement. Appl. Geochem. 22 (2), 249–275.

Lowers, H.A., et al., 2007. Arsenic incorporation into authigenic pyrite, bengal basin sediment. Bangladesh. Geochimica Cosmochimica Acta 71 (11), 2699–2717.

Ludin, A., Weppernig, R., Boenisch, G., Schlosser, P., 1998. Mass Spectrometric Measurement of Helium Isotopes and Tritium. Technical report no. 98-6. Lamont Doherty Earth Obs, Palisades, N.Y.

Mailloux, B.J., Trembath-Reichert, E., Cheung, J., Watson, M., Stute, M., Freyer, G.A., van Geen, A., 2013. Advection of surface-derived organic carbon fuels microbial reduction in Bangladesh groundwater. Proc. Natl. Acad. Sci. 110 (14), 5331–5335.

McArthur, J.M., et al., 2004. Natural organic matter in sedimentary basins and its relation to arsenic in anoxic ground water: the example of West Bengal and its worldwide implications. Appl. Geochem. 19 (8), 1255–1293.

McArthur, J.M., et al., 2008. How paleosols influence groundwater flow and arsenic pollution: a model from the Bengal Basin and its worldwide implication. Water Resour. Res. 44 (11).

McArthur, J.M., Banerjee, D.M., Sengupta, S., Ravenscroft, P., Klump, S., Sarkar, A., Disch, B., Kipfer, R., 2010. Migration of As, and 3H/3He ages, in groundwater from West Bengal: Implications for monitoring. Water Res. 44, 4171–4185.

Mladenov, Natalie, Zheng, Yan, Miller, Matthew P., Nemergut, Diana R., Legg, Teresa, Simone, Bailey, Hageman, Clarissa, Moshiur Rahman, M., Matin Ahmed, K., McKnight, Diane M., 2009. Dissolved organic matter sources and consequences for iron and arsenic mobilization in Bangladesh aquifers. Environ. Sci. Technol. 44 (1), 123–128.

Mladenov, N., Zheng, Y., Simone, B., Legg, T., McKnight, D., Nemergut, D., Radloff, K.A., Rahman, M.M., Ahmed, K.M., 2015. Dissolved organic matter quality in a shallow aquifer of Bangladesh: implications for arsenic mobility. Environ. Sci. Technol. http://dx.doi.org/10.1021/acs.est.5b01962 (available online only).

Meng, X.G., Korfiatis, G.P., Jing, C.Y., Christodoulatos, C., 2001. Redox transformations of arsenic and iron in water treatment sludge during aging and TCLP extraction. Environ. Sci. Technol. 35 (17), 3476–3481.

Neumann, R.B., et al., 2010. Anthropogenic influences on groundwater arsenic concentrations in Bangladesh. Nat. Geosci. 3 (1), 46–52.

Planer-Friedrich, B., Härtig, C., Lissner, H., Steinborn, J., Süß, E., Hassan, M.Q., Zahid, A., Alam, M., Merkel, B., 2012. Organic carbon mobilization in a

Bangladesh aquifer explained by seasonal monsoon-driven storativity changes. Appl. Geochem. 27, 2324–2334.
Polizzotto, M.L., et al., 2006. Solid-phases and desorption processes of arsenic within Bangladesh sediments. Chem. Geol. 228 (1–3), 97–111.
Polizzotto, M.L., Kocar, B.D., Benner, S.G., Sampson, M., Fendorf, S., 2008. Near-surface wetland sediments as a source of arsenic release to ground water in Asia. Nature 454 (7203), 505–U5.
Poppe, L.J., Hastings, P., Polloni, C., 2000. USGS East Coast Sediment Analysis: Procedures, Database and Georeferenced Displays. U.S. Geological Survey Open-File Report 00–358.
Postma, D., Larsen, F., Hue, N.T.M., Duc, M.T., Viet, P.H., Nhan, P.Q., Jessen, S., 2007. Arsenic in groundwater of the Red River floodplain, Vietnam: controlling geochemical processes and reactive transport modeling. Geochimica Cosmochimica Acta 71 (21), 5054–5071.
Postma, D., Larsen, F., Thai, N.T., Trang, P.T.K., Jakobsen, R., Nhan, P.Q., Murray, A.S., 2012. Groundwater arsenic concentrations in Vietnam controlled by sediment age. Nat. Geosci. 5 (9), 656–661.
Radloff, K.A., Zheng, Y., Michael, H.A., Stute, M., Bostick, B.C., Mihajlov, I., Van Geen, A., 2011. Arsenic migration to deep groundwater in Bangladesh influenced by adsorption and water demand. Nat. Geosci. 4 (11), 793–798.
Radloff, K.A., et al., 2008. Considerations for conducting incubations to study the mechanisms of as release in reducing groundwater aquifers. Appl. Geochem. 23 (11), 3224–3235.
Schlosser, P., Stute, M., Sonntag, C., Münnich, K.O., 1989. Tritiogenic 3 He in shallow groundwater. Earth Planet. Sci. Lett. 94 (3), 245–256.
Schroth, A.W., Bostick, B.C., Graham, M., Kaste, J.M., Mitchell, M.J., Friedland, A.J., 2007. Sulfur species behavior in soil organic matter during decomposition. J. Geophys. Res. 112, G04011. http://dx.doi.org/10.1029/2007JG000538.
Sorzano, L., 1969. Determination of ammonia in natural waters by phenol-hypochlorite method. Limnol. Oceanogr. 14, 799–801.
Stookey, L.L., 1970. Ferrozine—a new spectrophotometric reagent for iron. Anal. Chem. 42 (7), 779–781.
Stute, M., et al., 2007. Hydrological control of as concentrations in Bangladesh groundwater. Water Resour. Res. 43 (9).
Stute, M., Clark, J.F., Schlosser, P., Broecker, W.S., Bonani, G., 1995. A 30,000- yr continental paleotemperature record derived from noble gases dissolved in groundwater from the San Juan Basin, New Mexico. Quat. Res. 43 (2), 209–220.
Swartz, C.H., Blute, N.K., Badruzzman, B., Ali, A., Brabander, D., Jay, J., Harvey, C.F., 2004. Mobility of arsenic in a Bangladesh aquifer: Inferences from geochemical profiles, leaching data, and mineralogical characterization. Geochimica Cosmochimica Acta 68 (22), 4539–4557.
Van Geen, A., Zheng, Y., Versteeg, R., Stute, M., Horneman, A., Dhar, R., …, Ahmed, K.M., 2003a. Spatial variability of arsenic in 6000 tube wells in a 25 km2 area of Bangladesh. Water Resour. Res. 39 (5).
van Geen, A., et al., 2004. Testing groundwater for arsenic in Bangladesh before installing a well. Environ. Sci. Technol. 38 (24), 6783–6789.
van Geen, A., et al., 2006. Preliminary evidence of a link between surface soil properties and the arsenic content of shallow groundwater in Bangladesh. J. Geochem. Explor. 88 (1–3), 157–161.
van Geen, A., et al., 2008. Flushing history as a hydrogeological control on the regional distribution of arsenic in shallow groundwater of the Bengal Basin. Environ. Sci. Technol. 42 (7), 2283–2288.
van Geen, A., Bostick, B.C., Trang, P.T.K., Lan, V.M., Mai, N.N., Manh, P.D., Berg, M., 2013. Retardation of arsenic transport through a pleistocene aquifer. Nature 501 (7466), 204–207.
van Geen, A., Zheng, Y., Stute, M., Ahmed, K.M., 2003b. Comment on “Arsenic mobility and groundwater extraction in Bangladesh” (II). Science 300 (5619), 584C–584C.
Van Genuchten, M.T., Alves, W.J., 1982. US Dept. of Agriculture, Agricultural Research Service. Analytical Solutions of the One-Dimensional Convective-Dispersive Solute Transport Equation. USDA Technical Bulletin No. 1661. 152p.
Webb, S.M., 2005. SIXpack: a graphical user interface for XAS analysis using IFEFFIT. Phys. Scr. 2005 (T115), 1011.
Weinman, B., et al., 2008. Contributions of floodplain stratigraphy and evolution to the spatial patterns of groundwater arsenic in Araihazar, Bangladesh. Geol. Soc. Am. Bull. 120 (11–12), 1567–1580.
Weiss, R.F., 1968. Piggyback sampler for dissolved gas studies on sealed water samples. Deep-Sea Res. 15 (6), 695-&.
Wood, W.W., Kraemer, T.F., Hearn, P.P., 1990. Intragranular diffusion: an important mechanism influencing solute transport in clastic aquifers? Science 247 (4950), 1569–1572.
Zheng, Y., Van Geen, A., Stute, M., Dhar, R., Mo, Z., Cheng, Z., …, Ahmed, K.M., 2005. Geochemical and hydrogeological contrasts between shallow and deeper aquifers in two villages of Araihazar, Bangladesh: Implications for deeper aquifers as drinking water sources. Geochimica Cosmochimica Acta 69 (22), 5203–5218.

Please cite this article in press as: Radloff, K.A., et al., Reversible adsorption and flushing of arsenic in a shallow, Holocene aquifer of Bangladesh, Applied Geochemistry (2016), http://dx.doi.org/10.1016/j.apgeochem.2015.11.003

Reversible adsorption and flushing of arsenic in a shallow, Holocene aquifer of Bangladesh

Supplementary Materials

Kathleen A. Radloff, Yan Zheng, Martin Stute, Beth Weinman, Benjamin Bostick, Ivan Mihajlov, Margaret Bounds, M. Moshiur Rahman, M. Rezaul Huq, Kazi M. Ahmed, Peter Schlosser and Alexander van Geen

Table of Contents

A1. Hydrology

A complete list of all of the monitoring wells at Site K including the well depth and ground elevation relative to one location in the village is given in Table A1.1.

A1.1 Manual *vs*. Logger Comparison

In order to quantify the net intra-aquifer gradient, an annual average water level calculated from the dry season (February or March) to the following dry season was estimated using both pressure transducer data and the biweekly manual measurements. A comparison of the annual average water level from 7 leveloggers (using the daily measurement at midnight) and the biweekly manual measurements show good agreement between the two methods; slope of 1 and no offset with a r^2 of 0.80 or 0.84, depending on time period used (Figure A1.1A, Table A1.2). While daily fluctuations of water level can influence manual measurements (due to the timing of measurements), the effect of these differences on the annual average estimates did not significantly alter the examination of this data. The manual water level measurements have the advantage of having a 2 year complete record for 12 wells (6 locations and up to 3 depths), thus were used for this analysis. Ten wells are located along the transect from K240 (also referred to as KW12) to the stream and 2 wells are located west or east of this transect (KW14 and 16, respectively). The lowest average water level was recorded in the village (K240/KW12) and water levels increased towards the stream (Figure A1.1B). There was no difference in water level among the wells screened at 7, 10 or 15 m at K240 and K150/KW10. At K60/KW8, water level decreased with well depth by ~4 cm, suggesting the potential for downward flow. However the 7m well had a similar water level as the 7m well located near the irrigation well, so this gradient may instead reflect downward flow induced by irrigation, since hydraulic conductivity increases with depth and may channel the flow in that layer to the irrigation well.

Lateral gradients along the transects show net groundwater flow northward towards the village with an estimated gradient of 2.8 x10-4 (± 0.8 x10-4). Combined with hydraulic conductivity measurements (Supplementary Material, A4) in the shallow aquifer at our study site, this gradient corresponds an annual average Darcy flux of groundwater of -2.7 ± 0.7 m/yr in the shallow (<15 m) portion of the aquifer and a northward velocity of 9 m/yr taking into account porosity.

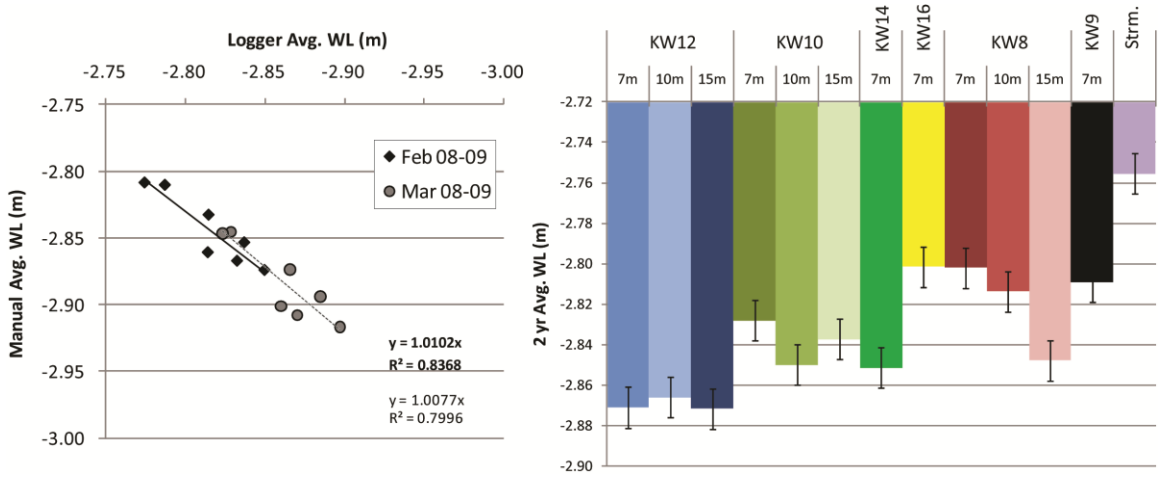

Figure A1.1 Annual average water levels from manual and logger measurements. A) The annual average water level based on the biweekly manual measurements and 20 minute averaged logger measurements are compared for 7 wells for two time periods. B) The two-year average water levels are shown based on biweekly measurements for 12 wells and the stream. Wells are ordered based on their location along the transect.

A1.2 Manual water levels

Manual water level measurements were made every 2 to 3 months in 21 shallow (<15 m) wells to investigate site-wide groundwater gradients in the different seasons to expand on the main transect (Figure A1.2, Table A1.3). At the onset of the dry season, the stream level is 0.3 m higher than the groundwater in the nearest well (KW9) and a water level depression is observed in the wells located nearest to irrigation wells (Figure A1.3A). By March the irrigation- induced depression has disappeared and there is a significant gradient from the stream north to the village (Figure A1.3B). If the well survey is simplified to estimate the gradient from stream towards the village (north to south only with no consideration of east to west or depth variation), there is a -3.5 x 10^{-4} m/m gradient (r^2 = 0.52) and a -0.2 m difference between the stream and the nearest well (Figure A1.3B). During the pre-flood, the difference between the stream and the aquifer has grown to -1.6 m and the northward gradient increased to -8.1 x 10^{-4} m/m (r^2 = 0.72, Figure A1.3C). As the flood approaches, the aquifer-stream difference decreases again to -0.45 m, but the intra-aquifer gradient remains steep (-6.9 x 10^{-4} m/m, r^2 = 0.62, Figure A1.3D). In 2008 and 2009, the flood period was limited and no measurements of intra-aquifer gradients were made. During the post-flood, the water level in the aquifer is between 0.5 and 0.6 m higher than the stream and there is no intra-aquifer gradient (r^2 = 0.03 and 0.22 in Figure A1.3 E and F, respectively).

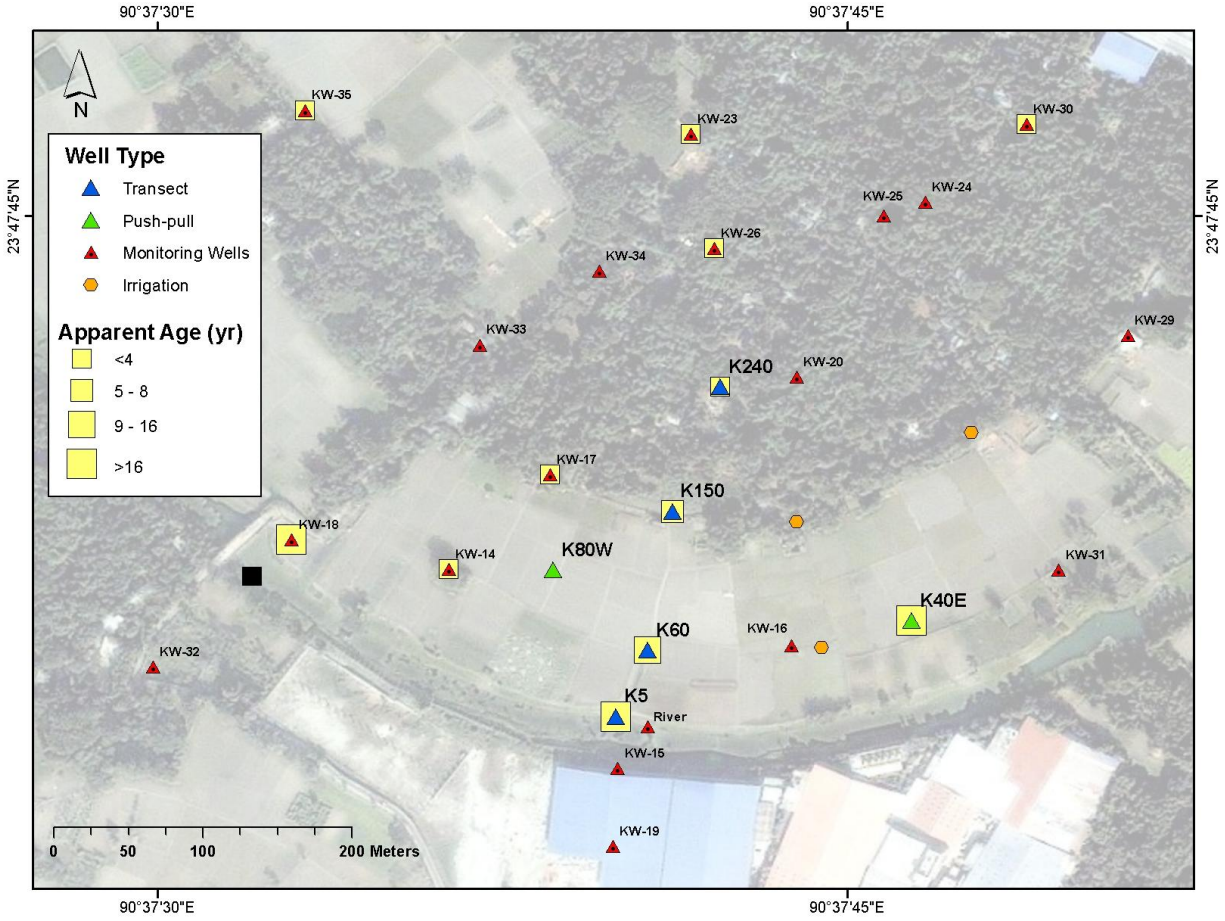

Figure A1.2. Map of all monitoring wells. Manually measured water levels (m) were normalized to K240 (located in the village). Yellow squares indicate the apparent groundwater ages for the shallowest well as determined by ^{3}H-^{3}He dating.

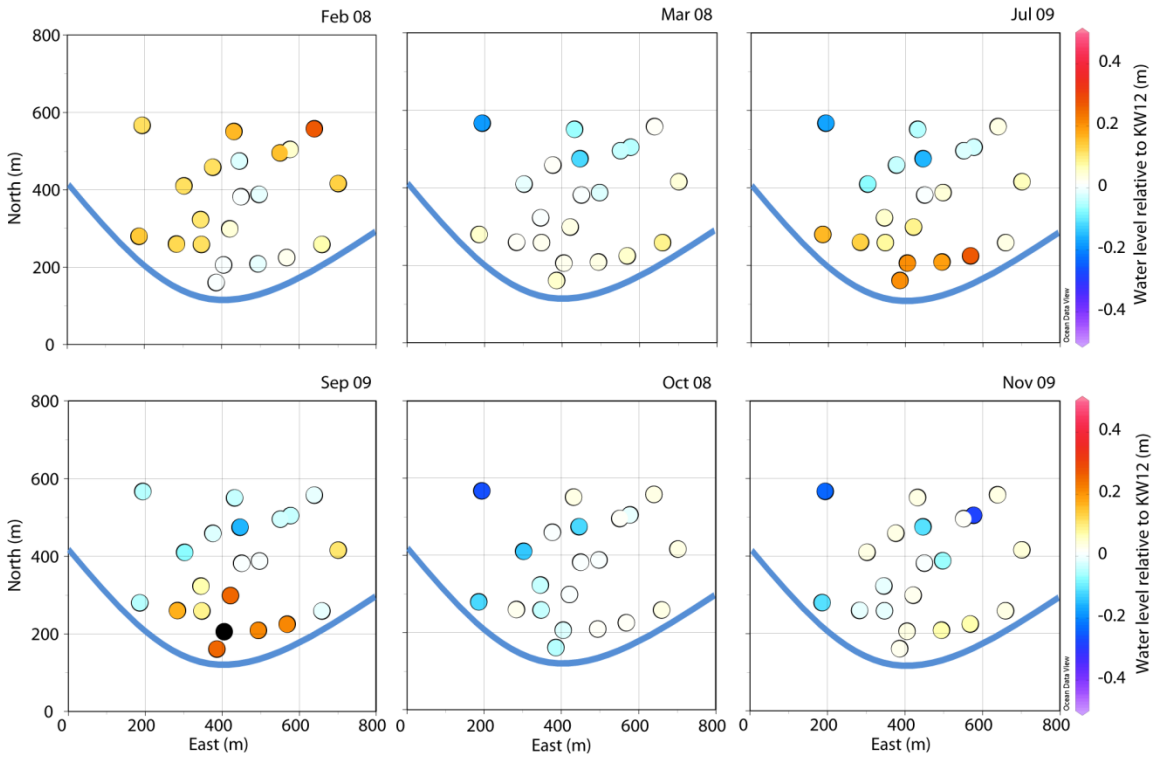

Figure A1.3. Map of relative water levels at six discrete time points. Manually measured water levels (m) were normalized to KW12 (located in the village). Wells with water levels above K240/KW12 are colored in orange and below it in blue, with the darker the color indicating a larger difference. Black dots indicate wells that were not measured. The approximate location of the stream is represented with a blue line.

A1.3 Stream as Hydraulic Boundary

The stream provides one hydraulic boundary to this site (Figure A1.4). At all times of year, the stream water level hydraulically separates the groundwater on either side of it. As was observed in the annual hydrograph, the water level in the aquifer is lower than the stream in the dry and pre-flood seasons and the magnitude of this difference increases with time. During the dry season, the gradient between the stream and aquifer is small, but towards the village (as indicated in the red-orange lines). The gradient increases in the pre-monsoon time when the stream level is rapidly rising and the aquifer levels are lagging (shown in blues) and reaches a maximum difference of 1 m. After the flooding has receded (post-monsoon, November to December), the gradient reverses and the aquifer is nearly 1m higher than the stream (shown in pink-purple).

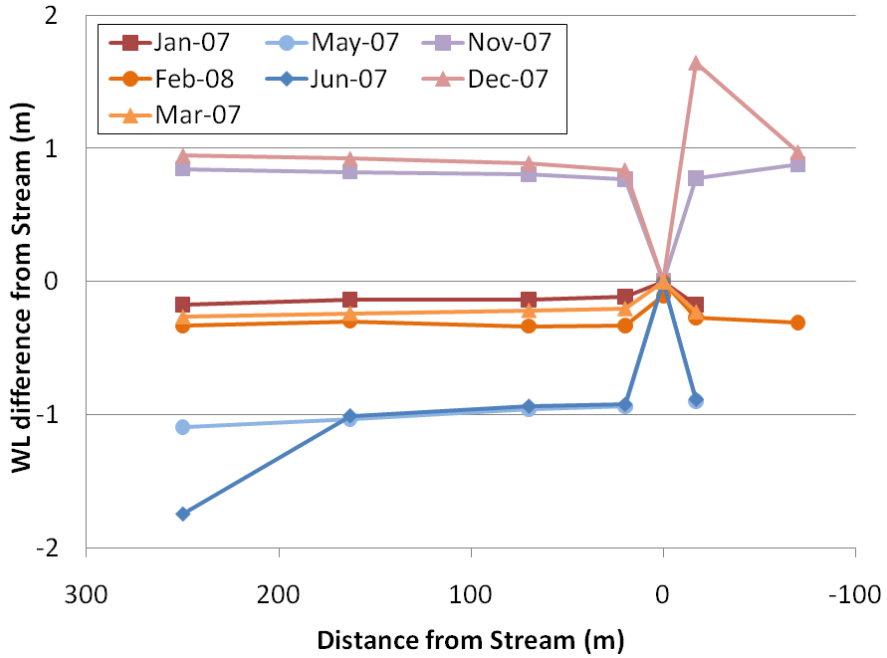

Figure A1.4. Water levels normalized to the stream at discrete times. Using the biweekly measurements, water levels in the 7 m wells along the transect from K240/KW12 to KW19 were normalized to the stream (data from the bridge location) and shown relative to their distance from the stream. Seven time points were chosen to represent the dry season (red-orange), the pre-monsoon (blue) and the post-monsoon (pink-purple).

A1.4 Irrigation Pumping

Irrigation influences groundwater flow and the overall water balance of the site. There are three irrigation wells in the southern fields at Site K (Figure 1, main text). The well KW16 is located about 20 m from one of the irrigation wells; the observation well is screened at 7 m with a 1 m screen, while the irrigation well is screened from approximately 10 to 15 m. The depression cone from the irrigation well can be observed at KW16 using the 20 minute- averaged readings from the pressure transducer. The irrigation season typically begins in January and extends into March or April, depending on when the rain begins, however the most intensive irrigation occurs in January and February with near daily pumping (Figure A1.5). Irrigation induces a transient 5 to 15 cm decrease in water level at KW16, while the overall water level is also dropping over this period. By April, irrigation typically ceases and the groundwater begins to rise (onset of the pre-flood season).

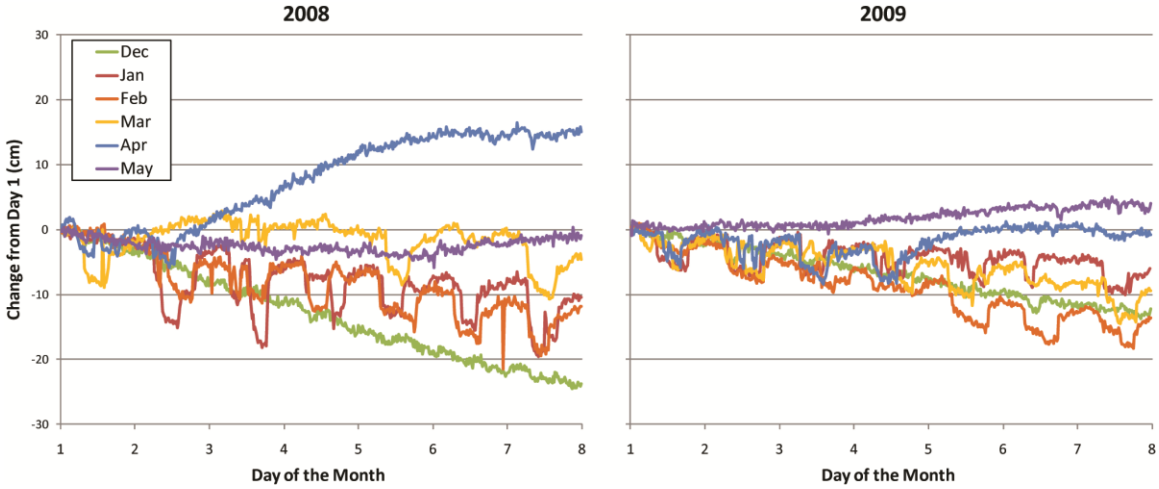

Figure A1.5. Water levels at KW16 normalized to the first day of the month. Using the pressure transducer, water levels (m) at KW16 were normalized to the water level at midnight on the first day of the month. Readings from the first week of each month from December to May are shown for 2008 and 2009.

The groundwater age data (see A2) supports the finding that irrigation pumping can cause local changes in groundwater flow. At KW16, the well located closest to an irrigation well, the apparent groundwater age decreased from 7 to 3.5 yrs between 2007 and 2008 and may indicate that local pumping is enhancing recharge nearby or is pulling younger water towards the well. The apparent groundwater age is 35 yrs at 7, 10 and 15 m depth at K40E, which is located within 60 m of a irrigation well and may suggest that irrigation pumping is drawing older, deeper groundwater through the more conductive 15 m depth and results in some groundwater mixing here. Similarly, a small vertical gradient at K60 may reflect downward flow induced by irrigation, since hydraulic conductivity increases with depth and may result in greater flow towards the irrigation well with depth.

A1.5 Factory Water Use

A large cotton-spinning mill, the Vai Vai Spinning Mill, was built sometime between 2003 and 2006 on the southern side of the stream and expanded in 2008. It began operation around the time when water level surveys were initiated (in 2007). The factory operates 5 shallow aquifer wells (<40 m) and 2 deeper aquifer wells and the plant wastewater is discharged into the stream. The discharge volume is not known, but the factory pumps an estimated 400,000 L/day from the deeper aquifer (R. Mozumder, personal communication).

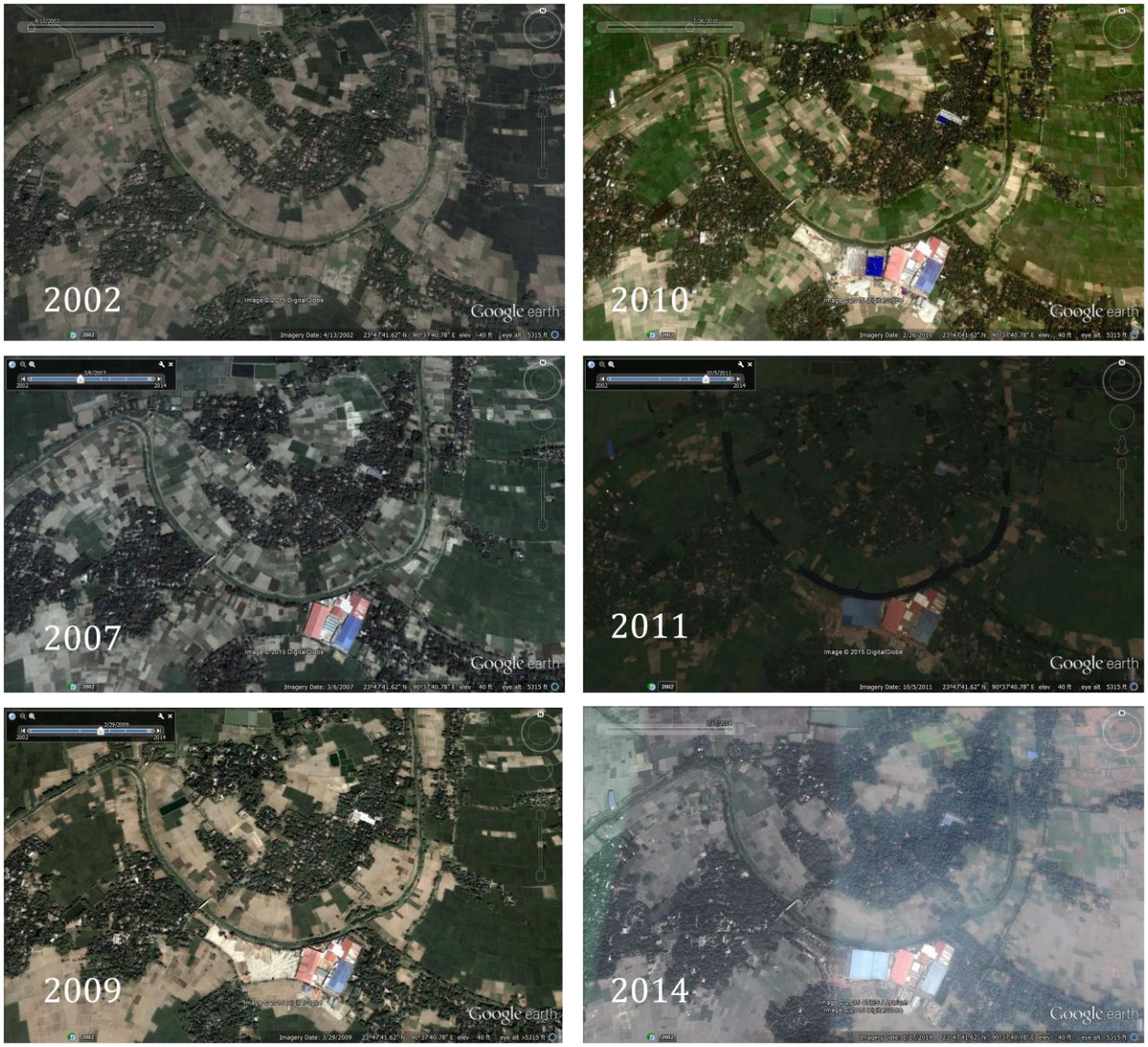

Figure A1.6. Satellite Images of the Site K area from 2002 to 2014. The satellite images obtained from Google Earth show that construction began after 2002 and the initial mill was present and operational in 2007. The mill began an expansion in 2008, resulting in the loss of 2 monitoring wells.

A2. Groundwater Age Dating

A2.1 ^{3}H-^{3}He Dating

An extensive (33 well) survey of ^{3}H and ^{3}He concentrations in groundwater in the shallow (<15 m) aquifer was conducted and was used to estimate the apparent age of the groundwater using ^{3}H-^{3}He dating, referred to as the ^{3}H-^{3}He ages. All of the shallow wells at Site K have been recharged since the bomb peak and had detectable tritium. The section of shallow wells from the site shows an increase in age from the village towards the stream with ages ranging from recent (~0.5 yr) to 36 years (Figure A2.1, Table A2.1). The wells in the village are at least 7 m deep and have young groundwater, suggesting a high vertical recharge rate and deep penetration of recharge water. Older groundwater (>30 years) is located near the stream both on and off the main transect (at K60/KW8 and K5/KW9 as well as KW18 and K40E/KW22). The samples from K60-20m and K5-20m contained unexpectedly low ^{3}H levels and were understaturated in Ne indicating that some de-gassing of these samples has occurred in the aquifer, possibly due to methane generation. This is consistent with the methane measurements in the shallower wells and the high level of degassing observed at K60-30m and K5-30m, which prevented ^{3}H-^{3}He sample collection. In addition, the three samples (K150- 30m, K60-20m and K5-20m) show evidence of terrigenic He input and the age estimates were corrected using total He and Ne measurements and the ratio of ^{3}He/^{4}He to differentiate the He from tritogenic and terrigenic sources.

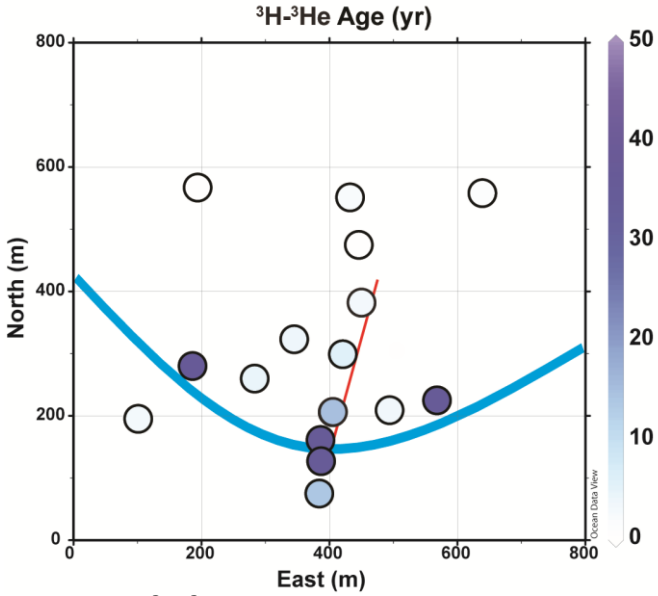

Figure A2.1. ^{3}H-^{3}He ages in a section view and along the transect. ^{3}H-^{3}He ages in section view of the shallow wells at the site. Darker blue indicates older groundwater. Transect location is indicated by the red line.

The estimated ages were confirmed by comparing the original content of ^{3}H (measured in TU) of the water and to this historical records of tritium content in precipitation in Asia (Stute et al., 2007). All of the samples from Site K, except for two, fall along the tritium input curve for older groundwater (Figure A2.2). The tritium input curve has not been updated since 1995, but the more recent groundwater appears to follow the slow decreasing trend in tritium and corresponds well with other young water measured in Araihazar (Stute et al., 2007). The two samples with unexpectedly low TU (KW8.4/ K60-20m and KW9.4/K5-20m) are both deep and were understaturated in Ne indicating that some de-gassing of these samples has occurred in the aquifer, possibly due to methane generation. We did not attempt to collect

samples at KW8.5/ K60-30m and KW9.5/K5-30m, due to the visible bubbling in the pumped groundwater. The deeper wells were not sampled for methane.

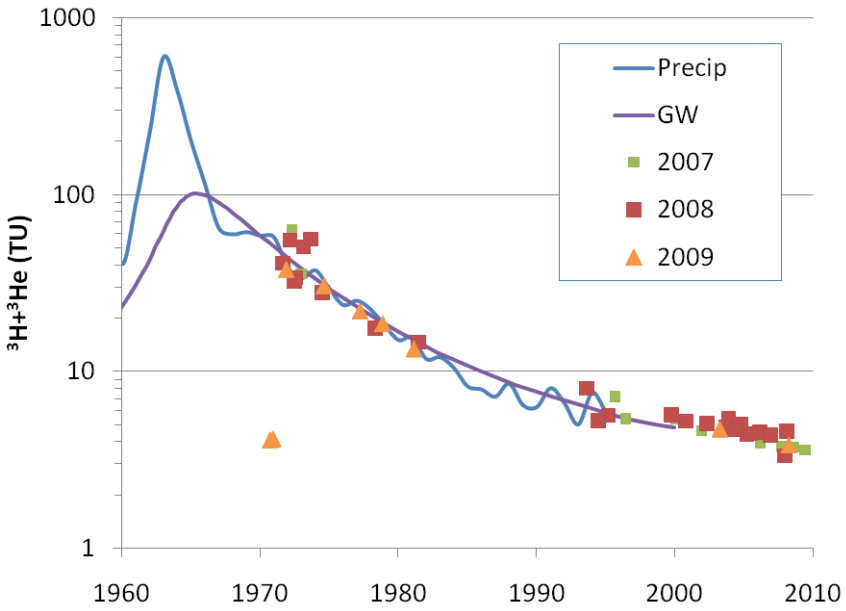

Figure A2.2. Sum of ^3H and tritogenic ^3He (in TU) compared to ^3H-^3He ages and the tritium input from precipitation in Asia. Tritium input curve and corresponding groundwater input curve were taken from Stute et al. (2007). Samples measured at Site K in 2007, 2008 and 2009 are shown.

A2.2 ^{14}C Dating

Groundwater age for younger waters can also be estimated from the comparing the $^{14}C/^{12}C$ ratio to modern carbon ratios, reported as the fraction modern carbon or FMC, however this approach requires the consideration of various sources of carbon in the aquifer and the half-life of ^{14}C (5,730 yrs). The alkalinity and ratios of $^{13}C/^{12}C$ and $^{14}C/^{12}C$ of DIC was measured in 16 wells along the transect (the 10 m depth was excluded). The alkalinity of the non-evaporated wells is relatively uniform (between 2 and 5 meq/L) and shows a slight increase towards the stream, but this increase is not significant at any particular depth ($p>0.01$) (Figure A3.1A). The five wells identified as having low deuterium excess also have elevated alkalinity (>6 meq/L). The $\delta^{13}C$ ‰ content of the groundwater at the beginning of the transect is typical of groundwater DIC with the major contribution of carbon coming from plant-derived organic carbon (-15 to -25‰) (Figure A1.3B). The $\delta^{13}C$ ‰ increases (gets heavier) towards the stream and with depth to a maximum of -7‰, suggesting carbonate dissolution is occurring.

The ^{14}C content of DIC, reported in FMC (fraction modern carbon), decreases along the transect and with depth, with a significant decrease where the alkalinity rises (Figure A1.3C). The measured FMC can be compared to the an atmospheric level of FMC predicted based on the ^3H-^3He apparent age, this ratio is known as the initial activity, A_0 and expresses the fraction of the carbon that is derived from atmospheric versus aquifer (carbonate) sources. In the wells with detectable tritium, this ratio is strongly correlated ($r^2= 0.6$, $n= 13$) with the alkalinity of the groundwater, with decreasing A_0 as alkalinity increases since the contribution of atmospheric carbon is declining age (Figure A1.3D). This relationship supports the observations from the $\delta^{13}C$ data that carbonate dissolution is occurring. In order to quantify the potential contribution of carbonate to the groundwater, the initial activity and alkalinity were used to calibrate a simple model were the alkalinity changes were completely attributed to carbonate dissolution of 4,000

year old (the approximate age of these sediments) or ^{14}C-dead carbonate. This allowed for the calculation of groundwater FMC at the time of recharge (and before dissolution of old or ^{14}C-dead carbonate), which was then compared to atmospheric levels of FMC in observed Germany (Levin and Kromer, 1997).

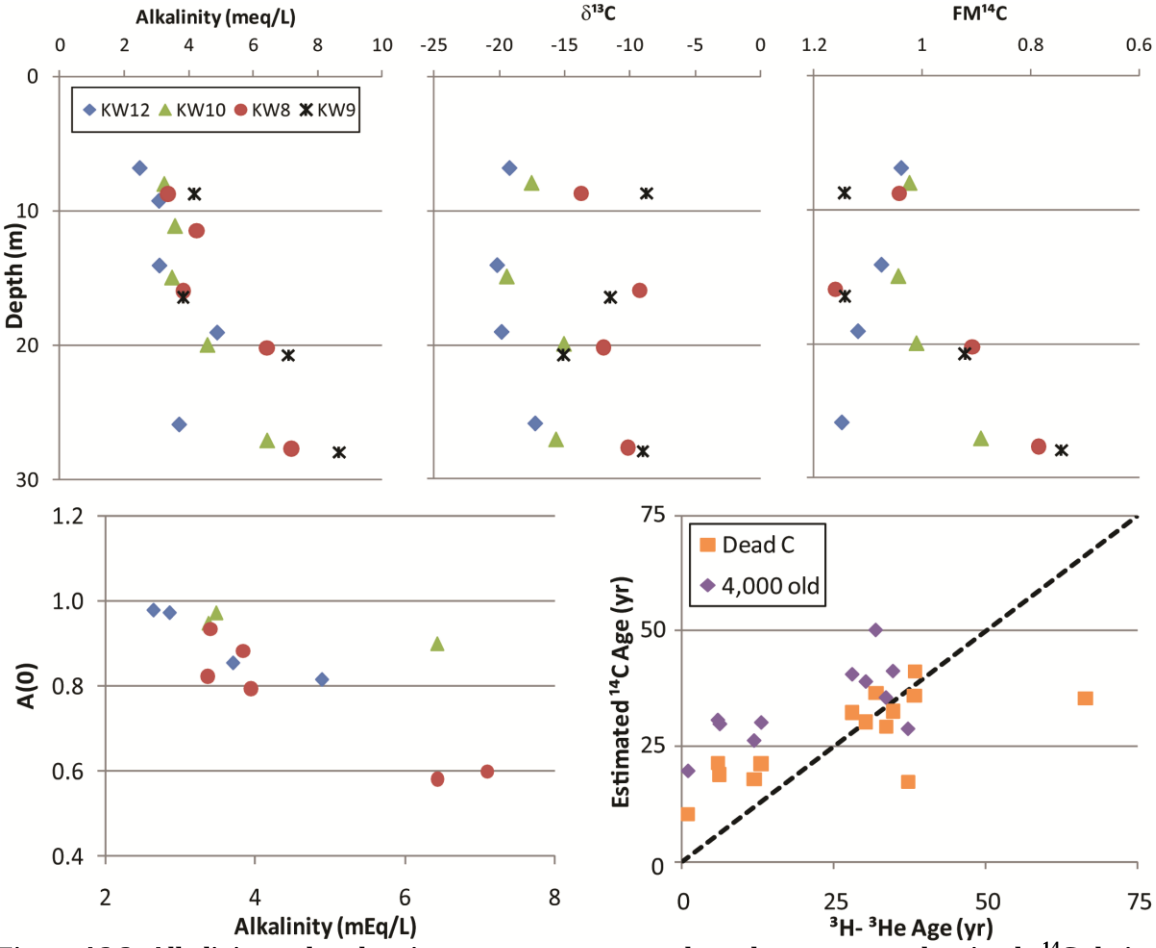

Figure A2.3. Alkalinity and carbon isotope measurements along the transect and a simple ^{14}C dating model. A) Alkalinity (meq/L) shown by depth in the 19 wells located along the transect. B and C) $^{13}C/^{12}C$ and $^{14}C/^{12}C$ ratios, reported as $\delta^{13}C$ and $FM^{14}C$, in 16 wells along the transect. D) Relationship between initial activity (A_0) and alkalinity. E) Comparison of the age estimates from the two simple ^{14}C dating models to ^{3}H-^{3}He apparent ages. Black dashed line indicates a 1:1 correlation of age estimates.

Groundwater age estimation using ^{14}C dating requires the consideration of multiple carbon sources within the aquifer, including atmospheric and carbonate components. The simple models applied here suggest that sufficient dissolution of carbonates, as indicated by the changes in alkalinity, is occurring and that estimating age in the older wells using a radiocarbon correction only is not sufficient. Both models were able to roughly estimate the known ^{3}H-^{3}He apparent age (Figure A1.3E). The models slightly overestimated the groundwater age of the younger (<20 yr) water at the site. The models assumed that changes in alkalinity were due solely to the dissolution of carbonate. Therefore moderate increases in alkalinity (like what was observed in the younger water) were attributed to more dissolved carbonate, which in turns suggests that the initial groundwater (before dissolution) had a higher initial FMC in order to reach the measured FMC. This resulted in older groundwater age estimates (FMC increases with time towards the bomb-peak) for this water. It is possible that much of these smaller alkalinity changes are more the result of microbial activity or other geochemical reactions and not completely due to carbonate

dissolution as the models assumed. The groundwater age estimates were much more accurate for water in the 15 to 50 years time frame.

If we consider the wells with the significant alkalinity increase, the models provide a significantly more accurate prediction of groundwater age than adjusting for radiocarbon decay alone, even though the FMC indicates that this water should not have bomb ^{14}C. The model predictions for these 5 wells ranged from 35 to 45 years, while accounting only for radiocarbon decay would suggest ages from 660 to 2,400 years. The measured ^{3}H-^{3}He apparent ages, on the other hand, ranged from 38 to 67 years in the 3 measured wells. The models estimated that the age the groundwater at KW8.5 and 9.5 is between 35 and 45 yrs and the actual age is likely somewhat greater due to the underestimation in the 3 similar wells (perhaps between 50 and 200 years), but far less than the initial 2,000 year estimate. Therefore all of the shallow (<30 m) groundwater at this site is relatively young.

A3. Groundwater Properties

A3.1 Additional parameters

The shallow aquifer site described here was completely anoxic, yet a range of redox conditions were present. In general, the shallow groundwater has increasingly reducing conditions along the transect towards the stream and with depth. Only the shallowest well in the village, 7 m at K240 had low concentrations of elements (As, Fe, Mn and P) sensitive to suboxic conditions. The typical redox sequence of elements can be observed in the rest of the aquifer.

The groundwater can be described as a near neutral HCO_3-Ca-Mg type, with nearly 90% of the anions being supplied by the alkalinity. The pH of the groundwater varies from 6.5 to 7 (Figure A3.1, Table A3.1). The K240 wells have lower pH than the five other locations, which show no spatial pattern and a slightly increasing pH from 10 to 30 m. Most wells have an alkalinity varying from 2.7 to 4.9 meq/L with a small increase in alkalinity towards the stream and little depth variability (Figure A3.1B). However the 5 deep wells nearest to the stream (20 m wells at K60 and K5 and the 30 m wells at K150, K60 and K5), have significantly higher alkalinities, ranging from 6.4 to 8.7 meq/L. Chloride concentrations tend to decrease towards the stream. In the K240 wells, dissolved Cl increased from 6 mg/L at the surface to over 50 mg/L at depth. The other wells have higher Cl concentrations at the surface (up to 20 mg/L) and lower concentrations at depth (1 to 9 mg/L). At K60 and K5 the Cl concentration in the 30 m wells are higher than the shallow wells.

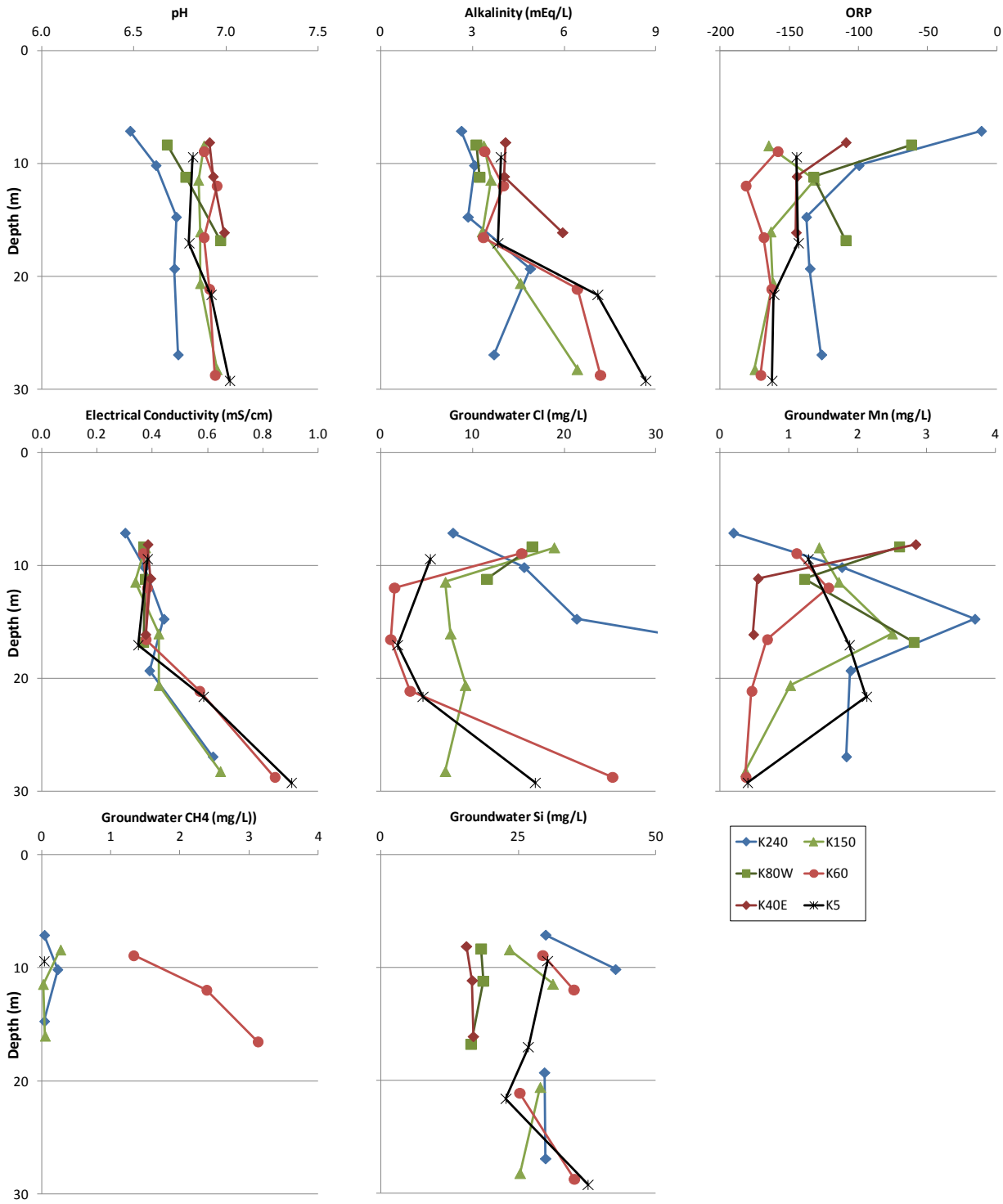

Figure A3.1 Additional groundwater characteristics. Vertical profiles extending from the surface to about 30 m depth are shown for 6 locations. Color indicates distance from stream, changing from blue in the village to green to red to black near the stream bank. Seven parameters are shown here: pH (A), Alkalinity in meq/L (B), oxidation-reduction potential (ORP) in mV (C), electrical conductivity in mS/cm (D), and given in mg/L are Cl (E), Mn (F), and methane (G).

A3.2 Arsenic timeseries

The concentration of groundwater As was remarkably stable in the wells along the transect, particularly for the wells with concentrations at or below 100 µg/L. All of the bi-weekly samples collected for the wells at K60, K5 and KW18 between well installation in December 2006 or May 2007 and March 2008 were analyzed. For the other wells, only the samples collected every 2 months between March 2007 and 2008 were analyzed (Figure A3.2, Table A3.2).

Only three wells displayed significant changes. At K60-10m and KW16, leveloggers installed in the wells confirm that floodwater entered these wells in late July 2007. The results from K60-10m are discussed more fully in the main text. At KW16, less frequent samples were measured, but the recovery appears to be slower. At KW18, another significant drop in As concentrations was observed, but the timing of the event does not correspond to the monsoonal flooding. It is therefore unknown what caused this perturbation. However, concentrations recover in approximately one month.

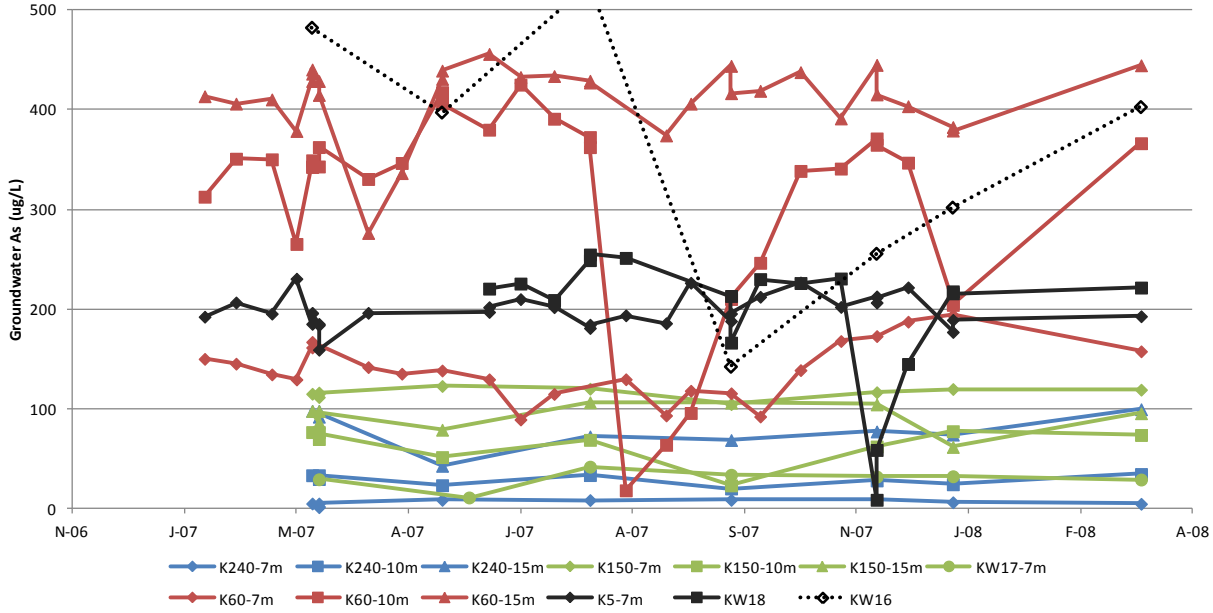

Figure A3.2 Groundwater As concentration over time along the transect. The wells approximate location along the transect is given by the color and the depth of the well by the shape. Blue symbols indicate the village wells at K240/KW12, green symbols for the fields at K150/KW10 and KW17, red symbols for K60/KW8 and black symbols for K5/KW9, KW16 and KW18. Diamonds represent the 7m depth wells, squares for the 10m depth wells and triangles for the 15m depth wells.

A3.3 Stable isotopes

Measurements of ^{2}H and ^{18}O in groundwater were used at Site K in the 17 shallow wells across the site to identify potential recharge sources of the aquifer. Furthermore, the stable isotope composition of groundwater with depth was explored using the 19 wells located along the transect from the village to the stream. The deuterium excess ($\delta^{2}H$-8*$\delta^{18}O$) of precipitation is approximately 10, while for evaporated waters, such as the stream or ponds during the dry season, it can be much lower. The shallow (<15 m) groundwater at Site K was comparable to precipitation at all locations (Figure A3.3A and C, Table A3.1). The groundwater in the deeper wells along the transect approaching the stream had a more evaporated signal. Five wells have particularly low deuterium excess (0 to 2.5 per mil) suggesting the source of this water was highly evaporated and not like the other locations.

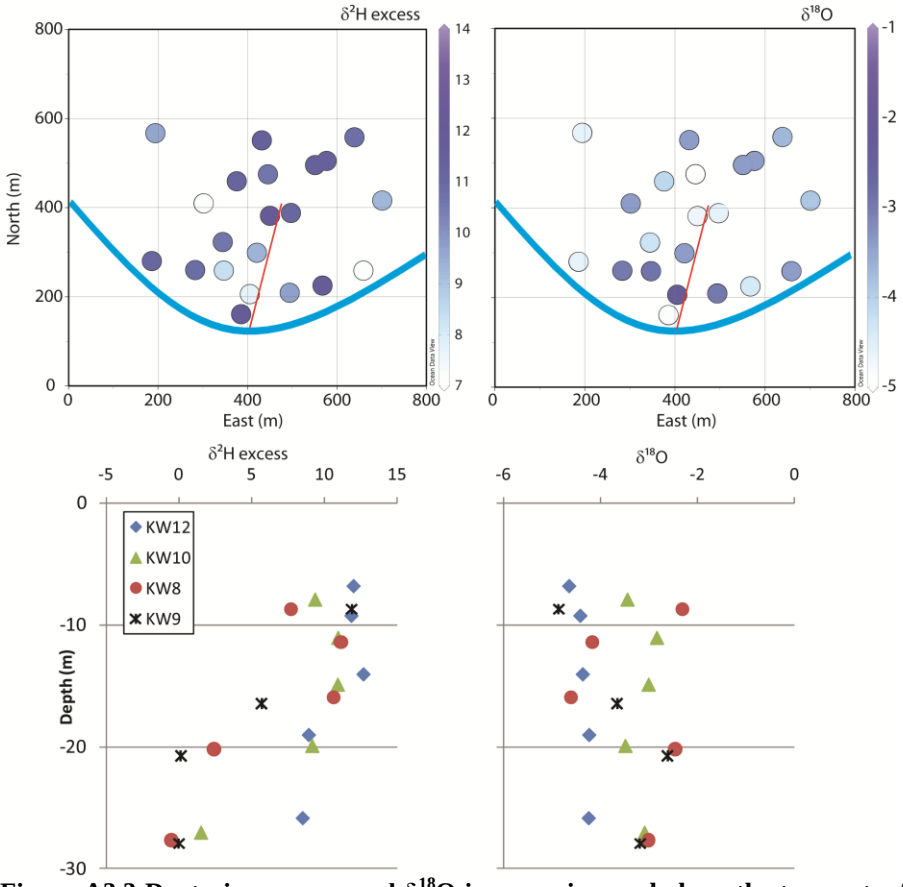

Figure A3.3 Deuterium excess and $\delta^{18}O$ in map view and along the transect. A and B) Deuterium excess (‰) and $\delta^{18}O$ (‰) in section view of the shallow wells at the site. Transect location is indicated by the red line. C and D) Deuterium excess and $\delta^{18}O$ with depth along the transect. Wells at each well nest are indicated by blue diamonds for K240/KW12, green triangles for K150/KW10, red circles for K60/KW8 and black stars for K5/KW9.

The seasonal timing of shallow (non-evaporated) groundwater recharge can be inferred using $\delta^{18}O$ ‰ (Figure A3.3B and D). The less negative $\delta^{18}O$ ‰ values indicate recharge from rains earlier in the monsoon. The wells in the southern rice fields along the transect have the least negative values indicating early rains, while the village and other field locations are more negative. The clear difference between the wells at K240/KW12 and K150/KW10, with $\delta^{18}O$ of approximately -5‰ and -3‰ respectively, suggests that the precipitation recharging K240/KW12 occurs later in the season than the recharge at

K150/KW10. The recharge in the village evidently does not occur until the site is more saturated with water, perhaps due to transpiration in the tree covered areas. The $\delta^{18}O$ at K60/KW8 suggests a non-uniform source of groundwater with depth. The patterns observed in the $\delta^{18}O$ data are also apparent in the $\delta^{2}H$ data (data not shown).

A4. Sediment Properties

A4.1 Additional parameters

Classification of sandy or fine-grained deposits was made with an electromagnetic (EM) survey of the land surface and was used to identify locations with higher recharge potential (Aziz et al., 2008). The EM survey of Site K (0.25 km^2) included the agricultural fields and stream bank and measured conductivities from 3 to 27 mS/m (n=1,278) with an average value of 12 ± 4 mS/m (Figure 1). The survey of the Araihazar region (~25 km^2) measured conductivities from 3 to 75 mS/m, with an average of 18 ± 8 mS/m (n=18,530) and were reproducible to 0.5 mS/m (Aziz et al., 2008). The EM conductivity at Site K is lower than Araihazar, in general, and suggests that the site is overlain by coarser materials. Several potential recharge zones were identified. In general, the EM conductivity increased from the village towards the stream, indicating more recharge potential near (or possibly in) the village. The agricultural fields to the west of the village were particularly conductive, as was a patch of land east of KW10 (and situated between two irrigation pumps).

XRF analysis showed no difference in the Ca and K content of the sediments between locations and a small decrease in K with depth, suggesting that the basic mineralogy of the sediments was uniform (Figure A4.1, Table A4.1). There was, however, a more significant decrease in Fe with depth at all locations from about 40 g/kg at the surface to 20 g/kg at 15 m (Figure 6, in main text). The field location had a slightly lower Fe content than the village or stream locations. The HCl- extractable Fe ranged from 3 to 27 g/kg and was highest in the shallowest sediment near the stream, consistent with a greater proportion of Fe-rich silts and clays (Figure A4.3). The ΔR and Fe(II)/Fe measurements from the HCl-extractions both showed an increasingly reduced sediment up to 10 m (Figure A4.1). Speciation of the HCl- extractable Fe, described as the ratio of Fe(II) to total Fe (or Fe(II)/Fe), ranges from 0.1 to 0.9, and is generally more reducing towards with stream and with depth (Figure 6). As reported in Radloff *et al*. 2008, vertical profiles of several of the locations also described here, exhibited fluctuations in Fe(II)/Fe ratio in the shallow zone, most notably from 4 to 9 m depth and was greatest at K150, where Fe(II)/Fe ratio increases from 0.1 to over 0.5 between 2 and 5 m depth at this location. The new coring data reported here show that the more oxic sediments (Fe(II)/Fe < 0.5) are found to a depth of 7 m at K280 and K240, but only to 2 m at K150 and K60. The most reduced sediment was found at K60 between 4 and 6 m depth with a Fe(II)/Fe of 0.9.

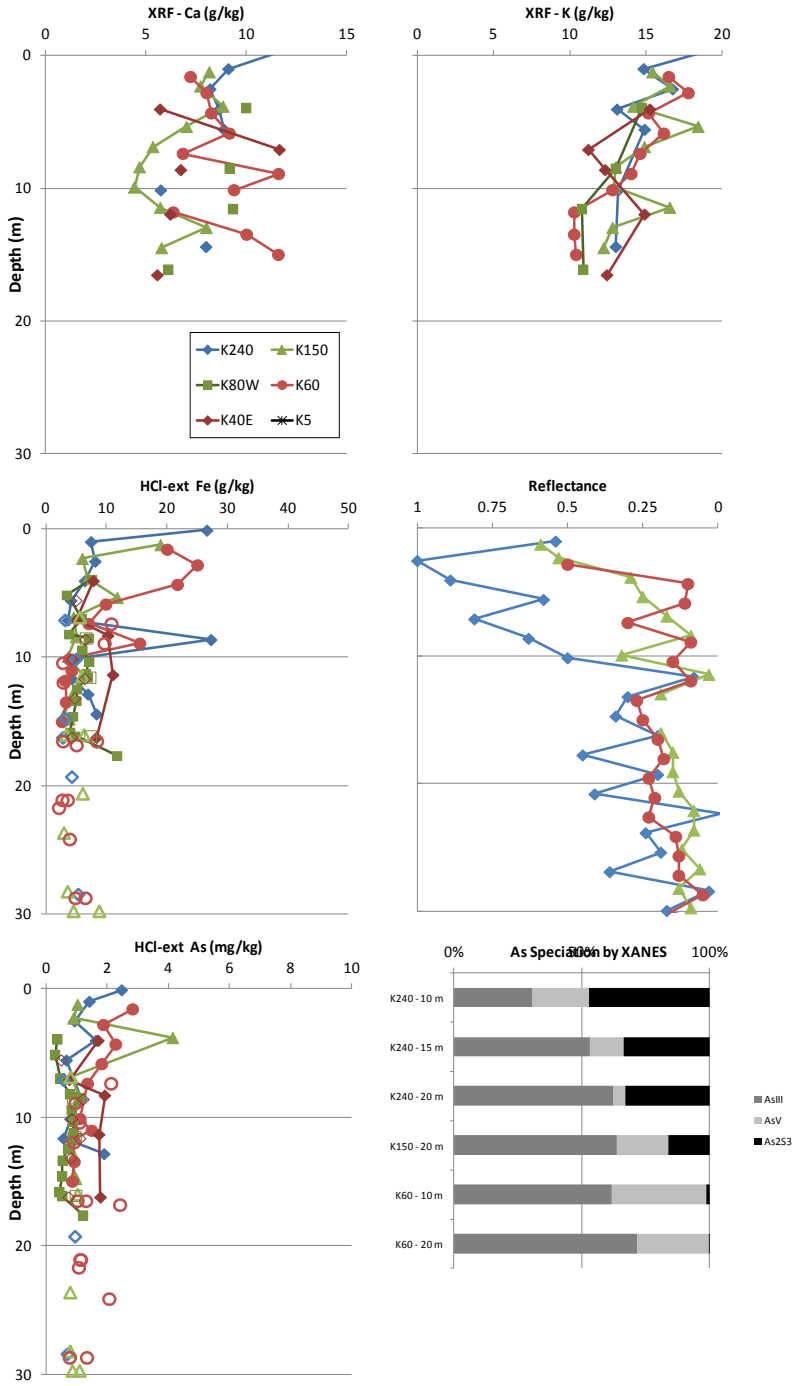

Figure A4.1 Additional sediment characteristics. Vertical profiles extending from the surface to about 30 m depth are shown for 5 locations. Color indicates distance from stream, changing from blue in the village to green to red to black near the stream bank. Sediment collected by coring are shown with solid markers and are connected by a line in the sandy portion of the aquifer. Sediment collected from needle sampling or as drill cuttings are shown as open markers. Six parameters are shown here: Ca and K by XRF in g/kg (A and B), HCl-extractable Fe in g/kg (C), reflectance given in dR (D), HCl-extractable As in mg/kg (E) and As speciation by XANES (F) given in percent of total.

A4.2 Extractable As

Sediment As concentrations are also quantified with hot HCl- and phosphate- extractions conducted in the field. HCl-extractable As ranges from 0.3 to 4.1 mg/kg and phosphate-extractable As ranges from 0.2 to 6.8 mg/kg in sediment collected in cores, as drill cuttings and from the needle sampler (Figure A4.1). HCl- and PO_4- extractable As is higher in the shallowest zone (<5 m depth). At K240, the PO_4-extractable As concentrations are frequently greater than the HCl extractions. However, at the other locations, PO_4-extractable As concentrations are less than or equal to the HCl- extractable As (Figure 5 and Figure A4.1). Overall, the PO_4-extractable As concentrations are highest in the village (K240), while the HCl-extractable As is generally highest near the stream (K40E and K60). In the deeper zone (>10 m depth) both HCl- and PO_4- extractable As concentrations are typically <2 mg/kg, which is <30% of the total As as measured by XRF, and there is little spatial difference.

Sediment extractions were also conducted on the 15 samples used in the adsorption experiment that received no As addition upon completion of that experiment (30 days). In the initial samples, the water extraction liberates the smallest amount of As, ranging from 0.01 to 0.7 mg/kg (Figure A4.2). The water-extractable As increased along the transect and with depth for K240 and K150, while the maximum concentration at K60 is at 10 m. Water-extractable As is predominately As(III), ranging from 60 to 95% of total As. For these initial samples, the phosphate extraction yields 0.1 to 1 mg/kg of As and is highest at K60. The batch PO4-extractions removed <20% of the total As, as determined by XRF, and are lower that the PO4-extractable As concentrations measured in the field on all samples collected. The batch PO4-extractable As is corrected for the adsorption or desorption of As that occurs in the bottle, based on the change in groundwater As, to estimate the adsorbed As at the time of sample collection. Speciation measurements show that As(III) comprises 50 to 90% of batch PO_4- extractable As.

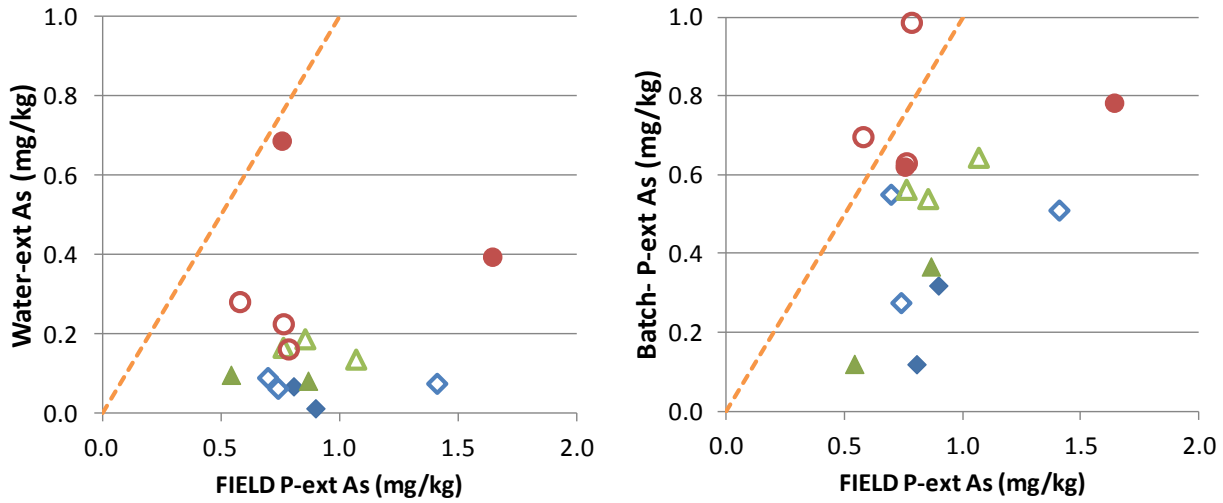

Figure A4.2 Additional extractable As measurements. The concentration of water and phosphate – extractable As from the batch isotherm samples is compared to the field-measured PO4-extractions, using the same colors and markers as Figure A4.1. Sediment collected by coring are shown with solid markers, while sediment collected from needle sampling or as drill cuttings are shown as open markers.

A4.3 Hydraulic Conductivity

Hydraulic conductivity was then estimated from the grain size method using two different approaches (Table A4.2). The most commonly used method was derived by Hazen and is based on the representative grain size, d_{10}, where 10% of the sediment is finer by weight and estimates conductivity with the equation:

$$K = 4558 * d_{10}^{1.96} \quad \text{(eq.1)}$$

The coefficient and exponent are derived from a study done on aquifer materials from Cape Cod (Shepherd, 1989). Alternatively, the Kozeny-Carman equation estimates K using the effective diameter, D_{eff}, of the sediment and is calculated from:

$$D_{eff} = \frac{1}{\sum \frac{f_i}{D_{li}^{0.5} * D_{si}^{0.5}}} \quad \text{(eq. 2)}$$

where f_i is the fraction of particles between two sieve sizes, and the average particle size between the two sieve sizes is calculated from $D_{li}^{0.5} \times D_{si}^{0.5}$ where D_{li} is the larger sieve size and D_{si} is the smaller sieve size in cm (Carrier, 2003). The Kozeny-Carmen equation is:

$$K = \frac{\gamma}{\mu} * \frac{1}{C_{K-C}} * \frac{1}{S_0^{\,2}} * \frac{e^3}{1+e} \quad \text{(eq. 3)}$$

and can be simplified to

$$K = 248.75(D_{eff}) \quad \text{(eq. 4)}$$

where γ is the unit weight of the fluid, μ is the viscosity of the fluid (γ/μ is 9.93 x 10^4 l/cm-s when the fluid is water at 20ºC), $C_{K\text{-}C}$ is the Kozeny-Carmen constant (usually taken to be 5 for uniform spheres), $S_0^{\,2}$ is the specific surface area and can be simplified to $(6/D_{eff})^2$, and e is the porosity 0.25.

Hydraulic conductivities were also measured in 35 wells by slug testing. Wells were pressurized using a hand pump and the temporal response of the hydraulic head was measured using a submerged pressure transducer (Leveloggers, Solinst). The approach and analysis employed here was slightly modified from Butler et al. by using a bicycle pump to pressurize the well, instead of a nitrogen tank (Butler et al., 2003). At least 3, and up to 12, slug tests were performed at each well tested. The slug test response curves were analyzed using the high conductivity Hvorslev model assuming the aquifer is confined and the formation thickness is greater than 10 m. The standard error of the measurements was about 3%.

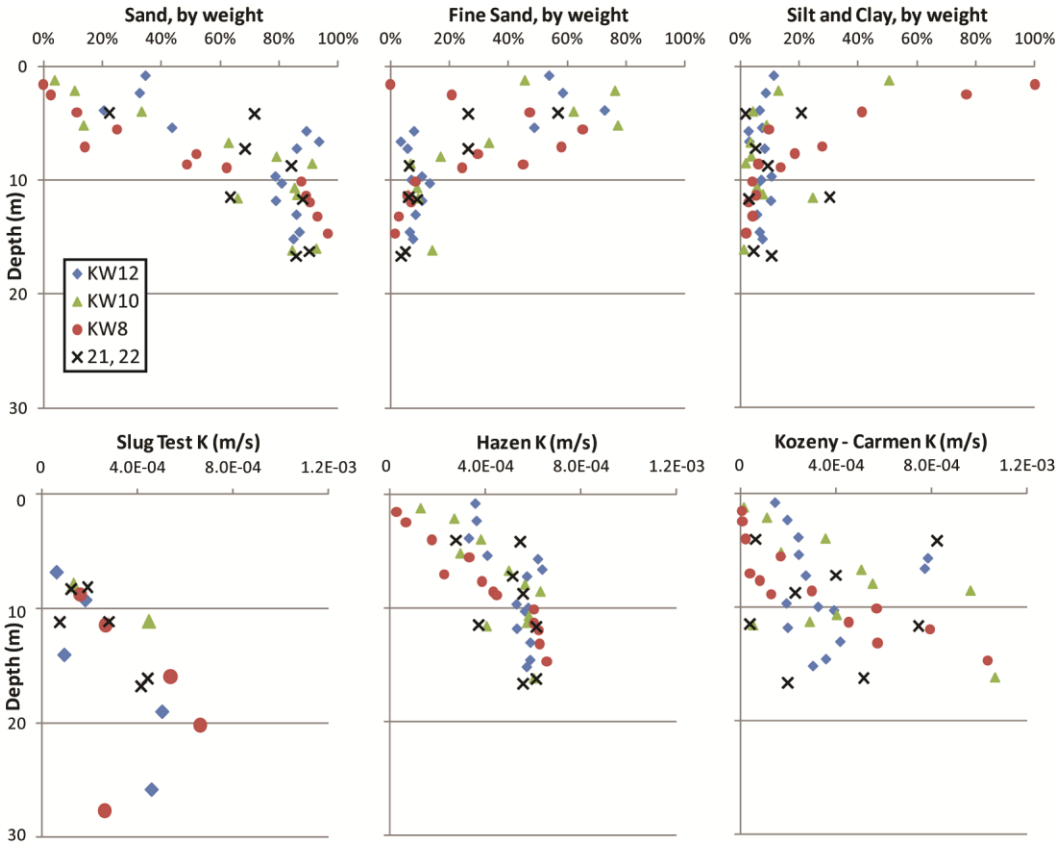

Figure A4.3. Distribution of grain size and hydraulic conductivities along the transect. The percent by weight of the sand (>150 µm), fine sand (63-150 µm), and silt/ clay (<63 µm) from the coarse fraction sieving are shown for 5 coring locations. Also shown are the hydraulic conductivities measured by slug testing at these locations and the conductivities predicted from the grain size analysis using the Hazen and Kozeny-Carmen methods.

Hydraulic conductivity was estimated from the observed grain sizes using two methods (Hazen and Kozeny-Carmen) and varied from 4.4 x 10^{-6} to 1.5 x 10^{-3} m/s (Table A4.2). This range of conductivities is typical of a sandy aquifer, where K values frequently vary by more than 2 orders of magnitude within the same hydrogeological unit (Fetter, 2001). Geometric means are typically used to describe the "average" K of such an aquifer. The Hazen method predicted little variability in K below 10 m, with the geometric mean of K of 5.7 x 10^{-4} m/s. The Kozeny-Carmen method, on the other hand, predicted a wider range of K, using the same data set. In general, the Kozeny- Carmen method predicted increasing K with depth and a difference in K between the locations. Below 10 m, K is lowest in the village and increases towards the stream, based on the slightly higher sand content in these sediments (geometric means of 3.0 x 10^{-4} m/s at KW12 and 5.0 x 10^{-4} m/s at KW8).

The predictions of K provided by the Kozeny-Carmen method are more closely aligned with the hydraulic conductivities measured with the slug tests. The slug test results also demonstrate increasing K with depth and towards the stream, however the measured K is about half of the predicted K from the Kozeny-Carmen method (Figure A4.3D). The lowest K (6.2 x 10^{-5} m/s) was observed in the shallow village well and the highest in a deeper well near the stream (6.6 x 10^{-4} m/s). The geometric mean of the wells with grain size data is 3.0 x 10^{-4} m/s (n=18) and of the entire site is 1.6 x 10^{-4} m/s (n=31), which is biased towards shallow wells in the village area.

A5. Batch Experiment

A5.1 Isotherms

After one month, the groundwater in the isotherm experiments was measured to reveal the partitioning of the added As between the groundwater and adsorbed phase (calculated from the loss in groundwater). The adsorption experiments were assumed to be at or near equilibrium, based on the results of the push-pull tests. Groundwater and sediment As data is given for each experiment in Tables A5.1 to A5.3. The K_d is evaluated for samples with additions up to 8,000 µg/L; the 15,500 µg/L addition is excluded due to the apparent saturation observed in some samples (resulting in less linear behavior). There was no discernible difference in the amount of As(III) or As(V) adsorbed on aquifer sands from the 6 intervals where both were added to separately (7 m and 10 m depth intervals at three locations). A summary of the calculated K_ds and the error, based on the estimated slopes, is given in Table A5.4. The groundwater concentrations for Fe and P is given for each experiment in Table A5.5

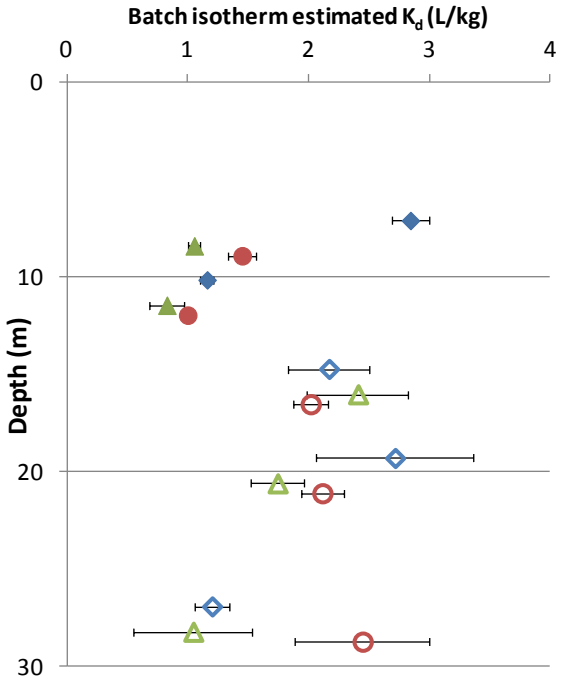

Figure A5.1. Vertical profile of K_d results. Vertical profiles extending from the surface to about 30 m depth are shown for 15 positions used in the As batch adsorption experiments. Color indicates distance from stream moving from blue (K240) to green (K150) to red (K60). Filled markers indicate sediments from cores, while open markers indicate sediment from drill cuttings.

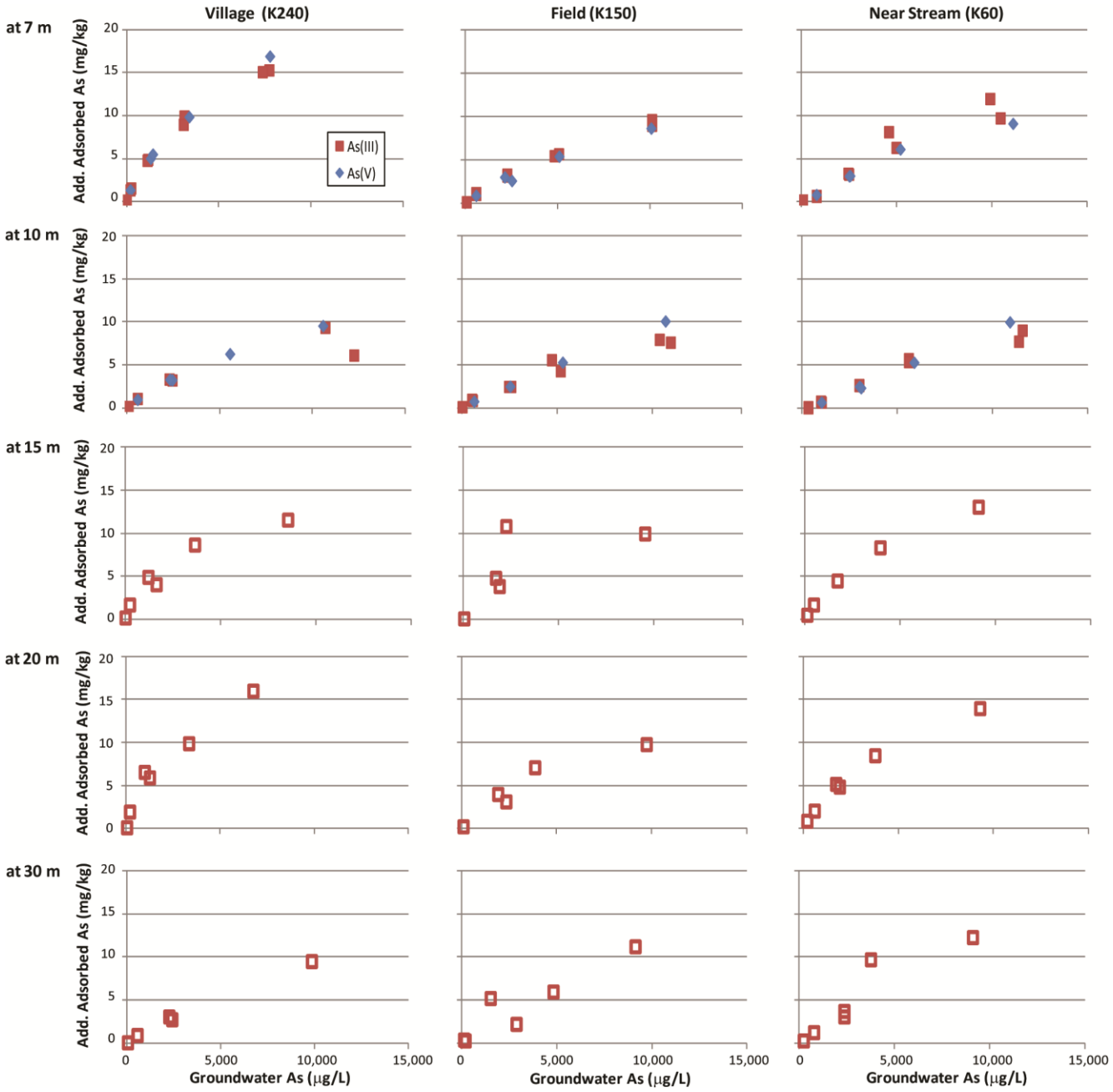

Figure A5.2. As batch adsorption experiments at Site K. The observed As adsorption isotherm is shown for each of the 15 positions, rows include samples from similar depths (7, 10, 15, 20 or 30 m), while the columns include isotherms from the same location (K240, K150 and K60). Red squares indicate samples with As(III) additions, while blue squares are for As(V) additions. Filled markers indicate sediments from cores, while open markers indicate sediment from drill cuttings.

A5.2 Arsenic Speciation and Extractions

Adsorption experiments for both As(III) and As(V) were performed on the core materials collected at 7 and 10 m at the three locations. As speciation was measured in both the groundwater and sediment at the completion of the adsorption experiment (Figure A5.3, Table A5.1 to A5.3). Dissolved As(III) accounted for 85% or more of the total As, even when high concentrations of As(V) are added in the batch experiments. The batch PO_4-extraction recovers 55 to 70% of the As adsorbed during the experiment and typically greater than 60% of the extracted As is As(III), with only a three outliers.

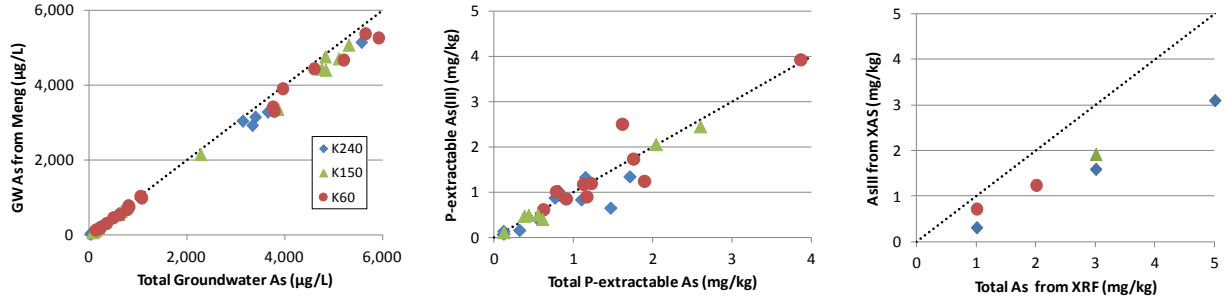

Figure A5.3. As speciation in the batch samples. Total groundwater As concentrations are compared to As(III) determined using the Meng column in panel A, with blue for K240, green for K150 and red for K60. Total P-extractable As concentrations are compared to As(III) determined using voltammetry in panel B using the same color scheme. Total sediment As concentrations from XRF are compared to As(III) estimates determined from XAS. These results include the samples were As(V) was added.

The samples receiving the As(V) addition had high concentrations of As(III) in the groundwater upon completion of the experiments, which suggest that either the As(V) was extensively reduced or the added As(V) displaced As(III) bound on the sediments. Displacement of As(III) bound to the sediments is supported by two findings. First, little As reduction was observed in the sediments, as measured PO_4-extractions. Second, the batch phosphate addition experiments, which competes particularly with As(V), produced only minor changes in groundwater As concentration. This finding coupled with the lack of saturation observed in the As batch experiments suggests that little As(V) was desorbed and that there were ample surface sites available for any desorbed As(III) or As(V). Assuming the As(V) additions simply displaced As(III) from the sediments, the indistinguishable batch adsorption curves do not therefore show that there is no difference in the partitioning of As(III) or As(V) on the sediment, but instead that the As(V) is so readily and completely adsorbed than only As(III) is left in solution and these experiments essentially just replicated the As(III) experiments. Taken together, these results strongly support that As(III) is the more labile species in these sediments and that As(III) equilibrium is the primary adsorption mechanism in this aquifer, which is agreement with earlier observations.

A5.3 Competition with phosphate

In order to estimate of the partitioning coefficient of phosphate, one sample from core material collected at 7 and 10 m, at each location, received a 4,000 µg/L addition of P as phosphate; ambient concentrations of P range from 30 to 1,600 µg/L in these samples (Figure 3 in main text). The phosphate Kd varies from 1.2 to 13.6 L/kg with the highest partitioning occurring at 7 m at K240, similar to the As results (Table 3 in main text). Only minor changes in groundwater As concentrations are observed with the phosphate addition (Table A5.6); the difference is <25% for all except the low As sample where the groundwater concentration increases from 10 to 14 µg/L.

Table A5.6. Effect of addition of P on As adsorption. The observed phosphate adsorption Kd is given for the 4 samples where approximately 4,000 µg/L of P was added. The As concentration in the sample of both initial and P addition samples as well as the percent change from no additional P is shown.

			Groundwater As		
	Depth	Phos Kd	No Added P	Added P	Diff.
	m	L/kg	µg/L	µg/L	%
K240	7	13.6	10	14	145%
	10	missing			
K150	8	1.2	80	91	113%
	11	2.1	99	75	76%
K60	9	1.9	210	234	111%
	12	3.7	362	355	98%

A6. Push-pull experiment

A6.1 Additional parameters

Groundwater As, Fe, P and S concentrations are shown for the five push-pull tests. Dashed lines indicate expected concentration if there was no reaction (estimated from change in [Br]); samples with significant dilution (e.g. $[Br]/[Br]_0<0.7$) are shown as unfilled diamonds. Complete groundwater analyses are given in Tables A6.1 to A6.5.

In the four experiments where groundwater with lower than ambient concentrations were added (desorption tests), there is a transition when the measured groundwater As concentration goes from being greater than the mixing curve (due to desorption) to being less, even though the dilution should have increased the measured groundwater As concentration in the desorption experiments. This typically occurred between 100 and 250 hr after injection. After 2 weeks, the bromide has been significantly diluted suggesting that the initial groundwater As concentration should be restored, however the measured concentrations are remain less than the initial (Table 1 in main text). The modeling scenarios replicate this pattern well. Model calculations of adsorbed As concentrations at the end of the experiment are significantly depleted (only 50 to 80% of the initial adsorbed sediment concentration). This suggests that groundwater As concentration didn't return to the ambient concentration since the incoming groundwater was replenishing the sediment. When these same wells were sampled two months later (in March 2008), the ambient concentrations had largely been restored (Table 1).

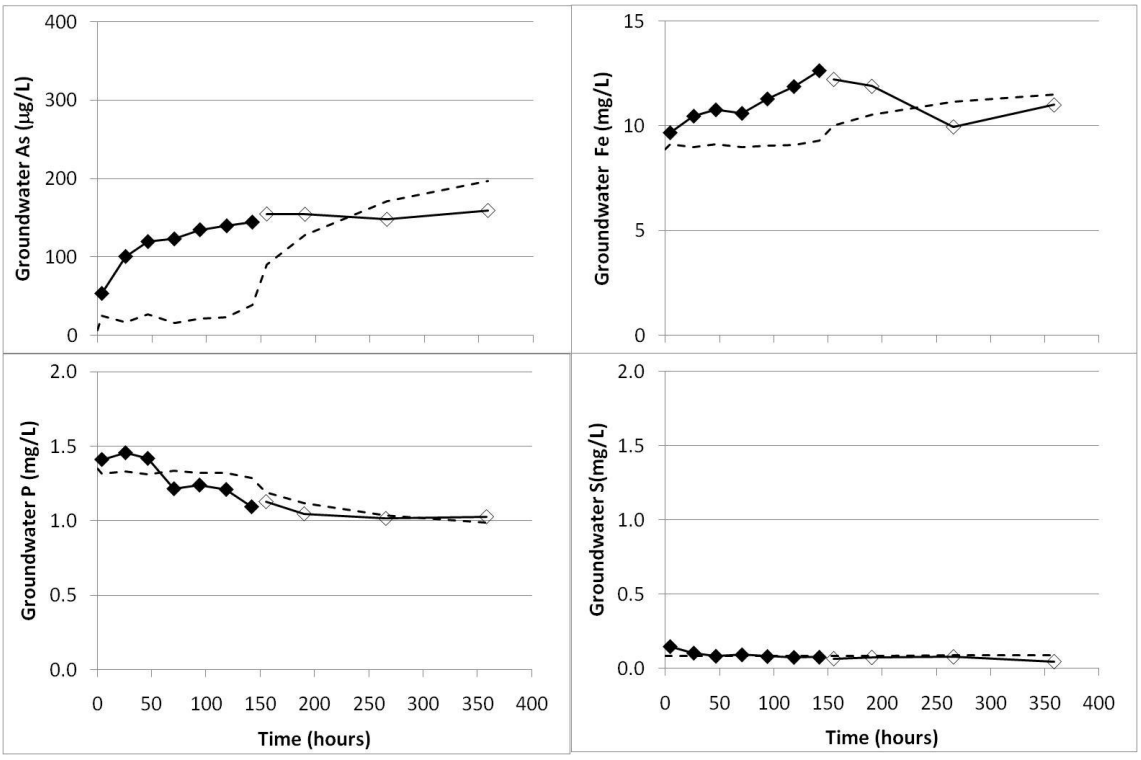

Figure A6.1. Desorption push-pull test: K40E – 7m

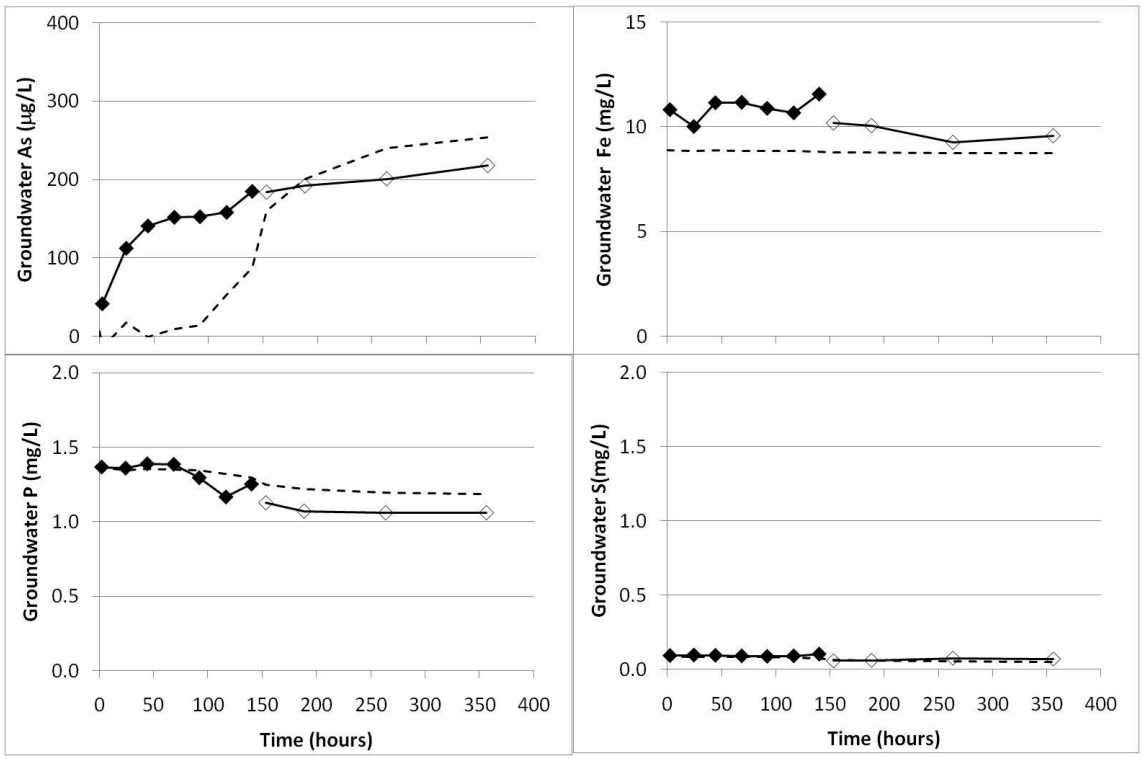

Figure A6.2. Desorption push-pull test: K40E- 10m

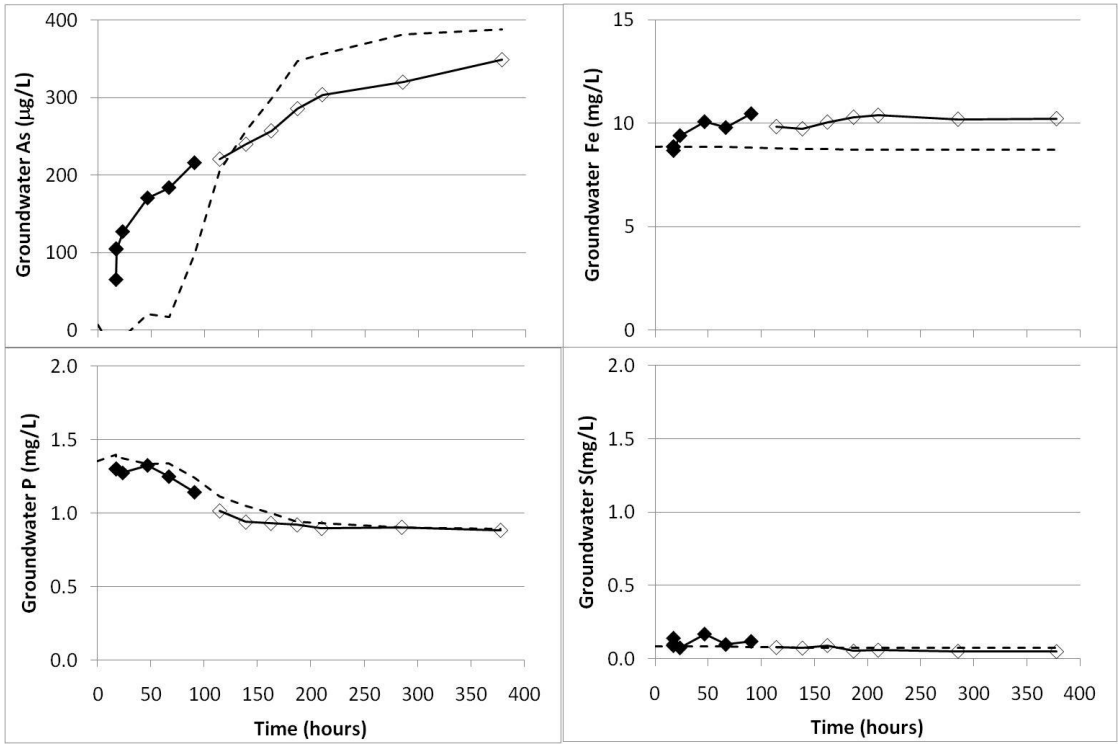

Figure A6.3. Desorption push-pull test: K40E-15 m

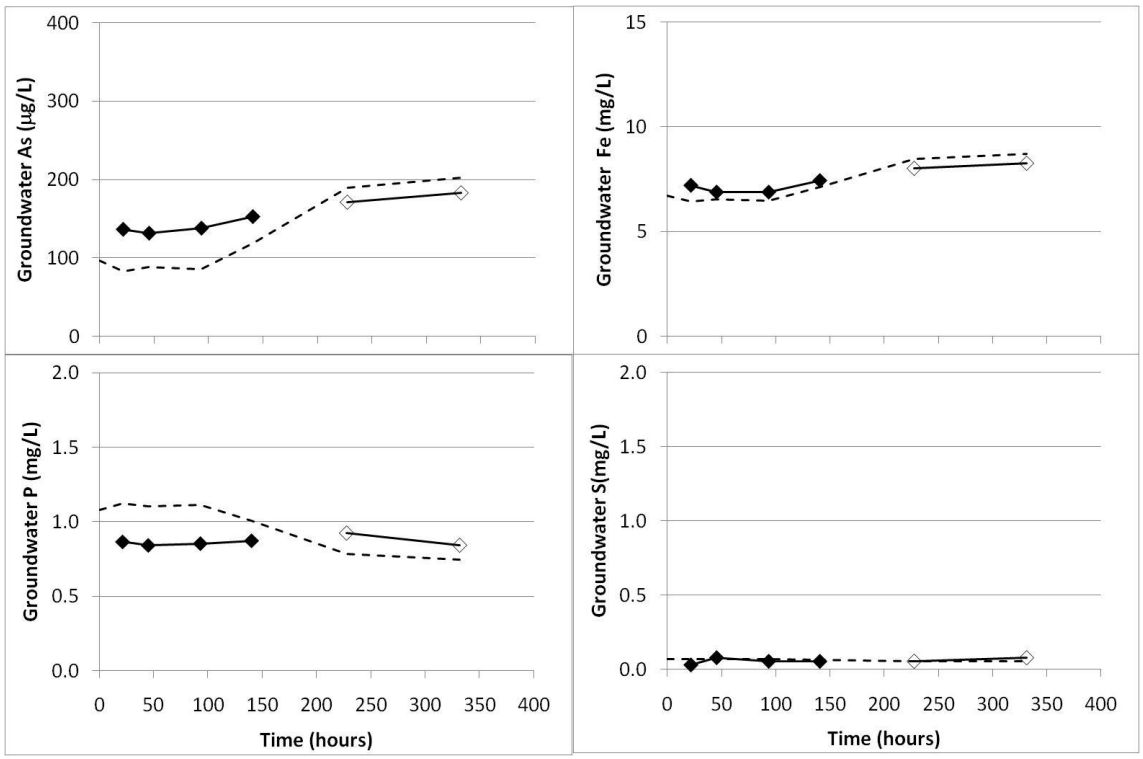

Figure A6.4. Desorption push-pull test: K80W-15m

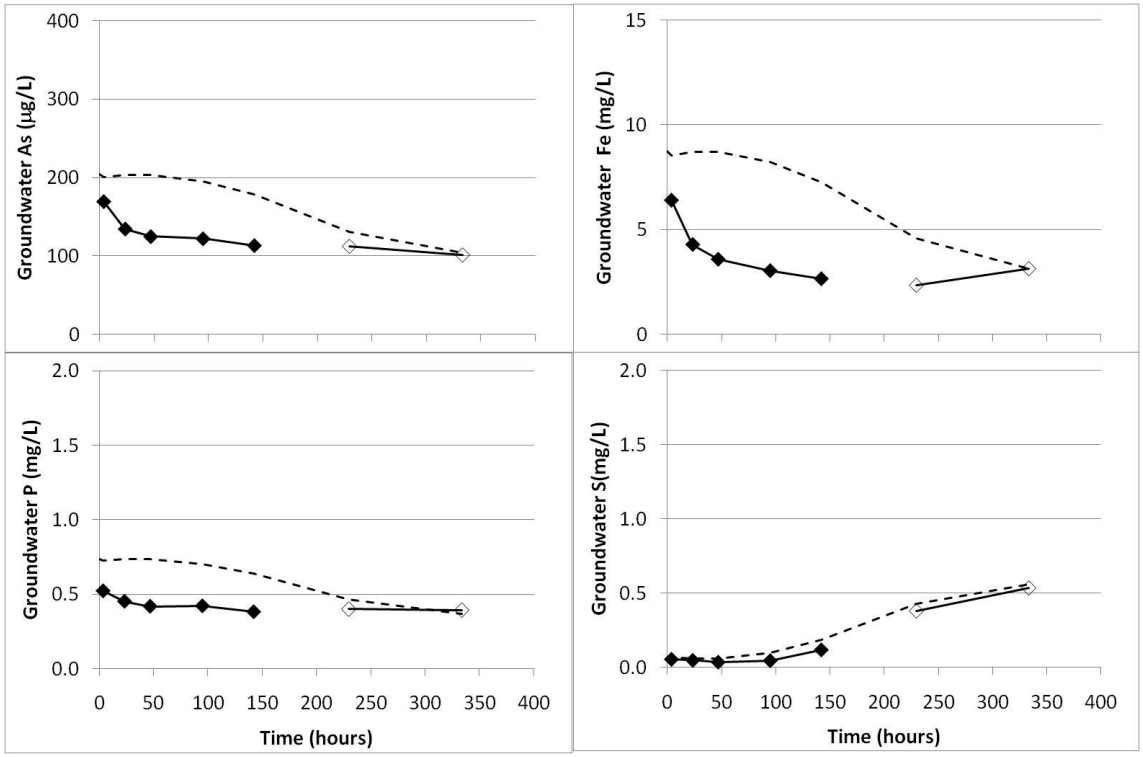

Figure A6.5. Adsorption push-pull test: K80W – 7m

A6.2 Additional model fitting

Model fitting using all of the nondiluted samples in all 5 five experiments was presented in the main text. Addition model fits for each experiment individually, using only the nondiluted sample or all of the samples, are shown below (Tables A6.6 and A6.7). The results from a third modeling scenario are also given. In this scenario, the portion of readily available adsorption sites is set to 20%, similar to other sandy aquifers, and best fit is achieved with a K of 0.42 L/kg.

Table A6.6. Model fitting for each experiment individually, using only the nondiluted samples.

			Desorption				Adsorption
		All 5	K40E- 7m	K40E- 10m	K40E- 15m	K80W- 15m	K80W- 7m
K=1.5	K	1.5	1.5	1.5	1.5	1.5	1.5
	kf	1.24	0.79	0.85	0.80	1.55	0.72
	xe	6%	9%	6%	7%	6%	14%
	kdiff	0.0006	0.0006	0.0004	0.0004	0.0003	0.0008
Single	K	0.17	0.22	0.15	0.26	0.12	0.29
	kf	0.02	0.03	0.02	0.02	0.04	0.08
	xe	--	--	--	--	--	--
	kdiff	--	--	--	--	--	--
xi=80%	K	0.42	0.64	0.43	0.47	0.50	1.05
	kf	0.38	0.35	0.25	0.12	0.59	0.51
	xe	20%	20%	20%	20%	20%	20%
	kdiff	0.0026	0.0017	0.0016	0.0030	0.0011	0.0011

Table A6.7. Model fitting for each experiment individually, using all samples.

			Desorption				Adsorption
		All 5	K40E- 7m	K40E- 10m	K40E- 15m	K80W- 15m	K80W- 7m
K=1.5	K		1.5	1.5	1.5	1.5	1.5
	kf		0.29	0.46	0.46	1.42	0.67
	xe		13%	7%	6%	5%	15%
	kdiff		0.0000	0.0003	0.0008	0.0006	0.0006
Single	K		0.19	0.20	0.49	0.38	0.35
	kf		0.04	0.01	0.01	0.01	0.06
	xe		1.00	1.00	--	--	--
	kdiff		0.0000	0.0000	--	--	--
xi=80%	K		0.95	0.45	0.72	0.49	1.75
	kf		0.18	0.24	0.08	0.79	0.29
	xe		20%	20%	20%	20%	20%
	kdiff		0.0000	0.0013	0.0022	0.0017	0.0000

A7. Flushing Model

A7.1 Description of the Flushing Model

We use the idealized Vogel model of an aquifer presented by Schlosser et al. (1989) to compare the vertical profiles of groundwater ages derived from 3H-3He data, first at the present study site and subsequently another dozen sites across the Bengal and the Red River basins (Klump et al., 2006; Stute et al., 2007; Postma et al., 2007; 2012; McArthur et al., 2010). The Vogel model predicts, for instance, groundwater ages of ~5 and 50 yr at 15 m depth below the water table for vertical flow velocities of 5 and 0.5 m/yr, respectively, in a 25 m thick aquifer. Vertical profiles of groundwater ages predicted are compared to the range of ages derived from ^{3}H-^{3}He data to estimate vertical flow velocities. For an order-of-magnitude lower vertical flow velocity of 0.05 m/yr, the model predicts that peak bomb input of ^{3}H and ^{14}C during the 1950s and 1960s should be detectable no more than a few meters below the surface. The constant vertical age profile requires that the velocity and shape of the theoretical flow paths are not identical in the lateral direction. The flowpaths transition from slower, nearly vertical flow to faster, more lateral flow approaching the discharge location. Some flowpaths with have shorter paths with lower velocities, while other flowpaths will be longer with higher velocities to reach the same depth.

We build on the Vogel model of the distribution groundwater ages to predict the evolution of the vertical distribution of As in groundwater over time using a simple one dimensional advection dispersion model (from van Genuchten and Alves, 1982). The underlying assumption is that groundwater As concentrations are controlled by adsorptive equilibrium with ambient aquifer sands and that the rate flushing of the aquifer is set by the profile of groundwater ages. At any given depth, the rate of flushing of an aquifer remains constant given that groundwater ages remain constant, regardless of the distance from the boundary of the watershed. Therefore, the observed groundwater age is used to estimate the velocity and flowpath distance parameters in the flushing model using the Vogel model. The implication of this simple but plausible model is that the evolution of exchangeable As retained in the sediment, and therefore As concentrations in groundwater, are both solely a function of depth and independent of lateral location. The "clock" for flushing starts after sediment deposition and after the onset of reducing conditions. The age of the aquifer sediment since deposition therefore provides an upper limit for the flushing time.

A7.2 Araihazar, Vietnam, Munshiganj, West Bengal, and Cambodia

The idealized flushing model was used to evaluate the groundwater As and age relationship at other sites were apparent groundwater ages were reported. The aquifer thickness was estimated based on geologic profiles of the site and the known minimum water levels. Vertical velocity was then estimated using the Vogel model. The assumptions are stated in table A7.1.

The highest vertical flow velocity of 5 m/yr (corresponding to a recharge rate of 1.5 m/yr, assuming a porosity of 0.3 for the shallow aquifer) was estimated for two low As sites within Araihazar, C and F, (Figure 7D, in the main text) and are comparable to the reported recharge rates of 0.5 and 1.1 m/yr which did not consider aquifer thickness (Stute et al. 2007). Similarly the vertical flow velocity at the two high As sites within Araihazar, A and B, was estimated to be 0.7 m/yr (0.2 m/yr recharge, Figure 7D, in the main text) from the Vogel model and the reported recharge was 0.1 m/yr (Stute et al., 2007). For the sites in Vietnam, the reported vertical velocities were used and agree with our estimates.

Table A7.1. Data used for estimating flushing rates and flushing time. The approximated aquifer depth and water levels were used to estimate aquifer thickness for the Vogel model, which was used to estimate the vertical velocity. The flushing time was then estimated by fitting the model results to the depth of the peak As concentration.

Site	Aquifer depth (m bgs)	Minimum water level (m bgs)	Aquifer Thickness (m)	Est. Vertical Velocity (m/s)	Flushing extent (yr)	Reference
Araihazar, Site K	**30**	**5**	**25**	**0.25 to 1**	**500**	**This Study**
Araihazar, Site A	15.5	5.5	10	0.7	200	Stute et al., 2007
Araihazar, Site B	35.5	5.5	30	0.7	200	Stute et al., 2007
Araihazar, Site C	20	5	15	5	50	Stute et al., 2007
Araihazar, Site F	20.5	5.5	15	5	75	Stute et al., 2007
Vietnam, H-transect	60	5	55	0.5*	200	Postma et al., 2012
Vietnam, Van Coc	35	5	30	0.25*	750	Postma et al., 2012
Vietnam, Phu Kim	20	5	15	0.5*	500	Postma et al., 2012
Vietnam, Phung Thuong	15	0	15	0.5*	1000	Postma et al., 2012
Munshiganj	72	2	70	0.5	750	Klump et al., 2005
West Bengal, AP	38	8	30	2	250	McArthur et al., 2010
West Bengal, FP	38	8	30	1	250	McArthur et al., 2010
Cambodia	67	7	60	0.05	5000	Benner et al., 2008 and Polizzotto et al., 2008

The results for the sites from Munshiganj, West Bengal, and Cambodia are given in Figure A7.1. Vertical velocity was estimated to be 0.5 m/yr in Munshiganj based on the limited samples up to 20 m depth (Klump et al., 2006) and is comparable to the vertical flow velocity of the lower recharging sites in Araihazar, including Site K. Vertical velocities ranged from 1 to 2 m/yr in West Bengal, based on samples up to approximately 30 m depth, and is intermediate to the vertical flow velocities observed in Araihazar (McArthur et al., 2010). Vertical velocity was reported to be 0.04 m/yr in Cambodia based on modeling and is not based on age data, due to the slow recharge through the 20-m thick clay layer (Polizzotto et al., 2008; Kocar et al., 2008; Benner et al., 2008). No peak bomb input of ^{3}H and ^{14}C should be detectable below a few meters and this is consistent with the absence of bomb-produced tracers in groundwater at this site (S. Fendorf, personal communication).

Shallow groundwater As concentrations can be approximated in Munshiganj using a flushing time of 750 yrs for samples less than 20 m and for a flushing time of 1,000 yrs for samples collected from 30 m depth. In West Bengal, high groundwater As concentrations are still present in the shallow aquifer, which suggests a flushing time of 250 yrs for the two sites. In Cambodia, groundwater As concentrations are shown across the site. Peak As concentrations found at 25 m can be approximated using a flushing time of 5,000 years.

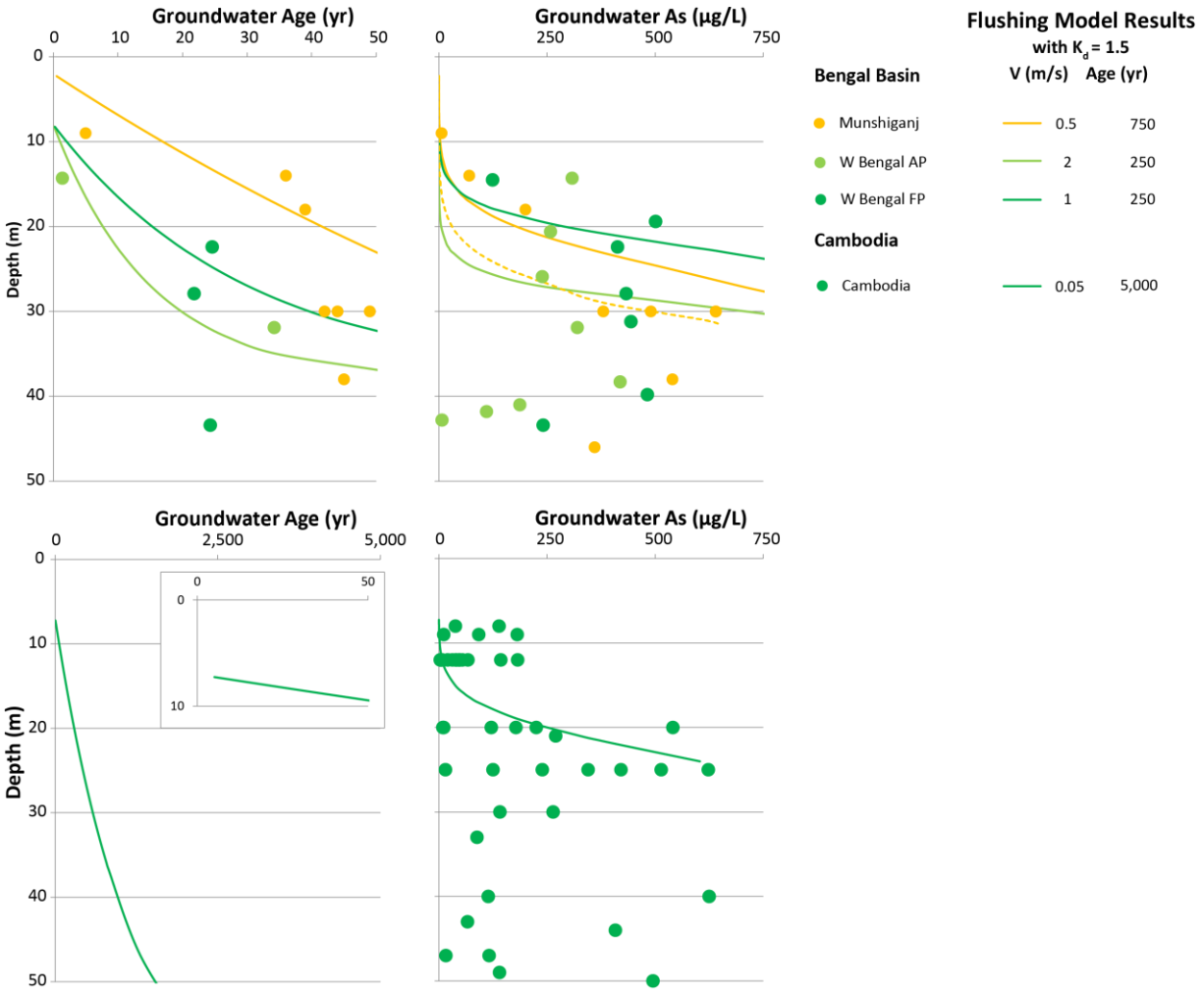

Figure A7.1. Idealized Flushing Model Results for Munshiganj, West Bengal and Cambodia. Measurements and model results for Munshiganj and West Bengal sites AP and FP are shown in Panels A and B (Klump et al., 2006 and McArthur et al., 2010); and for Cambodia in C and D (Polizzotto et al., 2008; Benner et al., 2008). Measured groundwater ages and modeled age profiles based on the Vogel model are shown in A and C. Groundwater As concentrations and modeled concentration based on the idealized flushing model for a K_d of 1.5 L/kg are shown in B and D.

Additional References

Carrier, W.D., 2003. Goodbye, Hazen; Hello, Kozeny-Carman. Journal of Geotechnical and Geoenvironmental Engineering, 129(11): 1054-1056.

Fetter, C.W., 2001. Applied Hydrogeology. Prentice Hall, Upper Saddle River, NJ, 598 pp.

Levin, I. and Kromer, B., 1997. Twenty years of atmospheric (CO2)-C-14 observations at Schauinsland station, Germany. Radiocarbon, 39(2): 205-218.

Shepherd, R.G., 1989. Correlations of permeability and grain-size. Ground Water, 27(5): 633-638.